NSF/CEE-82003

SCEGIT-101-82

PB82-202276

Research Initiation

PROBABILISTIC EVALUATION OF DAMAGE POTENTIAL IN EARTHQUAKE-INDUCED LIQUEFACTION IN A 3-D SOIL DEPOSIT

By

Achintya Haldar

Frank J. Miller

Technical Report of Research

Supported by

THE NATIONAL SCIENCE FOUNDATION

Grant No. PFR-8006348

March 1982

GEORGIA INSTITUTE OF TECHNOLOGY
A UNIT OF THE UNIVERSITY SYSTEM OF GEORGIA
SCHOOL OF CIVIL ENGINEERING
ATLANTA, GEORGIA 30332

Research Initiation

PROBABILISTIC EVALUATION OF DAMAGE POTENTIAL IN EARTHQUAKE INDUCED LIQUEFACTION IN A 3-D SOIL DEPOSIT

by

Achintya Haldar
Frank J. Miller

Sponsored by

The National Science Foundation
Grant No. PFR-8006348

Report No. SCEGTT-101-82

School of Civil Engineering
Georgia Institute of Technology
Atlanta, Georgia 30332

March 1982

ACKNOWLEDGEMENTS

This material is based upon work supported by the National Science Foundation under Grant No. PFR-8006348. Any opinions, findings, and conclusions or recommendations expressed in this publication are those of the authors and do not necessarily reflect the views of the National Science Foundation.

ABSTRACT

A probabilistic model is proposed here to evaluate the risk of liquefaction at a site considering the damage aspect of the problem. It is necessary to consider the minimum soil volume that will produce a noticeable amount of damage at a referenced location. Soil properties in this soil volume are modeled probabilistically in three dimensions. It is found in this study that the estimation of risk of liquefaction considering the weakest point in the deposit may not be meaningful in many cases. A considerable amount of uncertainty is expected in the estimation of the in situ relative density. A new relationship is proposed here between the SPT-value, inplace dry density, limiting densities and effective overburden pressure. The predictability of the Haldar and Miller relationship is superior to other presently available relationships. A model is also developed to estimate the in situ shear resistance of a deposit considering the effects of compliance, sample preparation methods, mean grain size, multidirectional shaking and some other secondary factors. All the earthquake-related load parameters are also considered probabilistically. The probabilistic model developed here could be used as an analytical tool to complement the deterministic procedures by providing information on the relative risk of liquefaction between various design alternatives.

TABLE OF CONTENTS

LIST OF TABLES

LIST OF FIGURES

Chapter 1

INTRODUCTION

1.1 General Remarks

Liquefaction of a soil deposit has an enormous damage potential in terms of human life, property damage, human suffering and environmental damage. The devastating damage due to soil liquefaction in Anchorage, Alaska and Niigata, Japan in 1964 is a very recent reminder of the critical nature of such events (11, 25, 42, 71). Soil liquefaction following earthquakes in these areas resulted in landslides, subsidence of foundations, formation of sand volcanoes, damage to earth structures, lateral movement of structures resting on soil, disruption of services, and loss of human life. These events, more than anything else, created a sensational amount of interest about the phenomenon among the research communities, and a sense of urgency among practicing engineers. Consequently, voluminous research efforts were exerted (3, 8, 12, 16, 21, 22, 45, 46, 57, 61, 68, 72, 75, 76, 79, 85). Due to the inherent complexities of the problem, the research was conducted in many areas related to the liquefaction phenomenon. Researchers are investigating the causes of the problem, but the damage associated with liquefaction is another aspect which should not be neglected. The technical as well as the economic aspect of the problem needs to be considered. This type of study will lead to the development of a decision analysis framework (26).

Liquefaction is caused by loss of shear strength of a deposit due to earthquake excitation. For proper evaluation, information on soil

properties affecting the liquefaction phenomenon and earthquake loading needs to be available. The estimation of in situ soil parameters can be obtained by directly measuring them in the deposit, or indirectly from empirical relationships or by measuring them in the laboratory using so-called "undisturbed" samples. Considerable error can be incurred during these processes (28, 30, 31, 52, 56, 59, 71, 93). The nonhomogeneity of the soil properties in the liquifiable volume has to be modeled in three dimensions. Long-distance fluctuations and local variations in soil properties can only be modeled effectively using probability theory. Seismic loading is also unpredictable. This necessitates the availability of a simple but efficient and practical probabilistic model to study the risk of damage associated with the liquefaction phenomenon.

1.2 Objectives and Scope of Study

This study will be limited to earthquake-induced liquefaction. "Cyclic Mobility" would be the most appropriate definition of the problem under consideration according to the most recent literature (7, 70). However, the term "liquefaction" will be used in this report instead of "cyclic mobility" since the former is the most widely used by practicing engineers.

It is necessary to develop a simple but efficient and practical probabilistic model considering damage during liquefaction. Thus, it is necessary to go one step beyond the evaluation of liquefaction potential. Limiting or eliminating damage during liquefaction would be a reasonable criterion for this type of approach.

The development of this type of sophisticated probabilistic model is, however, very complicated and needs to be done in several stages. The

objectives of this initial stage are twofold: (1) development of a probabilistic model considering all important parameters to evaluate risk of liquefaction at a point, and (2) extension of the model to consider the three-dimensional nonhomogeneous soil properties. This three-dimensional model will be developed further in subsequent studies.

This study attempts to review, identify and analyze all major parameters relevant to the liquefaction problem and the uncertainties associated with them. Normally consolidated, saturated sand deposits are considered in this study. Voluminous information available in the literature is used to develop this model. To facilitate application by practicing engineers, the proposed model is kept as simple as possible while retaining pertinent features of the existing deterministic evaluation method.

1.3 Report Organization

Chapter 2 is devoted to an extensive literature survey to identify all the important parameters relevant to the liquefaction phenomenon. To facilitate the discussion, these parameters are classified into three groups. They are (1) soil parameters, (2) parameters required to consider laboratory test and sampling effects, and (3) loading parameters.

In Chapter 3, the fundamentals of risk-based design concepts pertinent to the liquefaction problem are reviewed. The probabilistic concepts necessary to analyze uncertainties are described briefly. Finally, the chapter presents a risk model for evaluating liquefaction risk at a site, accounting for the effects of relevant uncertainties. This point model is then developed further to consider soil properties in three dimensions.

Chapter 4 is devoted to a detailed statistical evaluation of the soil parameters in the proposed liquefaction model. The uncertainty associated with the estimation of in situ relative density is evaluated for both direct and indirect methods. For the indirect estimation of relative density, a new relationship between the standard penetration test value and the in-place dry density is developed. This new relationship, called the Haldar and Miller relationship, is shown to be superior to all other presently available relationships. The in situ shear resistance of a deposit is also estimated by introducing a shear strength parameter. This shear strength parameter is corrected for factors including compliance effect, multi-directional shaking, sample preparation methods, mean grain size effect and all other factors identified in Chapter 2.

The parameters of earthquake loads pertinent to the liquefaction problem are identified and analyzed probabilistically in Chapter 5. The probabilistic characteristics of earthquake magnitude, equivalent number of uniform stress cycles corresponding to an earthquake magnitude, design acceleration, etc. are developed.

The liquefaction risk at a site is evaluated in Chapter 6. This chapter also suggests a procedure for a probabilistic evaluation of the liquefaction potential of a site. The probabilistic method is applied to a site in the San Francisco Bay area.

The summary and principal conclusions are presented in Chapter 7.

Chapter 2

LITERATURE REVIEW

2.1 General Remarks

There is general agreement about the mechanism by which the onset of liquefaction occurs during an earthquake. It is generally recognized that the basic cause of liquefaction in a saturated cohesionless soil deposit during an earthquake is the buildup of pore water pressure due to the application of cyclic shear stresses induced by the ground motions. These stresses are generally considered to be due primarily to upward propagation of shear waves in a soil deposit, although other forms of wave motions are also expected to occur. As a consequence of the applied cyclic stresses, the cohesionless soil tends to become more compact with a resulting transfer of stress to the pore water. The soil grain structure rebounds to the extent required to keep the volume constant, and this interplay of volume reduction and soil structure rebound determines the magnitude of the increase in pore water pressure. If sufficient pore water pressure is produced, the effective stresses are reduced to zero, and the deposit loses its ability to withstand shearing stresses and assumes the character of a viscous liquid. This essentially leads to liquefaction. To understand this complicated behavior of a soil deposit, a series of experiments with various degrees of complexity were carried out in the laboratory. Understanding the behavior of soils under various laboratory conditions would essentially lead to the development of a reasonable and acceptable liquefaction model.

2.2 Laboratory Studies

In the past the majority of the research into liquefaction of sands under cyclic loading has been done with laboratory experiments. Field and loading conditions were duplicated as closely as possible in the laboratory to reproduce the in situ soil behavior. Of course, the degree to which the results are representative of in situ soil behavior depends on how closely the field conditions have been simulated. In the initial stages of this experimental work, the triaxial test was used extensively to simulate field conditions (7, 12, 22, 39, 43, 45, 46, 49, 56, 73, 75, 78). It is still widely used to study the cyclic strength of saturated sands, but the test may not reproduce the in situ state of stress on the soil element adequately (7, 12, 25, 29, 41, 61, 70, 72, 75, 97). To overcome the inherent deficiencies in the triaxial test, the simple shear test was developed (20, 22, 23, 38, 61, 64, 75). Though the simple shear test is an improvement over the triaxial test, it has some shortcomings also. For example, application of a uniform shear stress across the width of the sample or development of complementary shear stresses along the side of the sample are difficult to obtain (25, 35, 70, 75, 96). Most of the drawbacks of the simple shear device are eleminated in the ring torsional simple shear device (35, 36, 41, 77, 95, 96, 97, 98). All the aforementioned tests were small-scale tests. The difficulties they encountered can be eliminated by large-scale tests. In large-scale shaking table tests, a sealed saturated sample of soil is placed on a shaking table and a surcharge is placed on top. An electronic actuated ram applies the cyclic lateral load. This test has several advantages over the aforementioned small-scale tests; for example, large saturated sand samples can

be tested; boundary effects can be minimized; in situ soil conditions can be reproduced more closely; and the sample can be subjected to uniform accelerations under plane-strain conditions at low frequencies (12, 54). When conducted properly, large-scale shaking table tests can provide the most representative information on liquefaction of sands under cyclic loading.

Past research, both experimental and analytical, and field investigations have led to several methods of liquefaction potential evaluation. These are discussed in the following section.

2.3 Methods of Liquefaction Potential Evaluation

Earthquake-induced liquefaction is a very complex problem, and several methods with various degrees of complexity are available to help solve the problem. For the purpose of this discussion, the currently available methods of liquefaction potential evaluation can be classified into the following major categories:

(1) Method based on evaluation of stress conditions in the field and laboratory determination of stress conditions causing liquefaction - the simplified method suggested by Seed and Idriss (72).

(2) Cyclic stress analysis by means of ground response analysis: (a) neglecting pore pressure buildup as the earthquake progresses (71), (b) considering pore pressure buildup as the earthquake progresses (21, 47), based on knowledge of maximum ground surface motion or by deconvolution of a known ground surface motion (18, 69), (c) allowing partial drainage during earthquake loading (18).

(3) Empirical methods based on observation of the performance of sand deposits in previous earthquakes (42, 58, 74, 91), and

(4) Probabilistic Methods (9, 15, 17, 18, 29, 94).

The merits and demerits of the methods mentioned in Item Nos. 1, 2, and 3 are beyond the scope of this report. However, as stated earlier, a probabilistic method of liquefaction potential evaluation has definite advantages over the deterministic methods (18, 25, 29, 94).

The limitations of the currently available probabilistic methods need some mention here. They can be separated into two groups: methods based on the case histories of liquefaction available in the literature and methods relating laboratory experimental results and dynamic analysis of the deposit. Methods suggested by Christian and Swiger (9) and Yegian and Whitman (94) belong to the first group. The method suggested by Christian and Swiger is basically a multivariate statistical method called discriminant analysis. The authors even wrote in their paper that "Numerous assumptions are made in such analysis, including that the variates or parameters are normally distributed and that the variances and co-variances of individual cases (liquefaction and nonliquefaction) are the same as those for all cases taken together." Moreover, statistics of the two normal populations are estimated from sparse and unreliable data (18). Estimation uncertainty is not considered at all. Yegian and Whitman (94) used historical data but avoided making the questionable assumption of the existence of two binormal populations with the same covariance matrix. But they did not address many important factors that are presently throught to significantly affect liquefaction potential.

Methods relating laboratory experimental results and dynamic analysis are suggested by Donovan (15), Faccioli (17), Fardis and Veneziano (18),

and Haldar and Tang (29). Donovan assumed the probability density function of the shear stress-time history envelope of an earthquake followed the Rayleigh distribution. The seismic activity of the region as well as the uncertainties in soil parameters affecting liquefaction were not considered. Faccioli applied one-dimensional amplification theory to find the probabilistic characteristics of the shear stress process, considering an earthquake as a stationary random process with given power spectral density function. He did not consider uncertainties in soil parameters. Fardis and Veneziano considered an essentially one-dimensional mechanical model based on many assumptions (70, 99). Seed (70) wrote, "They do require, however, the determination of more material properties in order to make the analysis and some of them are vulnerable to testing errors or require further study before they are fully understood." Questions are frequently raised on the modeling of any future earthquake time history (from a known spectrum or any other way), damping characteristics of the deposit, finite element modeling, etc. Seed (70) suggested, "more simplified approach seems to offer a more practical and less vulnerable alternative at the present time." Haldar and Tang (29) used a relatively simple method commonly used by practicing engineers. It is the slightly modified simplified method suggested by Seed and Idriss (72). This method considered the uncertainties in the soil deposit and the earthquake loading. In that respect it is complete, but it will only estimate the probability of liquefaction at a point in the deposit.

An extension of the method suggested by Haldar and Tang is very appealing since it has some desirable features. If the extension is made very carefully, it will be an important tool available to engineers to

study the liquefaction phenomenon. This careful extension, using a different approach to the problem, is the objective of this study.

2.4 Soil Liquefaction Parameters

The factors to be considered in the proposed model of liquefaction potential evaluation are numerous. For simplicity of discussion, these factors are divided into three groups. They are soil parameters, parameters related to laboratory test and sampling effects, and loading parameters. These parameters and their effects on liquefaction potential are described in the following sections.

2.4.1 Soil Parameters

The soil parameters characterize the type of soil and the physical state in which the soil exists. They can be identified as relative density, initial confining pressure, overconsolidation ratio, earth pressure coefficient at rest, mean grain size and gradation, drainage, angularity or particle shape, soil fabric, method of deposition, age of deposit and seismic history, degree of saturation, temperature and viscosity of pore water, etc.

Relative density D_r, is one of the important parameters in a liquefaction potential evaluation study. All field and laboratory investigations suggest that an increase in D_r results in an increase in the resistance to liquefaction (12, 20, 22, 45, 56, 61, 70, 72, 73, 75).

From field and laboratory studies it has been found that the initial confining pressure, σ_o, on the soil element greatly affects the soil's resistance to liquefaction. The resistance to liquefaction will increase

with an increase in the initial confining pressure (22, 61, 70, 71, 72, 73, 75, 96).

An overconsolidated soil will result when a surcharge applied to the soil is later removed. The overconsolidation ratio, OCR, is the ratio of the preconsolidation pressure to the overburden pressure. An increase in the OCR will result in an increase in the liquefaction resistance of the soil (37, 70). Overconsolidated soil deposits will not be considered in this study.

Earth pressure coefficient at rest, K_o, a measure of the lateral confining pressure on a soil element, has a significant effect on liquefaction resistance. An increase in K_o will result in an increase in the liquefaction resistance (7, 22, 35, 37, 70, 75).

The type of soil greatly affects the liquefaction resistance of a soil deposit (8, 45, 66, 70, 72, 75). For cohensionless soils, the soil type is perhaps most easily characterized by the grain size distribution. Among many parameters, the mean grain size, D_{50}, is generally considered to represent the soil type. The general ranges of D_{50} which will be critical to the liquefaction problem are between 0.02 mm and 0.6 mm (45). Laboratory studies show that within this range of D_{50} sizes, vulnerability to liquefaction increases with decreasing D_{50} sizes for a given earthquake excitation. Soil deposits with a uniform gradation (66) are considered to be the most liquefiable soils.

Drainage will dissipate excess pore water pressures during a cyclic load; therefore, the resistance to liquefaction is increased by drainage of the soil (70).

Much work needs to be done in the area of the effect of angularity

or particle shape on the liquefaction resistance. However, it seems reasonable that if the soil particles are more angular in shape, the soil structure will be more stable; hence, the soil will have a greater resistence to liquefaction.

The soil fabric or soil structure is characterized by the orientation and arrangement of the grains and interparticle contact planes. A change in the soil fabric will result in a change in the soil's resistance to liquefaction (43, 56, 70). Mulilis, Seed and Chan (56), using triaxial tests have found that the distribution of the apparent long axes of sand grains apparently has no effect on liquefaction resistance, but samples that had a higher distribution of normals to interparticle contact planes parallel to the loading axis exhibited a greater resistance to liquefaction.

Through laboratory tests, it has been observed that the method in which the soil was deposited has a significant effect on liquefaction resistance (43, 56, 70). Ladd (43) has found that samples prepared in a moist condition exhibited greater liquefaction resistance than samples prepared dry for the triaxial test; however, the method of densification had very little effect. On the other hand, Mulilis, Seed and Chan (56) found that the method of densification does affect strength, and that samples densified by high frequency vibrations in the moist condition were strongest in their set of triaxial tests.

The age of the soil deposit has a significant effect on the cyclic strength of a soil. With time, cementation or welding of interparticle contact planes occurs, which strengthens the soil and increases its resistence to liquefaction (70).

The strength of a soil deposit is affected by its previous strain history. Finn, Bransby and Pickering (20) have observed that static shear strains or cyclic shear strains below certain threshold values increase the strength of the soil, but strains larger than the threshold values will decrease strength. Mori, Seed & Chan (54) subjected soil samples to a series of small shocks in order to simulate a prior seismic history, and found that the soils' resistance to liquefaction increased.

The soil will liquefy less readily during an earthquake if the soil conditions are less conducive to increases in excess pore water pressure; therefore, a reduction in the degree of saturation, S_o, will result in an increase in the cyclic strength of the soil (77).

The temperature and viscosity of pore water is expected to affect the cyclic strength of the soil, but the systematic effects resulting from these factors are not known clearly.

2.4.2 Parameters Related to Laboratory Test and Sampling Effects

Often laboratory tests are conducted using representative soil samples obtained from a deposit to evaluate the liquefaction potential of the deposit. The outcome of this type of evaluation will greatly depend on the quality of the sample used, the type of laboratory test and conditions of the test, etc. Some of the important parameters are quality of samples (i.e., undisturbed, disturbed or reconstituted samples), method of sample preparation, type of test, compliance effect, frequency and form of cyclic load used, etc.

Ideally, an undisturbed soil sample obtained from a deposit should be used in a laboratory investigation. Unfortunately, in the case of a

liquefaction study, it is extremely difficult to collect undisturbed samples from a loose, saturated sand deposit. However, extreme care should be taken during sampling to keep the degree of disturbance as small as possible. Mori, Seed and Chan (54) have shown that even in the most carefully conducted undisturbed soil sampling, a small amount of sample disturbance still occurs. This disturbance is significant enough to change the relative density and destroy the effects due to cementation or long-term loading and seismic history. Often, disturbed or reconstituted samples are used for test specimens. These type of samples will fail to consider the effect of cementation, long-term loading or seismic history of the deposit, etc.

The effects of method of preparation of samples have been discussed in Section 2.4.1.

Triaxial, simple shear, torsional shear, and large-scale shaking table tests are used in the laboratory to study the liquefaction potential. The load conditions used in these tests have been discussed in Section 2.2. In addition, strength as measured from the triaxial test can vary depending on the diameter of the sample, and the state of stress concentrations at cap and base (22, 61, 70, 75). Various reasons for stress concentration have been identified by Haldar (25). Strength as measured from the simple shear device can vary depending on if smooth or rough plattens are used, the magnitude of the seating load, development of complimentary shear stresses and the preparation of the simple shear test specimens (22, 61, 70, 75). Boundary effects and length-to-height ratios of soil samples can significantly affect results from large-scale shaking table tests (12, 70).

The test specimens in the laboratory are enclosed by a rubber membrane. The penetration of the membrane in spaces between sand particles will produce compliance error. Test results from laboratory investigations are expected to have compliance error to some degree. Compliance in the testing apparatus causes a fictitious increase in the cyclic strength of the test specimen (12, 23, 70). It has been observed that large-scale shaking table tests give values for cyclic strength close to those which would be found in situ.

The frequency and form of cyclic load applied to a specimen in the laboratory may not have a significant effect on the liquefaction potential evaluation. The effect of the loading frequency on the shear strength of the sample has been investigated in several research programs (45, 61). Peacock and Seed (61) have shown that for an applied uniform cyclic shear stress with a frequency in the range from 1/6 to 4 cycles/sec, the frequency of the cyclic shear stress does not affect cyclic strength in simple shear tests. Yoshimi and Oh-Oka (97) have found that for soil specimens tested in a ring torsion apparatus, the cyclic strength is independent of the frequency of the applied shear stress for frequencies in the range of 1 to 12 cycles/sec.

Tests have shown that the form of the applied shear stress history can have an effect on the cyclic strength of a soil (39, 40, 41, 96, 97). Yoshimi and Oh-Oka (97) have found that soil specimens subjected to complete or partial shear stress reversals will undergo liquefaction, but will not liquefy if subjected to unreversed shear stress cycles. Ishihara and Yasuda (41) found that the cyclic strength of a soil is greater for shock type than vibration type random shear stress applications.

2.4.3 Loading Parameters

Earthquake-induced liquefaction is under consideration in this study. All parameters of earthquake loading related to the liquefaction problem need to be evaluated. They are earthquake acceleration, magnitude, duration of shaking, multi-directional shaking, stress reduction factor, etc.

A site's vulnerability to liquefaction during an earthquake increases as the intensity of ground shaking increases. The maximum ground surface acceleration, a_{max}, is a measure of the intensity of ground shaking. For a given intensity of ground shaking a_{max}, the site will liquefy only when the duration of ground shaking exceeds a certain value. If the load-time history of an earthquake is converted to an equivalent number of uniform stress cycles, N_{eq}, then the duration of the ground shaking can be represented by N_{eq}. Since the duration of the ground shaking depends on the magnitude of the earthquake, N_{eq} will also depend on the magnitude of the earthquake.

Ordinarily, a soil specimen is subjected to a cyclic shear stress in only one direction in the laboratory. However, ground motion induced by an earthquake is multi-directional. Laboratory tests have shown that the resistance of soil to liquefaction under multi-directional ground shaking is less than if the shaking was in one direction (12, 38, 62, 70, 76).

As a soil column deforms during earthquake excitation, the shear stress at a point depends on the depth of the point from the ground surface. A stress reduction factor, r_d, is introduced to account for this (72). The maximum value of r_d is 1.0 at the ground surface. At other depths, the value of r_d is less than 1.0.

2.5 Summary

There are many factors involved in evaluating the liquefaction potential of a site. Some of these factors affect the liquefaction potential to a greater degree than do others. The relationship of these factors to the liquefaction potential and the uncertainties they introduce need to be accounted for in a probabilistic model of liquefaction.

Chapter 3

RELIABILITY MODEL

3.1 General Remarks

The safety or reliability of an engineering system or of a component of the system is essentially the measure of its capacity to meet the demands. If the capacity of the system and the demand on the system are known, the safety of the system can be assessed by comparing the capacity to the demand. In the present study the shear resistance mobilized by a volume of soil, τ_R, represents the capacity of the system and the shear stress generated during earthquake shaking, τ_A, represents the demand on the system. Liquefaction will occur when τ_R is less than τ_A.

In order to assess whether a soil deposit subjected to earthquake shaking is safe from liquefaction, τ_R and τ_A must be known. Unfortunately, these parameters are difficult to estimate. However, design decisions are often required to be made regardless of the state of completeness or quality of information available. Moreover, in view of the unavoidable errors in the modeling of soil behavior and of the unpredictability of the earthquake loading, τ_R and τ_A are intrinsically random. Therefore, a systematic probabilistic model of τ_R and τ_A is necessary.

In this chapter the basic probabilistic and statistical modeling techniques that are used will be presented briefly. These tools will be used to model the probabilistic characteristics of τ_R and τ_A considering all the known sources of uncertainties in them. Finally, with τ_R and τ_A modeled as random variables, the risk of liquefaction will be evaluated.

3.2 Concept of a Random Variable

Randomness in a parameter such as τ_R means that more than one outcome is possible; in other words, the actual outcome is (to some degree) unpredictable. The possible outcomes are usually a range of measured or observed values; moreover, within this range certain values may occur more frequently than others. Mathematical representation of a random variable is thus a primary task in any probabilistic formulation.

The mathematical representation of a random variable can be described graphically in the form of a histogram or frequency diagram as shown in Fig. 3.1a (2, 60). For a more general representation of the randomness, the frequency diagram can be fitted to some theoretical probability density function $f_X(x)$. By integrating the probability density function thus obtained, a probability distribution function, $F_X(x)$ can be obtained (see Fig. 3.1b). $F_X(x)$ is the probability that the random variable X will have a value less than or equal to x.

To describe the probability density function uniquely, some parameters of the distribution need to be estimated. The estimation of these paramters, which are called statistics, is itself a major part of the uncertainty analysis. These parameters or statistics need to be evaluated or estimated on the basis of a set of observed data obtained from the population. Among the most important statistical parameters are the mean value μ, which denotes the average or expected value of the random variable and the standard deviation σ, which denotes the dispersion of a random variable with respect to the mean value. Another commonly used parameter is the variance, which is the square of the standard deviation. The mean value and the variance can also be interpreted as, respectively, the centroidal distance

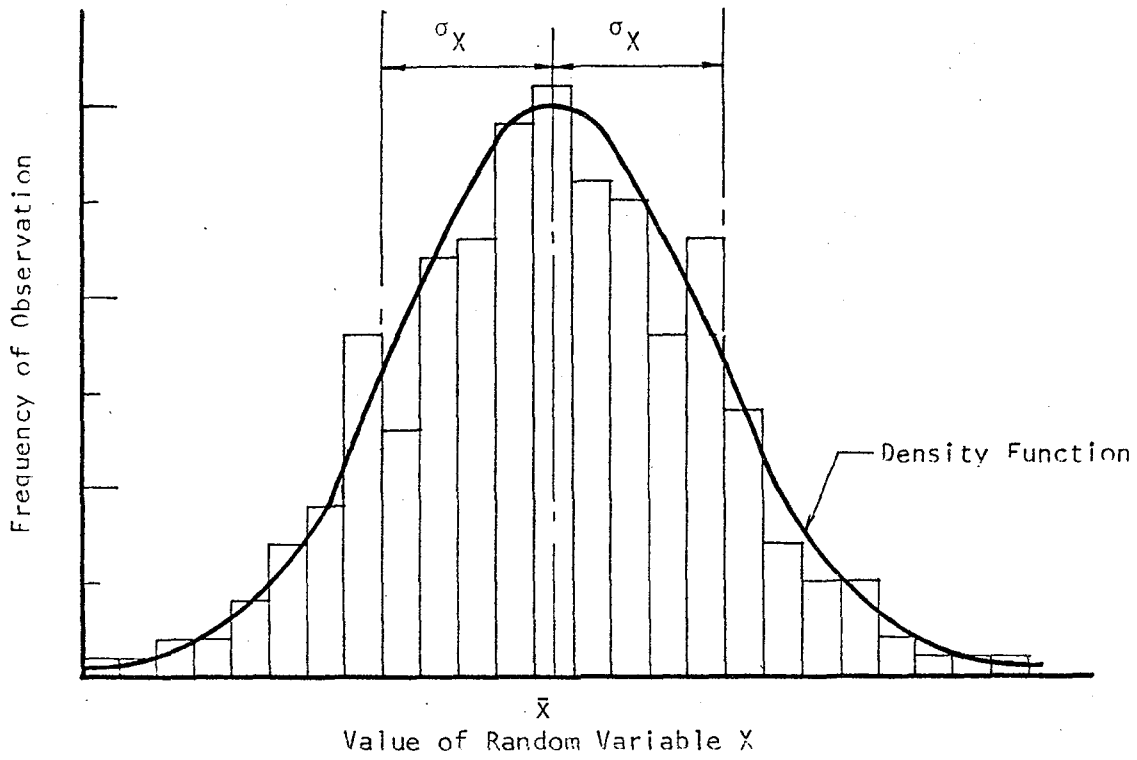

Fig. 3.1a A Typical Histogram or Frequency Diagram

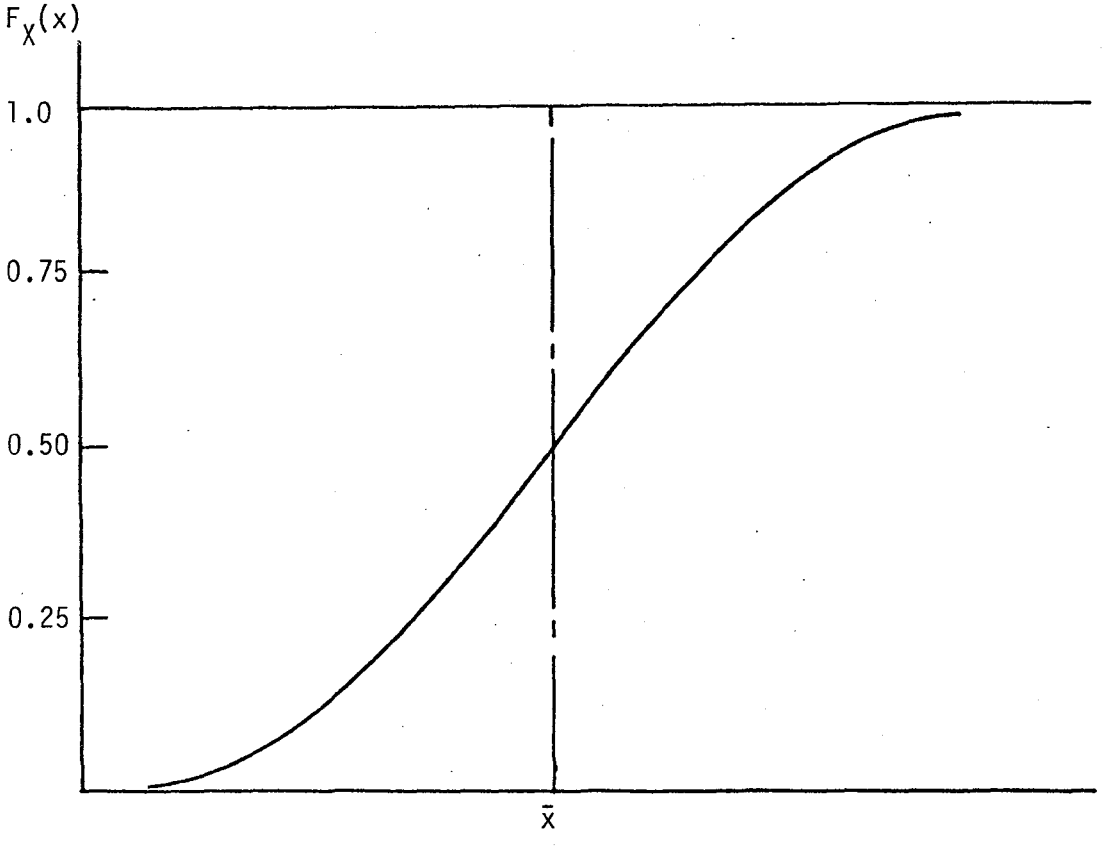

Fig. 3.1b A Typical Probability Function, $F_X(x)$

and the central moment of inertia of the density function. For most engineering problems, the absolute dispersion about the mean value may not be as important as the ratio of the degree of dispersion to the mean value. Hence, the coefficient of variation (COV) is often preferred. COV is the ratio of the standard deviation and the mean value.

If N number of observed values of a random variable X are available, then an estimate of the mean μ_X is the familiar average $\bar{x}$, i.e.

$$\mu_X \simeq \bar{x} = \frac{1}{N} \sum_{i=1}^{N} x_i \tag{3.1}$$

in which x_i's are the observed values of X. The corresponding variance, Var(X), standard deviation, σ_X, and COV, δ_X, can be estimated as

$$\text{Var}(X) = \frac{1}{(N-1)} \sum_{i=1}^{N} (x_i - \bar{x})^2 \tag{3.2}$$

$$\sigma_X = \sqrt{\text{Var}(X)} \tag{3.3}$$

and

$$\delta_X = \frac{\sigma_X}{\bar{x}} \tag{3.4}$$

When the density function of a random variable is available, the mean and variance of the random variable X can be estimated as

$$\mu_X = \int_{-\infty}^{\infty} x\, f_X(x)\, dx \tag{3.5}$$

and

$$\text{Var}(X) = \int_{-\infty}^{\infty} (x-\mu_x)^2\, f_X(x)\, dx \tag{3.6}$$

Different methods for estimating these parameters are available; among these are the method of moments and the method of maximum likelihood. These are also sometimes called the point estimators. It may be desirable to mention here that there are centain properties that are desirable in a point estimator. They are unbiasedness, consistency, efficiency and suffi-

ciency. In the method of moments, the parameters of the distribution are estimated from the mean and variance (and higher moments, if necessary) of the random variable. In some cases such as in the case of normal distribution, the moments, i.e., mean and variance, represent the parameters of the distribution. In the method of maximum likelihood the parameters of the distribution are estimated directly. The principle behind this method is as follows: for the given observations or simple values, x_1, x_2, ..., x_n, the estimated value of the parameter is the value most likely to produce these observed values. Unless it is specifically mentioned, the method of moments is used to estimate the parameters of a distribution in this study.

In general, to develop a probabilistic model the underlying distribution of a random variable as well as the statistics needs to be known. In practice the choice of the probability distribution may be dictated by mathematical convenience. In many cases, the functional form of the required probability distribution may not be easy to determine, or more than one distribution may fit the available data. Under certain circumstances, the basis or properties of the physical process may suggest the form of the required distribution. In some cases, the required probability distribution may be determined empirically based entirely on the available observed data.

More complete discussions of the descriptors of a random variable are available elsewhere (2, 60).

3.3 Estimation of Uncertainties

3.3.1 General Remarks

As discussed in Section 3.1, the uncertainties in τ_R and τ_A need to be analyzed and assessed in a systematic way. The estimation of uncertainties will depend on the source of information. The following sections describe the procedures for evaluating the uncertainties for some typical sources of information which will be used in subsequent chapters.

3.3.2 Single Random Variable

The uncertainty associated with a single random variable can be estimated with the help of a histogram or frequency diagram, density function, mean, variance, standard deviation, COV, etc. They are described in Section 3.2.

3.3.3 Function of Single Random Variable

In many geomechanics problems, the uncertainty associated with one random variable needs to be estimated indirectly from the information on uncertainty on another random variable. For example, X is a random variable and its density function representing the randomness is known. Y is another random variable whose uncertainty is of great concern in a particular problem. However, there is no direct information available on Y. But Y is functionally related to X as

$$Y = g(X) \tag{3.7}$$

Knowing the functional relationship g and the uncertainty associated with X, the uncertainty in Y in terms of density function can be shown to be

$$f_Y(y) = f_x(g^{-1}) \left| \frac{dg^{-1}}{dy} \right| \tag{3.8}$$

where g^{-1} represents $g^{-1}(y)$, the inverse function of g.

3.3.4 Function of Multiple Random Variables

Uncertainty analysis in this case is generally involved. The closed form analytical solution can be used only in some special cases. Three such cases which will have major engineering significance are (i) Sum and differences of independent normal variables, (ii) Products and quotients of independent lognormal random variables, and (iii) Sum of independent random variables with poisson distributions. The details of these cases will not be discussed here but can be found elsewhere (2, 28). However, it can be shown that the sum and differences of independent normal variables is normal, the products and quotients of independent lognormal variables is lognormal and the sum of independent poisson random variables is poisson.

3.3.5 General Approximate Method

The discussions made in Sections 3.3.3 and 3.3.4 are valid when the random variables X_i's are known in terms of statistics (mean, variance, etc.) as well as their distributions. In many geomechanical problems, however, the density function may not be known; information may be limited to the mean and variance of the original variate X_i. Furthermore, even when the density functions are known, the integrations indicated by Eq. 3.6 may be difficult to perform. Moreover, in the case of multiple random variables, the functional forms among variables could be something other than those described in Section 3.3.4. For these reasons, the approximate mean and variance of the function Y would be practically useful and may be obtained as follows. However, the density functions of Y may not be known. If Y is a function of several random variables, that is

$$Y = g(X_1, X_2, \ldots, X_n) \tag{3.9}$$

then expending the function $g(X_1, X_2, \ldots, X_n)$ in a Taylor series about the mean values $\mu_{X_1}, \mu_{X_2}, \ldots, \mu_{X_n}$, one would obtain

$$Y = g(\mu_{X_1}, \mu_{X_2}, \ldots, \mu_{X_n}) + \sum_{i=1}^{n} (X_i - \mu_{X_i}) \frac{\partial g}{\partial X_i} + \frac{1}{2} \sum_{i=1}^{n} \sum_{j=1}^{n} (X_i - \mu_{X_i})(X_j - \mu_{X_j}) \frac{\partial^2 g}{\partial X_i \partial X_j} + \ldots \tag{3.10}$$

where the derivatives are evaluated at the mean values of X_i's.

Truncating the series at the linear terms, the first-order approximate mean and variance of Y can be obtained as

$$E(Y) \simeq g(\mu_{X_1}, \mu_{X_2}, \ldots, \mu_{X_n}) \tag{3.11}$$

which indicates that the mean of the function is approximately equal to the function of the means; and

$$\mathrm{Var}(Y) \simeq \sum_{i=1}^{n} E_i^2 \, \mathrm{Var}(X_i) + \sum_{i}^{n} \sum_{\neq j}^{n} E_i \, E_j \, \mathrm{COV}(X_i, X_j) \tag{3.12}$$

where E_i and E_j are constants and are the values of the partial derivatives $\partial g/\partial X_i$ and $\partial g/\partial X_j$, respectively, evaluated at the mean values. If X_i and X_j are statistically independent, for all i and j, Eq. 3.12 reduces to

$$\mathrm{Var}(Y) \simeq \sum_{i=1}^{n} E_i^2 \, \mathrm{Var}(X_i) \tag{3.13}$$

The above approximate mean and variance may also be improved by including the higher-order terms of the Tyalor series expansion of $g(X_1, X_2, \ldots, X_n)$. If X_i and X_j are statistically independent, the second-order mean of Y would be

$$E(Y) \simeq g(\mu_{X_1}, \mu_{X_2}, \ldots, \mu_{X_n}) + \frac{1}{2} \sum_{i=1}^{n} \left(\frac{\partial^2 g}{\partial X_i^2}\right) \mathrm{Var}(X_i) \tag{3.14}$$

In many engineering problems, second-order mean and first-order variance would improve the accuracy of the estimation. Although the method is approximate, the method is very powerful and will be used in this study.

3.3.6 Reported Ranges

In many cases only the upper and lower bound of a random variable are known. In this case a probability density function may be prescribed, such as uniform or triangular, between the upper and lower bounds. The mean, variance and COV of the random variable can be estimated from the properties of the prescribed density function. Properties of these distributions are treated in more detail in Refs. 2 and 25.

3.4 Regression Analysis

When dealing with two or more variables, the functional relation between the variables is often of interest. However, if the variables are random, there will be no unique relationship between the variables. Thus, a probabilistic relationship between variables is necessary and can be developed using regression analysis techniques.

The functional relationship between the response or dependent variable and the regressor or independent variables can be developed using a scatter diagram (53). The unknown regression coefficients can be estimated by the method of least squares satisfying all the basic assumptions of regression analysis (2, 53). The basic assumptions can be summarized as:

1. The true relationship between the dependent and independent variables or their transformations is linear, or at least may be well

approximated by a straight line.

2. The error term ε has a zero mean. ε is a random variable representing the differences between the observed and the predicted values of the dependent variable.
3. The error term ε has a constant variance σ^2
4. The errors are uncorrelated, and
5. The errors are normally distributed.

Assumptions 4 and 5 imply that the errors are independent random variables. Standard summary statistics, in particular the r^2 and $\hat{\sigma}^2$ values, and residual analysis can be used to determine how well the regression model satisfies the aforementioned assumptions. This will be discussed briefly in the following sections.

3.4.1 r^2-Value - Coefficient of Determination

The total variability (S_x) in the observations of a dependent variable X in a regression analysis has two components: the amount of variability in the observations $\{X_i\}$ accounted for by the regression line (SS_R) and the residual variation left unexplained by the regression line (SS_E). The total variability of X can be written as:

$$S_X = SS_R + SS_E \tag{3.15}$$

SS_R, generally known as the regression sum of squares, can be calculated as

$$SS_R = \sum_{i=1}^{n} (\hat{X}_i - \bar{x})^2 \tag{3.16}$$

in which n is the total number of observations, $\hat{X}_i$ is the predicted value of X for a given set of independent variables obtained from the regression model and $\bar{x}$ is the mean value of X. SS_E, generally known as the error sum

of squares, can be estimated as

$$SS_E = \sum_{i=1}^{n} (x_i - \hat{x}_i)^2 \qquad (3.17)$$

in which x_i is the i-th observation. All other parameters were defined earlier.

The quantity r^2 is defined as

$$r^2 = \frac{SS_R}{S_X} = 1 - \frac{SS_E}{S_X} \qquad (3.18)$$

Since S_X is a measure of the variability in X without considering the effect of the regressor variable Y, and SS_E is a measure of the variability in X after Y has been considered, then the r^2-value refers to the proportion of variation in X explained by the independent variables. Thus, $0 \leq r^2 \leq 1$, and when r^2 is close to 1 it implies that most of the variability in X is explained by the regression model.

3.4.2 Mean Square Error $\hat{\sigma}^2$

The unbiased mean square error, which is also sometimes called the residual mean square, can be estimated as

$$\hat{\sigma}^2 = \frac{SS_E}{n-2} \qquad (3.19)$$

All the parameters have been described earlier. As can be seen from Eq. 3.17, when the error in the prediction is small, $\hat{\sigma}^2$ will be small. A smaller value of $\hat{\sigma}^2$ is always desirable.

3.4.3 Residual Analysis

The residual, e_i, in a regression analysis is usually defined as the observed value of the dependent variable minus the predicted value,

i.e.,

$$e_i = x_i - \hat{x}_i$$

Physically, the residual is a measure of the variability in X not accounted for by the regression model. Thus, any local deviations from the aforementioned assumptions will show up in the residuals (53).

Though several statistical techniques are available (53), residual plotting is probably the most informative in residual analysis. Partial residual plotting (PREP) can reveal non-linearities in the model if more than one regressor is used. Non-zero mean or non-constant variance of the error term e or correlated errors can be revealed by plotting the residuals versus the observed and predicted values of the dependent variable, and the residuals versus the values of the independent variables.

More thorough discussions of the aforementioned regression techniques as well as multiple regression, nonlinear regression and regression with non-constant variance techniques are widely available in the literature (2, 32, 53).

3.4.4 Computation of Mean and Variance of a Random Variable from its Conditional Mean and Conditional Variance

As discussed in Section 3.4, from the regression analysis the conditional mean and conditional variance of a dependent variable, say X, are obtained for a given value of an independent variable, say Y. The conditional mean and variance are denoted as $E(X|Y = y)$ and $Var(X|Y = y)$, respectively, To obtain the unconditional mean and variance of the dependent variable X, the probabilistic characteristics of the independent variable Y need to be considered. The unconditional mean, E(X), and

the unconditional variance, Var(X), can be shown to be (2);

$$E(X) = E_Y \left[E(X|Y)\right] \tag{3.21}$$

and

$$Var(X) = E_Y \left[Var(X|Y)\right] + Var_Y \left[E(X|Y)\right] \tag{3.22}$$

The subscript Y on E and Var emphasizes that the expectation and variance are with respect to Y. The first term in Eq. 3.22 represents the average scatter about the regression line, whereas the second term represents the uncertainty in the predicted mean value due to variability in Y. When Var(X|Y) is a constant, the first term of Eq. 3.22 may be estimated by Eq. 3.19. By using first-order approximation, the value of $Var_Y\left[E(X|Y)\right]$ can be estimated as

$$Var_Y \left[E(X|Y)\right] = Var(Y)\left\{\frac{\partial}{\partial Y} E(X|Y)\right\}_0^2 \tag{3.23}$$

in which $\left\{ \right\}_0$ denotes that the function is evaluated at the mean value.

3.5 Bases of Reliability Analysis

3.5.1 Extended Reliability Concept

Consider a random variable X. For the liquefaction problem X could represent τ_R or τ_A. In practice, the random variable X is assumed to have a predictive model $\hat{X}$. Errors may arise in the predictive model because of insufficient observed data on the random variable X, indirect observation of the values of X, or the use of a simplified predictive model. To compensate for the error in the predictive model $\hat{X}$, a corrective factor N can be introduced such that

$$X = N \hat{X} \tag{3.24}$$

in which $\hat{X}$ is a random variable with mean $\bar{X}$, standard deviation $\sigma_{\hat{X}}$, and COV $\delta_{\hat{X}}$, and N can be assumed as a random variable with mean $\bar{N}$, standard deviation σ_N, and COV Δ_X. The parameter $\delta_{\hat{X}}$ is a measure of the basic randomness of the data, as described in Section 3.3, and can be generally calculated from the observed data, or, in some cases, by using engineering judgement (81). On the other hand, Δ_X represents a measure of the prediction and modeling uncertainties in X, which mainly includes errors in the model mean $\bar{X}$. Applying first-order approximate analysis and using Eq. 3.24, the mean and overall uncertainty (measured by COV Ω) of X can be shown to be

$$\mu_X = \bar{N}\bar{X} \tag{3.25}$$

and

$$\Omega_X = \sqrt{\delta_X^2 + \Delta_X^2} \tag{3.26}$$

where N and X are assumed to be statistically independent.

Sometimes it may be convenient or necessary to assume that the corrective factor N is the product of several component factors. There will be a corrective factor N_i due to each factor. The overall corrective factor N_X, can be modeled in the following way:

$$N_X = \prod_{i=1}^{k} N_i \tag{3.27}$$

By using first-order approximation one gets

$$\bar{N}_X = \prod_{i=1}^{k} \bar{N}_i \tag{3.28}$$

and, assuming statistical independence between each corrective factor,

$$\Delta_X^2 = \sum_{i=1}^{k} \Delta_i^2 \tag{3.29}$$

where $\bar{N}_i$ and Δ_i are the mean and COV of the i^{th} corrective factor.

The random variable X can be a function of several other random variables. Using the concept of Eq. 3.24 and introducing a corrective factor N_f, the above statement can be expressed as

$$X = N_f \hat{f} (X_1, X_2, \ldots, X_n) \tag{3.30}$$

and

$$X_i = N_i \hat{X}_i \tag{3.31}$$

Expanding the function f in a Taylor series about the true means of $X_1, X_2, \ldots, X_n$, respectively, and truncating the series at the linear terms, the statistics of X can be approximated in the following way (81):

$$\mu_X = \bar{N}_f \hat{f} (\mu_1, \mu_2, \ldots, \mu_n) \tag{3.32}$$

and assuming N_f is uncorrelated with all other variables X and X_is are statistically independent,

$$\Omega_X^2 = \Omega_f^2 + \frac{1}{\mu_X^2}\left[\sum_{i=1}^{n} \left(\frac{\partial f}{\partial X_i}\right)_o^2 \sigma_i^2\right] \tag{3.33}$$

where $(\ )_o$ denotes that the expression is evaluated at the mean values of the variables and $\sigma_i = \Omega_i \mu_i = \Omega_i \bar{N}_i \bar{X}_i$.

The probabilistic modeling techniques presented in the previous sections may now be applied to the liquefaction problem. In the next section the predictive model of τ_A and τ_R will be developed for a point in a soil deposit. A later section will extend these "point" predictors to include the effects of local random fluctuations of the soil parameters in a volume of the deposit. Major parts of Chapter 4 and 5 will be devoted to systematic assessment of the uncertainties of all the parameters in the predictive models of τ_R and τ_A. These uncertainties will be combined using

extended reliability concepts presented in Section 3.5, into a probabilistic model for evaluation of liquefaction potential.

3.6 Predictive Model for τ_R and τ_A

Seed and Idriss (72) suggested a simplified deterministic procedure to evaluate the liquefaction potential of a site. As discussed in Chapter 2, it has some advantages as well as some shortcomings. Keeping its basic simplicity, this method will be extended here in a probabilistic sense. A brief review of the modified Seed and Idriss method developed in this study is presented in the following section.

3.6.1 Liquefaction Model

Consider a soil column as shown in Fig. 3.2. If the soil column is assumed to behave as a rigid body and the design maximum acceleration is assumed to be a_{max}, the maximum shear stress on the soil element can be expressed as

$$(\tau_{max})_{Rigid} = \frac{\gamma_s h}{g} a_{max} \tag{3.34}$$

in which γ_s is the saturated unit weight of the soil and g is the acceleration due to gravity. As the soil column deforms it will experience a shear stress less than $(\tau_{max})_{Rigid}$. This reduced stress τ_{max} can be given by

$$\tau_{max} = r_d \frac{\gamma_s h}{g} a_{max} \tag{3.35}$$

in which r_d is a stress reduction factor. The acceleration-time history of an actual earthquake is very irregular. An equivalent uniform acceleration of intensity S_L, which will be determined in Chapter 5, can be

introduced. Thus, the equivalent uniform shear stress, τ_A, can be written as

$$\tau_A = S_L \, r_d \, \frac{\gamma_s h}{g} \, a_{max} \tag{3.36}$$

τ_A as calculated by Eq. 3.36 will act on the soil element for a number of significant stress cycles, N_{eq}. The value of N_{eq} depends on the duration of ground shaking, and thus on the magnitude of the earthquake. The relationship of N_{eq} and earthquake magnitude will be discussed in more detail in Chapter 5.

The shear resistance of the soil element, τ_R, that will be mobilized to resist the applied shear stress can be evaluated from properly conducted laboratory test results as will be discussed in Chapter 4. To model the shear resistance effectively, a shear strength parameter, R, can be introduced such that

$$R = \frac{\tau_R}{\sigma_m' D_r} \tag{3.37}$$

in which σ_m' is the average effective normal stress and D_r is the relative density. The parameter R was introduced by Haldar (25, 29). σ_m' can be estimated as

$$\sigma_m' = \frac{\sigma_1' + \sigma_2' + \sigma_3'}{3} \tag{3.38}$$

in which σ_1', σ_2', and σ_3' are the effective stresses in three directions at a point in the deposit. Eq. 3.38 can be simplified as

$$\sigma_m' = \frac{1 + 2 K_o}{3} \, \sigma_v' \tag{3.39}$$

in which K_o is the coefficient of earth pressure at rest and σ_v' is the effective vertical stress at a point. The in situ value for R can be inferred from laboratory test results if the value for R measured in the

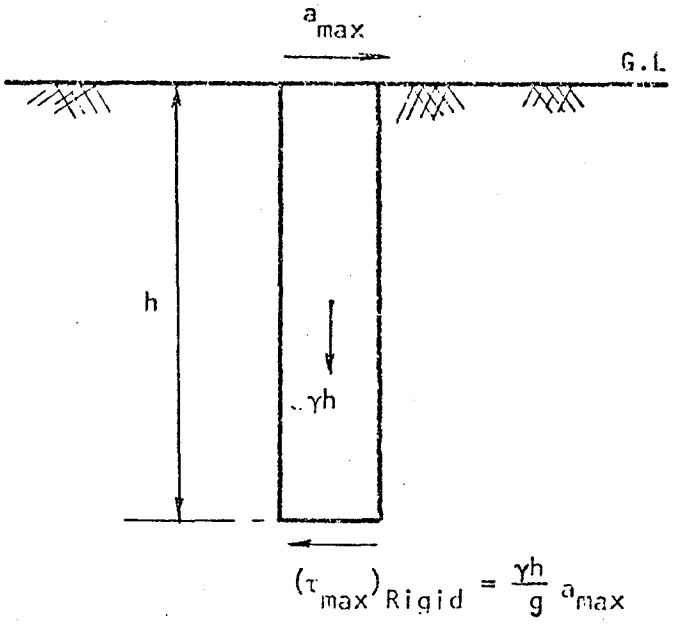

Fig. 3.2 Shear Stress Developed Due to Earthquake Acceleration

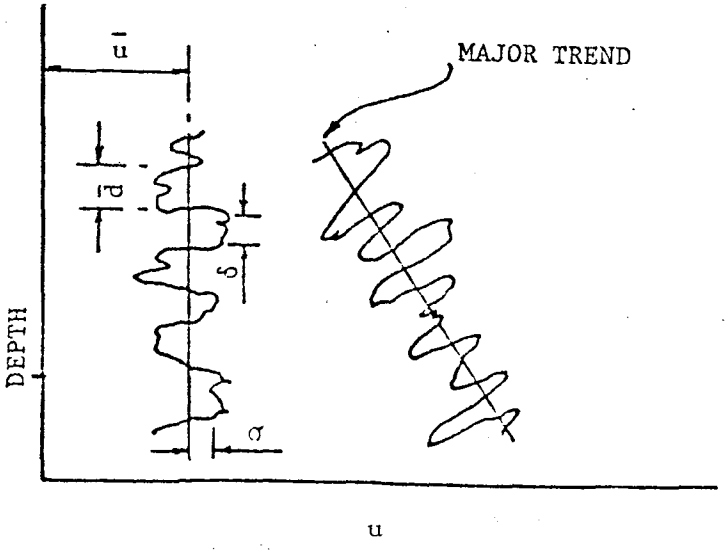

Fig. 3.3 Main Descriptors of the Local Random Fluctuations of the Soil Property, u

laboratory is modified by a corrective factor, C_r, i.e.

$$R_{field} = C_r \cdot R_{Lab} \tag{3.40}$$

Replacing R_{field} by Eq. 3.37, the in situ shear resistance, τ_R, at a particular point in a deposit can be estimated from laboratory test results by the following expression:

$$\tau_R = C_r \, R_{Lab} \, \sigma'_m \, D_r \tag{3.41}$$

σ'_m and D_r values need to be estimated in the in situ conditions. Liquefaction will occur when τ_A is greater than τ_R.

3.6.2 Probabilistic Liquefaction Model

To develop a probabilistic model, the probabilistic characteristics of all the parameters in Eqs. 3.36 and 3.41 need to be evaluated. This will be discussed in detail in Chapters 4 and 5. Assuming that the mean value and COV of each paramter are known, the following statistics of τ_A can be obtained assuming statistical independence between parameters in Eq. 3.36

$$\mu_{\tau_A} = S_L \; \mu_{r_d} \; \mu_{\gamma s} \cdot h \; \frac{\mu_{a_{max}}}{g} \tag{3.42}$$

$$\Omega^2_{\tau_A} = \Omega^2_{r_d} + \Omega^2_{\gamma_S} + \Omega^2_{a_{max}} \tag{3.43}$$

The values of g, S_L and h are assumed to be known.

Because of the various simplifying assumptions and empirical approximations, the model represented by Eq. 3.41 is only an estimate of the in situ shear resistance of the soil mass. A corrective factor, N_{τ_R}, can be introduced such that

$$\tau_R = N_{\tau_R} \, \hat{\tau}_R \tag{3.44}$$

where $\hat{\tau}_R$ is the predictive model of τ_R defined by Eq. 3.41. Using first-order approximate analysis, the mean and COV of τ_R become

$$\mu_{\tau_R} = \mu_{N_{\tau_R}} \cdot \mu_{C_r} \cdot \mu_R \cdot \mu_{\sigma'_m} \cdot \mu_{D_r} \tag{3.45}$$

and

$$\Omega^2_{\tau_R} = \Omega^2_{N_{\tau_R}} + \Omega^2_{C_r} + \Omega^2_R + \Omega^2_{\sigma'_m} + \Omega^2_{D_r} \tag{3.46}$$

assuming N_{τ_R}, C_r, R, σ'_m and D_r are uncorrelated random variable.

Since τ_A and τ_R are individually random variables, the event $\{\tau_R \leq \tau_A\}$ is uncertain. Hence, the risk of liquefaction failure can be defined by the probability

$$p_f = p(\tau_R \leq \tau_A) \tag{3.47}$$

or

$$p_f = \int_0^\infty \int_0^{t_A} f_{\tau_R, \tau_A}(t_R, t_A)\, dt_R\, dt_A \tag{3.48}$$

where $f_{\tau_R, \tau_A}(t_R, t_A)$ is the joint density function of τ_R and τ_A. Haldar (25) noted that τ_R and τ_A can be considered as statistically independent random variables for all practical purposes. Thus, Eq. 3.48 reduces to

$$p_f = \int_0^\infty \int_0^{t_A} f_{\tau_R}(t_R)\, f_{\tau_A}(t_A)\, dt_R\, dt_A \tag{3.49}$$

As discussed in Section 3.2, there is usually not enough data available in practice to justify or ascertain a particular density function. However, reliability analysis is useful in a comparative rather than in an absolute sense. Hence, a prescribed density function for Eq. 3.49 would provide a consistent relative measure of risk. For the present reliability analysis, the primary objective is the systematic assessment of uncertainties associated with the liquefaction phenomenon and the development of a

consistent basis by which design alternatives can be compared.

In this study, for the sake of simplicity lognormal, distributions are prescribed for τ_A and τ_R in estimating the probability of liquefaction. Therefore, it can be shown that for lognormal variates, Eq. 3.49 reduces to

$$p_f = 1 - \Phi\left(\frac{\ln\left[\frac{\mu_{\tau_R}}{\mu_{\tau_A}}\sqrt{\frac{1+\Omega_{\tau_A}^2}{1+\Omega_{\tau_R}^2}}\right]}{\sqrt{\ln\left[(1+\Omega_{\tau_R}^2)\ (1+\Omega_{\tau_A}^2)\right]}}\right) \tag{3.50}$$

where $\Phi(\ )$ is the standard normal cumulative distribution function.

It can be seen from Eq. 3.50 that the risk depends not only on the ratio of μ_{τ_R} to μ_{τ_A}, but also on the uncertainties in τ_R and τ_A, an aspect of the problem completely neglected by a deterministic approach.

3.7 Three-Dimensional Modeling of Soil Parameters

3.7.1 General Remarks

Using the method outlined in the previous section, the risk of liquefaction at a point in the soil deposit can be evaluated. In practice, the liquefaction potential is evaluated at the weakest point in the deposit. However, soil deposits typically exhibit local variations about their average properties or about major trends (horizontally and vertically). Thus, the so-called "weakest point" in the deposit may be misleading as far as the liquefaction of the deposit is concerned. Moreover, a sufficient volume of sand has to undergo a considerable amount of strain in order to produce a noticeable amount of damage at the referenced location. Thus, evaluation of the risk of liquefaction at just a point in the soil deposit may not be appropriate. The local random fluctuations in the soil

properties affecting the liquefaction potential in the liquifiable volume must be considered. These random fluctuations of the soil properties can be incorporated into the point reliability model developed in Section 3.6.2 if appropriate modifications are made.

3.7.2 Main Descriptors of Local Random Fluctuation

Consider a soil property given by the random variable u(z). For the liquefaction problem the soil property could be the relative density of the deposit. The local variations of u(z) can be expressed with the help of two parameters as shown in Fig. 3.3. It can be expressed as the point standard deviation σ_u of the soil properties and the scale of fluctuation θ_u, which measures the distance within which the soil property u(z) shows relatively strong correlation of persistence from point to point. The quantity θ_u is closely related to the average distance between intersections (crossings) of u(z) and $\bar{u}$: small values of θ_u imply rapid fluctuations about the average, while large values of θ_u suggest that a slowly varying component is superimposed on the average value $\bar{u}$.

The scale of fluctuation, θ_u, can also provide a host of practical information; for example, to avoid wasteful redundancy in information gathering, sampling distances should be chosen in such a way that they are large in comparison with θ_u. On the other hand, when a soil property is being determined by two different tests, the locations of pairs of samples should be well within the correlation distance for maximum effectiveness.

The scale of fluctuation θ_u can be estimated in two ways. A procedure is described by Vanmarcke (87) when observations of soil properties are available at equidistant intervals. This approach uses the concept of coefficient of correlation between values of u at two points. When points

are located at very small intervals, the coefficient of correlation will be close to 1, and it usually decays as the distance increases. For an assumed theoretical correlation function model, the scale of fluctuation θ_u can be estimated. The other method can be used to estimate θ_u if a reasonably complete record of u(z) is available. It is based on the approximate relationship between the scale of fluctuation, θ_u, and the average distance, $\bar{d}$, between the intersections of the fluctuating property, u(z), and its mean $\bar{u}$. The average distance between mean crossings is approximately (87)

$$\bar{d} \simeq \sqrt{\frac{\pi}{2}}\,\theta_u \simeq 1.25\,\theta_u \qquad (3.51)$$

The details of these two methods will not be discussed here but can be found elsewhere (86, 87, 88, 89). For this initial phase of study, the scale of fluctuation for a parameter, such as the relative density, will be considered known. In the second phase, the scale of fluctuation for different sand deposits will be evaluated using field observations. A deposit could have three different scales of fluctuation in the three different directions. In this study, the scales of fluctuation will be used to estimate the statistics of spatially averaged soil properties.

3.7.3 Spatially Averaged Soil Properties

Consider a site being investigated for liquefaction potential. It is very likely that a very loose pocket of sand is located during the subsurface investigation. It is known that to cause noticeable damage to a structure located on the site, a sufficient volume of sand needs to liquefy. The evaluation of the site considering the loose pocket of sand

is thus obviously incomplete. Some sort of spatially averaged soil properties in the critical soil volume needs to be used for this purpose.

Consider a statistically homogeneous soil parameter, say relative density, for the liquefaction problem. The value of the soil parameter at a location x, y, and z from a referenced origin can be represented as u(x, y, z). The spatial average of the soil parameter u(x, y, z) over a volume Δv, $u_{\Delta v}$, can be estimated as

$$u_{\Delta v} = \frac{1}{\Delta v} \int_{\Delta x} \int_{\Delta y} \int_{\Delta z} u(x, y, z)\, dxdydz \tag{3.52}$$

in which $\Delta v = \Delta x \cdot \Delta y \cdot \Delta z$ and Δx, Δy, and Δz are the length of the soil volume in the x, y, and z directions, respectively. For a statistically homogeneous soil deposit the point mean $\bar{u}$ and variance Var(u) can be estimated by using Eqs. 3.1 and 3.2, respectively, from the field observation. The spatial mean, $\bar{u}_{\Delta v}$, and the spatial variance, $Var(u_{\Delta v})$, can be shown to be

$$\bar{u}_{\Delta v} = \bar{u} \tag{3.53}$$

and

$$Var(u_{\Delta v}) = \Gamma_u^2 (\Delta v)\, Var(u) \tag{3.54}$$

in which $\Gamma_u^2 (\Delta v)$ is called the variance function. It describes the decay of the variance of the spatial average as the averaging dimensions increase. If the correlation structure of u(x, y, x) is separable, then Eq. 3.54 reduces to

$$Var(u_{\Delta v}) = \Gamma_u^2 (\Delta x)\, \Gamma_u^2 (\Delta y)\, \Gamma_u^2 (\Delta z)\, Var(u) \tag{3.55}$$

in which $\Gamma_u^2(\Delta x)$, $\Gamma_u^2 (\Delta y)$, and $\Gamma_u^2 (\Delta z)$ are the variance functions in the X, Y, and Z directions, respectively.

The variance function can be calculated from the information on the

scale of fluctuation in a given direction. For all practical purposes, the variance function in the X direction can be estimated as (86, 89):

$$\left.\begin{aligned}\Gamma_u^2(\Delta x) &= 1.0;\ \Delta x \le \Theta_{u_x} \\ &= \frac{\Theta_{u_x}}{\Delta x};\ \Delta x > \Theta_{u_x}\end{aligned}\right] \tag{3.56}$$

in which Θ_{u_x} is the scale of fluctuation of u in the X direction. The variance functions in the other two directions can similarly be estimated from the knowledge of the corresponding scale of fluctuation.

3.7.4 Probabilistic Three-Dimensional Liquefaction Model

Using the three-dimensional soil modeling techniques described in Section 3.7.3, the point liquefaction potential evaluation model presented in Section 3.6.2 can be modified.

The predictive model of τ_A is given by Eq. 3.36. Though a_{max} and r_d are random variables, their spatial variability can be considered negligible. Directly, the spatial variability of γ_s will not be considered here; however, it will be considered directly when the spatial variability of the relative density is considered. Thus, for a liquifiable volume of V, the spatial mean and COV of τ_A can still be estimated from Eqs. 3.42 and 3.43, respectively.

Similarly, for a statistically homogeneous soil deposit, the spatial mean of τ_R can be calculated from Eq. 3.45. It is assumed that the spatial variability of the parameters N_{τ_R}, C_r, R, and σ'_m is small relative to D_r; hence, the spatial variance of τ_R over the volume V becomes

$$\mathrm{Var}(\tau_{R_v}) = \mu^2_{\tau_R} \left[\Omega^2_{N_{\tau_R}} + \Omega^2_{C_r} + \Omega^2_R + \Omega^2_{\sigma'_m} + \Gamma^2_{D_{r_x}}(\Delta x) \cdot \Gamma^2_{D_{r_y}}(\Delta y) \cdot \Gamma^2_{D_{r_z}}(\Delta z) \cdot \Omega^2_{D_r} \right] \tag{3.57}$$

Knowing the scales of fluctuation of D_r in the X, Y, and Z directions, Eq. 3.57 can be evaluated. It must be pointed out here that spatial variability of all the parameters can be considered similarly if the corresponding information on the scale of fluctuation is available.

Eqs. 3.42, 3.43, 3.45, and 3.57 can be used to establish the probabilistic characteristics of τ_A and τ_R in three dimensions. With this information, the risk of liquefaction can be evaluated for a given soil volume using the concept developed in Section 3.6.2.

Chapter 4

UNCERTAINTY OF RESISTANCE PARAMETERS

4.1 General Remarks

According to the probabilistic liquefaction model outlined in Chapter 3, the in situ shear resistance at a particular point of the soil deposit needs to be evaluated. All the parameters in the in situ shear resistance model have also been identified in Chapter 3. However, all these parameters are random variables. The major sources of uncertainties affecting these parameters are evaluated in this chapter.

4.2 Density Model

4.2.1 Relative Density

The looseness or denseness of a sand deposit is an important parameter in a liquefaction potential evaluation study. Among all the alternatives available to model looseness or denseness, namely, density, relative density, void-ratio, degree of compaction, etc., the relative density is most commonly used in a liquefaction study. In fact, it is used widely as a major description of the characteristics of cohesionless soils. Significant error can be incurred with the present methods for determining in situ relative density (30) and warrants a detailed discussion here.

The American Society for Testing and Materials suggested guidelines (ASTM D 2049-69) defining the relative density, D_r, as

$$D_r = \frac{\gamma_{max}}{\gamma} \frac{\gamma - \gamma_{min}}{\gamma_{max} - \gamma_{min}} \tag{4.1}$$

in which γ_{max}, γ_{min}, and γ are the maximum, minimum, and inplace dry density, respectively, of a cohensionless depsoit.

The basic drawback of this definition is that it is computed from the ratio of small differences between large numbers. This implies that small variations in the densities could lead to large errors in the computed relative density (29, 30). Despite its drawbacks, and since a better measure of sand denseness has not yet become available, the relative density can still be used as a measure of denseness of sand. However, the assoicated uncertainties need to be considered appropriately.

In situ relative density can be estimated in two ways: (1) Direct method and (2) indirect method. These are described in the following sections.

4.2.2 Direct Estimation of Relative Density

In the direct method, D_r is estimated explicitly using Eq. 4.1. Haldar and Tang (30) showed the mean and coefficient of variation (COV) of D_r to be

$$\bar{D}_r \cong \frac{\bar{\gamma}_{max}}{\bar{\gamma}} \frac{\bar{\gamma} - \bar{\gamma}_{min}}{\bar{\gamma}_{max} - \bar{\gamma}_{min}} \tag{4.2}$$

$$\text{and } \Omega^2_{D_r} \cong E_1^2 \Omega^2_{\gamma_{max}} + \left[\frac{(E_1 + 1)(1 - \bar{D}_r)}{\bar{D}_r}\right]^2 \cdot \Omega^2_{\gamma_{min}} + \left[\frac{E_1 + 1}{\bar{D}_r} - 1\right]^2 \cdot \Omega^2_{\gamma}$$

$$= E_1^2 \Omega^2_{\gamma_{max}} + E_2^2 \Omega^2_{\gamma_{min}} + E_3^2 \Omega^2_{\gamma} \tag{4.3}$$

where $E_1 = \bar{\gamma}_{min}/(\bar{\gamma}_{max} - \bar{\gamma}_{min})$; and γ, γ_{max}, and γ_{min} are assumed to be mutually independent. The coefficients E_1, E_2, and E_3 could be interpreted as the amplification factors for the unceratinties in each of these densities, respectively. The uncertainty in γ is amplified more than

that in γ_{max} or γ_{min}. These densities are generally evaluated with the ASTM D 2049-69 method. Travenas, et al. (82) estimated that the COV of γ_{min} and γ_{max} are 0.018 and 0.023, respectively, based on 62 tests. Moreover, they suggested that the intralaboratory (reproducibility) error is approximately one-third of the interlaboraotry error. Thus, the combined uncertainty, $\Omega_{\gamma_{min}}$ and $\Omega_{\gamma_{max}}$, may be estimated as 0.019 and 0.025, respectively.

The uncertainties associated with the existing procedures for estimating the in situ density of sands under the water table were discussed in great detail by Haldar (25) and Haldar and Tang (30). It was noted that the in situ density generally cannot be estimated within $\pm$ 2 pcf with present techniques.

Considering all the aforementioned uncertainties, Haldar and Tang (30) observed that the uncertainties in D_r in terms of COV could be of the order of 0.11 to 0.36. This uncertainty is not negligible.

In many practical cases, information on in situ γ values may not be available, at least in the initial stage of the project. In this sense, the relative density can not be estimated using the direct method. Thus, a reliable indirect method to estimate the relative density is a necessity from a practical point of view.

4.2.3 Indirect Estimation of Relative Density

The standard penetration test, which will be designated as SPT hereafter, is intended to measure the degree of compactness of the in situ soil. Since relative density also measures the same soil property, some correlation between SPT-values and D_r values may exist. The SPT-values

have been used to estimate in situ relative density of a cohensionless soil deposit since 1948, when Terzaghi and Peck (105) proposed an approximate relationship between the two. ASTM D 1586-67 designates the standard penetration resistance, N, as the number of blows required to drive a split-barrel sampler the last 12 in. of an 18 in drive by a 140 lb hammer falling 30 in. (4). Due to the very nature of the testing procedures and field environment, the SPT-value obtained from the field may be erroneous (13, 25). The guideline ASTM D 1586 may be incomplete in that sense, and contribute significantly to the uncertainties in SPT-values. For example, the guideline does not clearly state how to obtain a freefall of the hammer. The freefall of the hammer can be obtained by a trip hammer mechanism or by the rope and cathead device. The impact energies of the two devices are quite different. Moreover, it has been observed in laboratory tests that when the rope and cathead device is used, the impact energy can vary a great deal with the number of turns the rope makes around the cathead, the speed of the cathead and even the age of the rope (70). Moreover, the relability of the test is further reduced when drill rods of different size and weight, different sized samplers and different drilling procedures are used. Nevertheless, the indirect determination of relative density by measuring SPT-values was attempted in both laboratory and field investigations (5, 24, 50, 51, 55, 67, 84, 90, 92, 100).

Several relationships between the relative density and SPT-values have been proposed and summarized by Haldar (25). The most commonly used relationships are Gibbs and Holtz's equation (24), Bazaraa's equations (100), and Waterways Experiment Station (WES) equation (50, 51).

The relationship proposed by Gibbs and Holtz has been widely used by engineers for both dry and saturated sand. The results reported by Gibbs and Holtz can be approximately represented by the following equation for normally consolidated soil:

$$N = 20\ D_r^{2.5} + 10\ D_r^{2}\ \sigma_v' \qquad (4.4)$$

where N is the SPT-value in blows/ft, D_r is the relative density, and σ_v' is the effective overburden pressure in Kips/ft^2.

Bazaraa (100) collected approximately 1300 SPT-values for dry cohensionless soils at 25 different sites. Observing the trend of SPT-values with D_r and σ_v', Bazaraa proposed the following equations:

$$N = 20\ D_r^{2} + 40\ D_r^{2}\ \sigma_v';\ \sigma_v' \leq 1.5 \text{ Kips/ft}^2 \qquad (4.5)$$

and

$$N = 65\ D_r^{2} + 10\ D_r^{2}\ \sigma_v';\ \sigma_v' > 1.5 \text{ Kips/ft}^2 \qquad (4.6)$$

All the parameters were defined earlier.

WES equation is based on very carefully controlled laboratory tests of submerged sands conducted by Marcuson and Bieganousky (50, 51) at the U. S. Army Engineer Waterways Experiment Station. The equation can be represented as

$$D_r = 11.7 + 0.76 \left[\left| 222(N) + 1600 - 53(\bar{\sigma}_v) - 50(C_u)^2 \right| \right]^{1/2} \qquad (4.7)$$

where $\bar{\sigma}_v$ is the effective vertical stress in lb/in^2, C_u is the uniformity coefficient, and D_r is the relative density.

The aforementioned three relationships are shown in Figure 4.1. Gibbs and Holtz's equation seems to overestimate (unconservatively) the in situ relative density (13, 30). Probable reasons for this systematic bias have

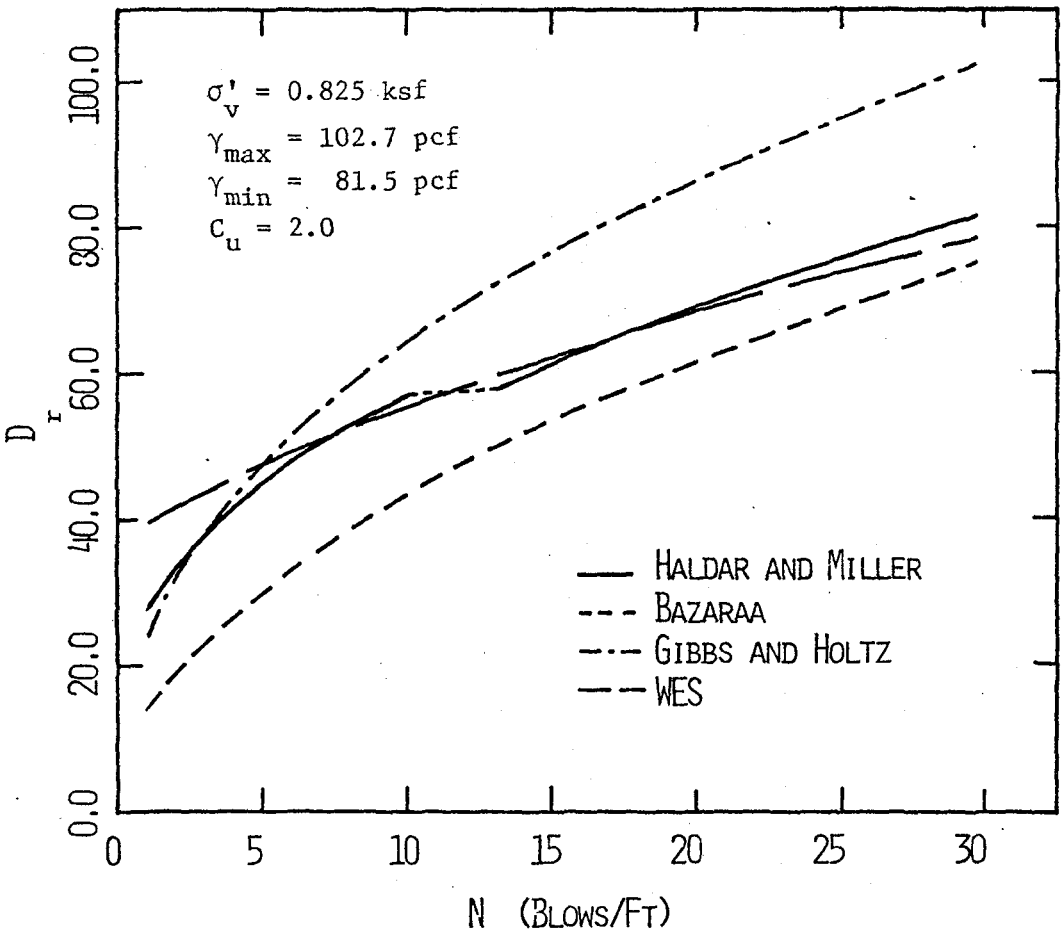

FIGURE 4.1 COMPARISON OF D_r - N RELATIONSHIPS

been discussed in detail by Haldar and Tang (30). Bazaraa's relationship is totally based on intuition. The data set he considered did not have any information on the in situ relative density and thus his relationship might not be reliable. WES equation is based on reliable information. However, it is based on nonstandard procedures (freefall of the hammer was obtained by trip hammer mechanism). Moreover, it will only predict D_r under laboratory conditions. It has never been calibrated to predict in situ relative density. From the above discussion, it is clear that a more complete relationship to predict the in situ relative density is needed.

4.2.4 A Proposed Model For Indirect Estimation of Relative Density

The proposed model is developed in two stages. First a laboratory relationship is proposed, and then it is calibrated using field data to predict the in situ relative density.

4.2.4.1 Indirect Estimation of Relative Density in the Laboratory

Indirect estimation of the relative density is traditionally made from the N and D_r relationship, as discussed in Section 4.2.3. It was also mentioned earlier that D_r is an error-prone parameter. Considerable error is expected in the estimation of in situ γ values. Thus, the predictability of the N and D_r relationship may not be very good. However, if a relationship between N and γ can be developed, the predictability of this relationship is expected to be much higher than that of the N and D_r relationship. The reliable estimate of γ thus obtained will improve the accuracy of the D_r values. The N-γ relationship will be meaningful

only if the information on γ_{max} and γ_{min} is incorporated in the proposed equation. Information on γ_{max} and γ_{min} can be obtained from the undisturbed samples collected from the site. In the following paragraphs, a relationship among N, γ, γ_{max}, γ_{min}, and σ'_v is developed using laboratory test results.

After an extensive literature search, three sources (24, 50, 51) of laboratory test results are obtained where all the aforementioned parameters are identified. The laboratory test results reported by Marcuson and Bieganousky (50, 51) are very recent and are expected to be more reliable than those reported by Gibbs and Holtz (24). The test conditions are significantly different between the United States Bureau of Reclamation (USBR) (24) and the Waterways Experiment Station (WES) (50, 51) studies. The major differences are identified in Table 4.1. It is quite obvious that the test results from these studies should not be combined for any statistical analysis. The proposed laboratory model is developed considering only the WES test results.

Four different sands were used in the WES study. These were Reid-Bedford Model sand (RBMS), Ottawa sand (OS), Platte River sand (PRS), and Standard Concrete sand (SCS). The limiting densities and grain size characteristics of these sands are given in Table 4.2. Tests were conducted under the effective overburden pressure σ'_v of 10 psi, 40 psi, and 80 psi. Cases where σ'_v = 80 psi may not be appropriate for a liquefaction study. They are not considered in this study.

The four different sands considered are quite different. Moreover, for RBMS, OS, PRS and SCS, 68, 8, 14, and 14 tests, respectively, were conducted. It may not be desirable to combine all the test results for

Table 4.1 Comparison of USBR and WES SPT Studies (from Ref. 51)

	Bureau of Reclamation Tests	WES Tests
1.	Applied overburden pressure by means of rigid plates and springs	Applied overburden pressure with flexible, fiberglass-reinforced rubber water bag
2.	Soil container was a solid wall tank, 3 ft. 1-1/2 in. in diameter, with sidewall friction present*	Soil container was a layered system of alternating steel and rubber rings to provide flexibility in the vertical direction to avoid sidewall friction
3.	Cathead with an unstated number of turns was used	Trip hammer was used
4.	Penetration tests were made through six holes in the loading plate	Penetration tests were made through a maximum of four holes
5.	Sand placement was by lifts compacted with a mechanical tamper	Various sand placement techniques during the first series. Compaction by vibrator during the second series
6.	Testing performed on submerged and dry specimens; recommendations were developed from the dry sand results	Testing performed on submerged specimens
7.	Rod lengths of 0, 32, and 65 ft. were studied	Rod lengths were limited. The minimum length was 5 ft. and the maximum length was 11 ft.
8.	A, B, and N rods were incorporated in the study	N rods were used exclusively

*Earth pressure cells were used to obtain intergranular vertical stress.

Table 4.2 Limiting Density and Grain Size Data For Sands in WES SPT Study

Sand	Limiting Densities (pcf)		Grain Size Data (mm)		
	γ_{max}	γ_{min}	D_{10}	D_{50}	D_{60}
RBMS	107.1	88.7	0.16	0.25	0.26
OS	109.1	93.0	0.15	0.21	0.22
PRS	122.7	102.8	0.47	2.10	2.50
SCS	120.6	103.7	0.28	0.50	0.60

Table 4.3 Regression Models Between $N^{1/2}$ and γ for RBMS

$E(N^{1/2} \mid \Gamma = \gamma) = a_o + a_1\gamma$				
σ'_v (ksf)	Regression Coefficients		Model Statistics	
	a_o	a_1	r^2	$\hat{\sigma}$
1.44	-30.559	0.3435	0.923	0.404
5.76	-30.066	0.3484	0.821	0.423

all four sands for statistical analysis. Since RBMS has the maximum number of test results, it is considered first to develop a relationship between N and γ. Other parameters are added to this basic equation whenever possible by considering other sands.

N and γ values are plotted for RBMS for σ'_v = 10 psi (1.44 ksf) and σ'_v = 40 psi (5.76 ksf) in Figs. 4.2 and 4.3, respectively. Observing the trend in Figs. 4.2 and 4.3, the following regression model is proposed.

$$E(N^{\lambda} | \Gamma = \gamma) = a_o + a_1 \gamma \qquad (4.8)$$

where Γ is a random variable which takes on values of γ, and λ, a_o, and a_1 are regression coefficients. The above form of the regression equation is selected to facilitate the use of the Box-Cox (101) transformation technique to obtain the most desirable regression equation. The objective is to find a value for λ, for which the mean square error, $\hat{\sigma}^2$, will be minimum. When $\lambda = 0$, it suggests that the best transformation of N should be Ln(N).

$\hat{\sigma}^2$ versus λ values for σ'_v = 5.76 ksf are plotted in Fig. 4.4. It can be seen from Fig. 4.4 that any value of λ between 0 and 0.5 would give the minimum $\hat{\sigma}^2$ value, since $\hat{\sigma}^2$ value is almost constant in this range. For this study λ is assumed to be 0.5.

$N^{1/2}$ and γ values are again plotted for σ'_v = 1.44 ksf and σ'_v = 5.76 ksf in Figs. 4.5 and 4.6, respectively. A definite improvement can be seen, since the data nearly plots as a straight line. The resulting regression coefficients, $\hat{\sigma}$, and r^2 values are given in Table 4.3 for the two cases.

Figs. 4.5 and 4.6 clearly demonstrate that the effect of effective overburden pressure, σ'_v, needs to be considered in the regression model. This effect can be accounted for by introducing a term, $a_2 \cdot \sigma'_v$, or a mixed

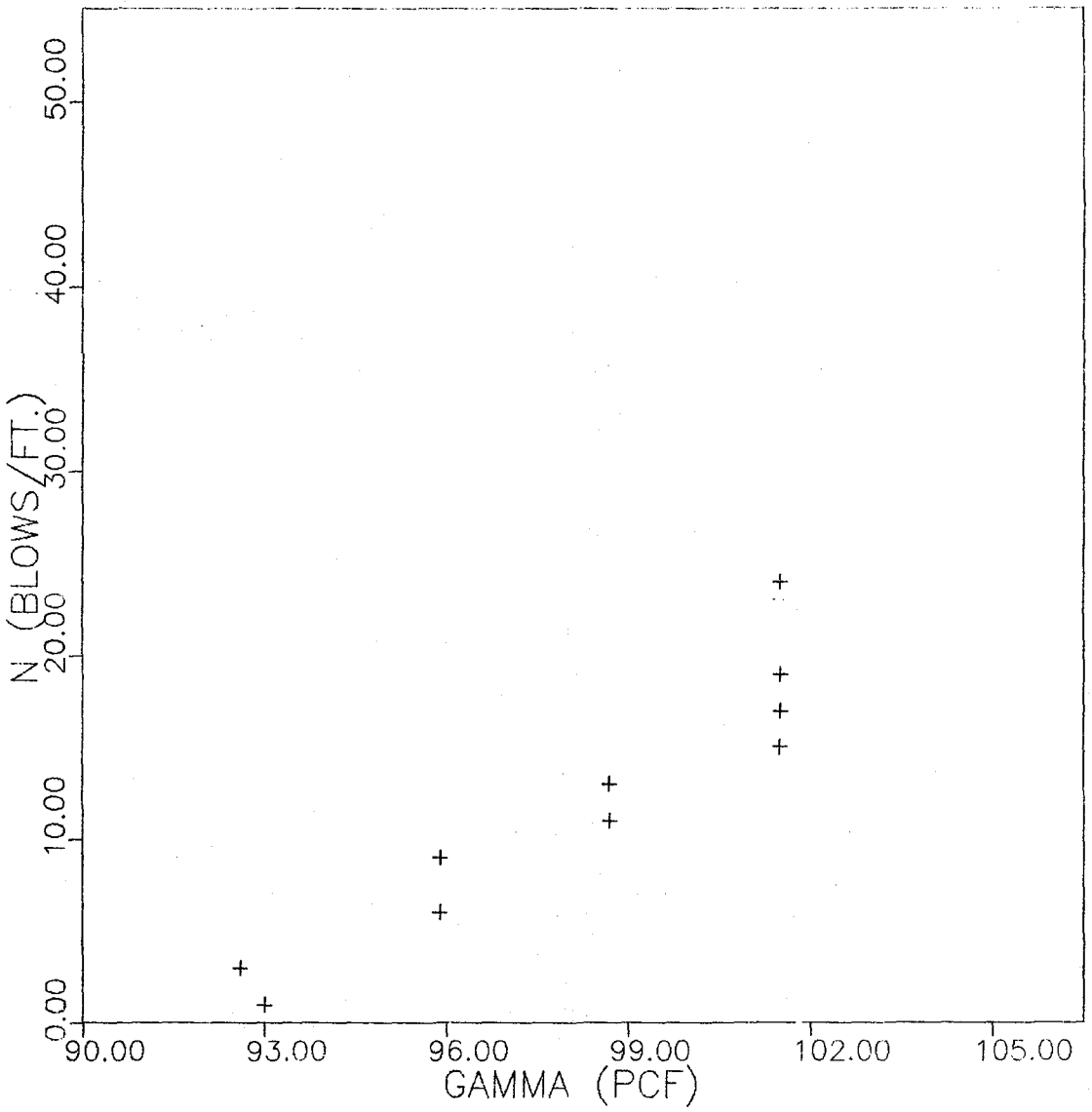

Fig. 4.2 SPT-Values, N, vs. In-Place Dry Density, Gamma, for RBMS, σ'_v = 1.44 ksf

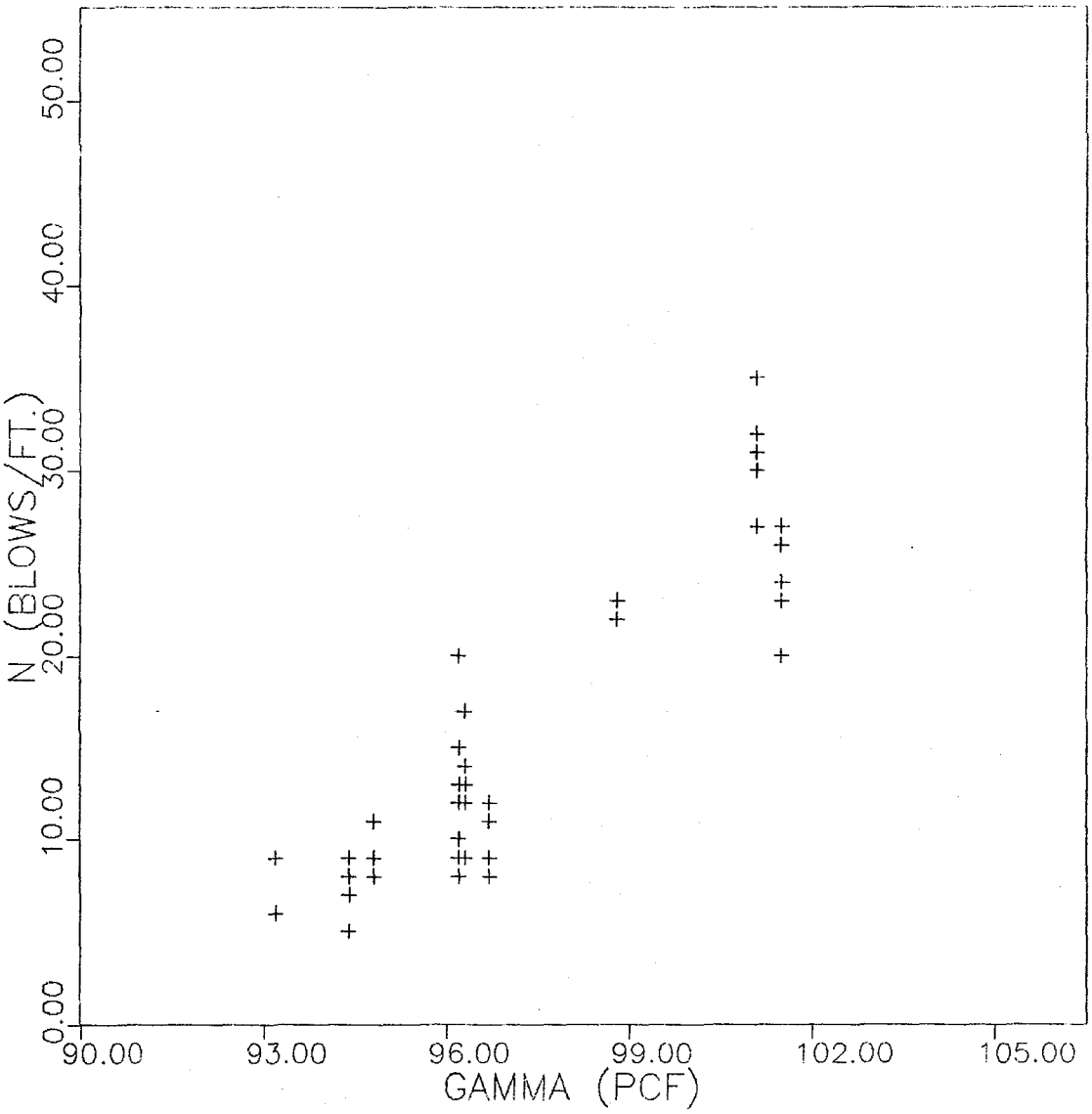

Fig. 4.3 SPT-Values, N, vs. In-Place Dry Density, Gamma, for RBMS, σ'_v = 5.76 ksf

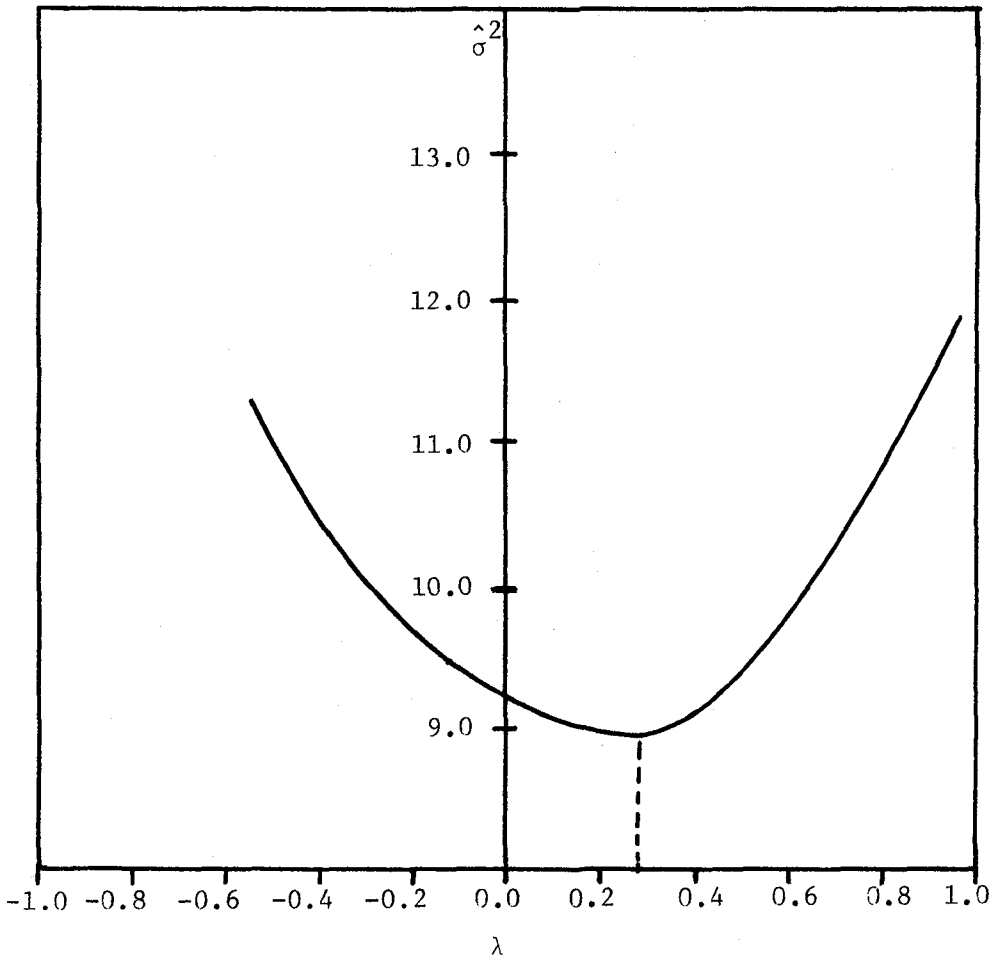

Fig. 4.4 $\hat{\sigma}^2$ Versus λ for RBMS, σ'_v = 5.76 ksf

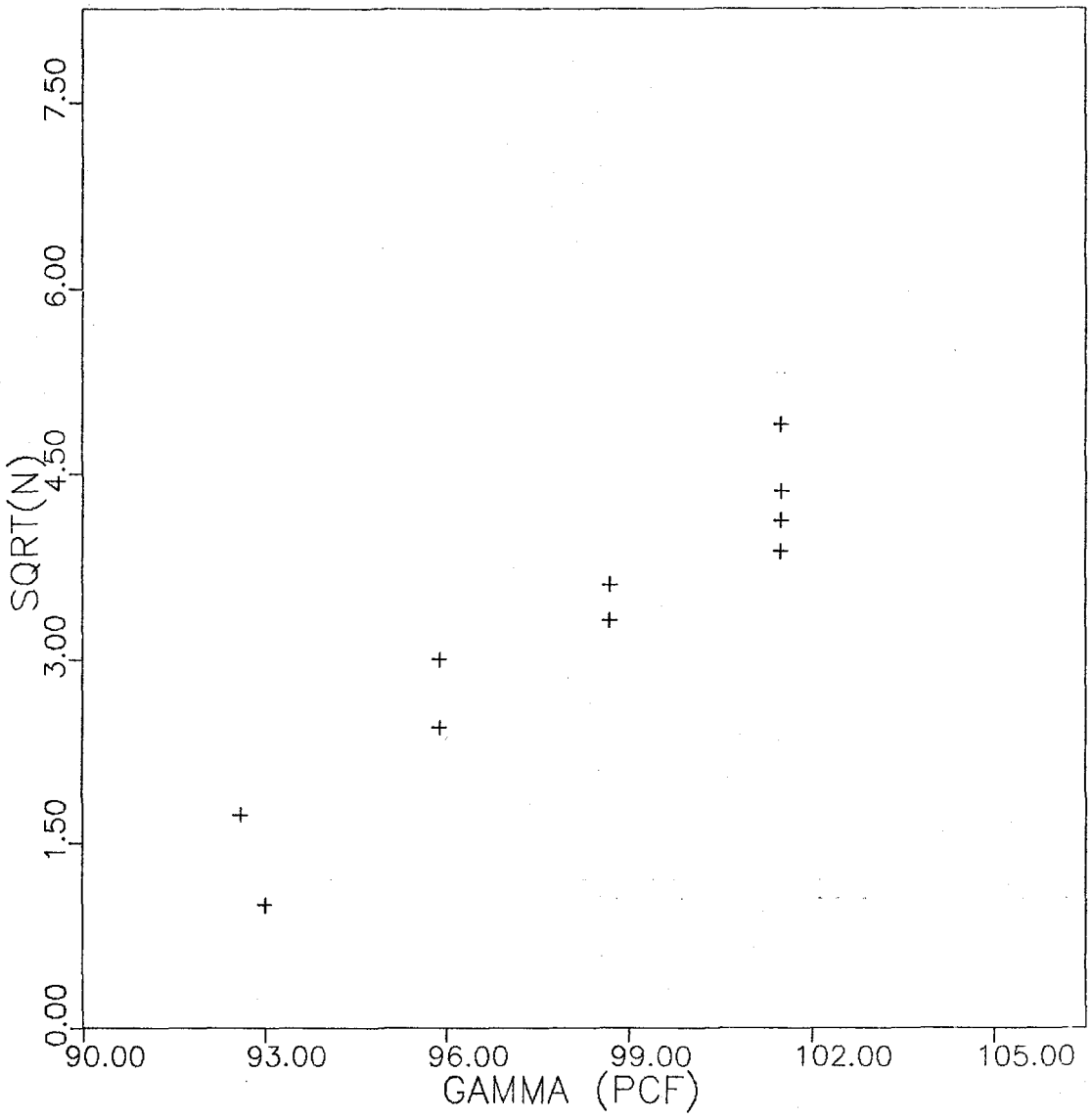

Fig. 4.5 $N^{1/2}$ vs. In-Place Dry Density for RBMS, σ_v' = 1.44 ksf

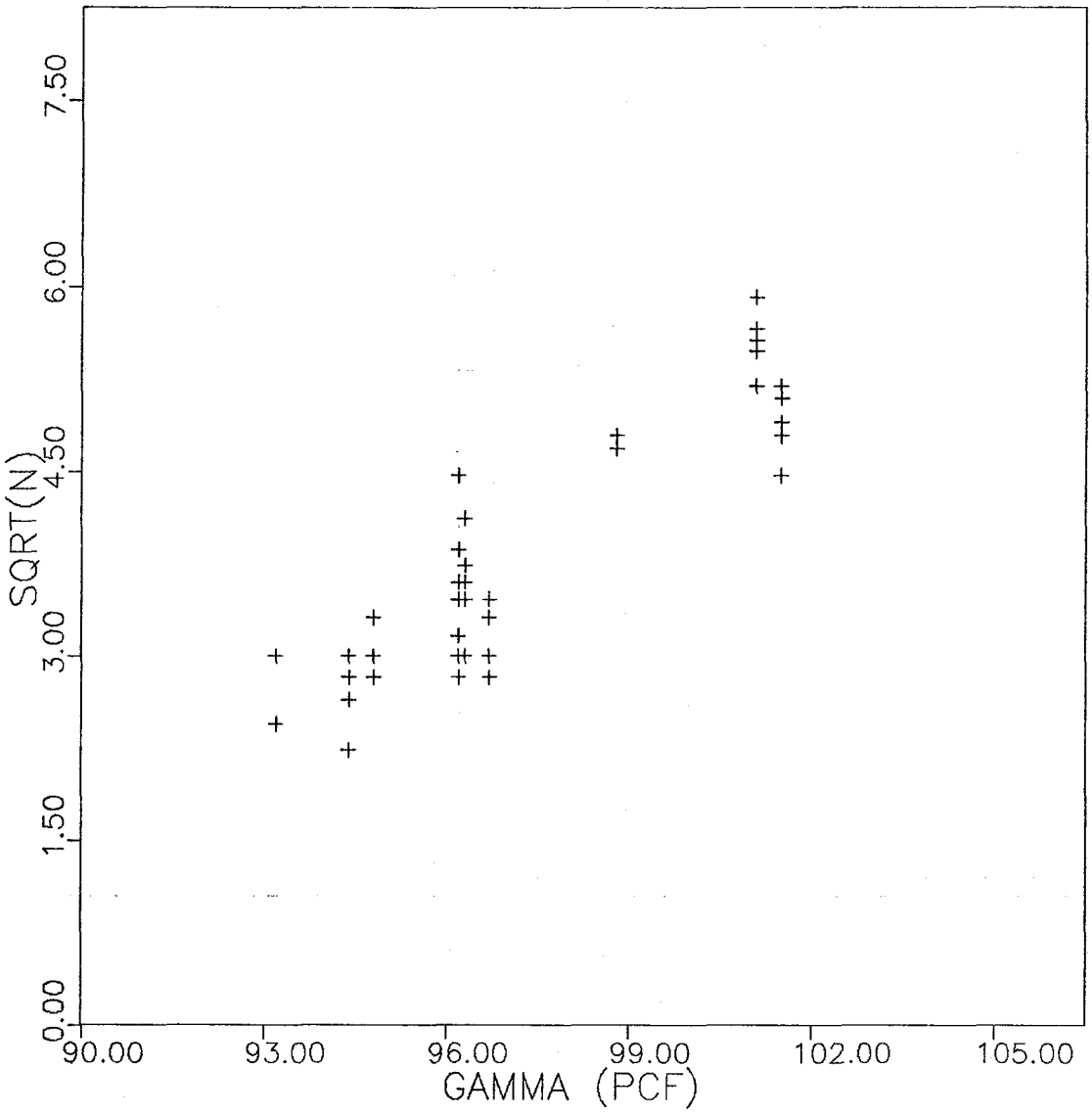

Fig. 4.6 $N^{1/2}$ vs. In-Place Dry Density for RBMS, σ'_v = 5.76 ksf

term, $a_3 \cdot \sigma'_v \cdot \gamma$, into the regression model (Eq. 4.8). The effect of sand type can also be introduced in Eq. 4.8 by considering γ_{min} and γ_{max} parameters. After extensive research, the following form of the regression equation considering all the parameters involved is found to be the best:

$$E(N^{1/2} | \Gamma_{max} = \gamma_{max}, \Gamma_{min} = \gamma_{min}, \Gamma = \gamma, \Sigma'_v = \sigma'_v) = a_o + a_1\gamma + a_2\gamma\,\sigma'_v + a_3\gamma_{min} + a_4(\gamma_{max} - \gamma_{min}) \quad (4.9)$$

The variance of the above equation is found to be constant.

Considering all types of sands, namely, RMS, OS, PRS, and SCS, and considering 104 results obtained from the WES test program, a regression analysis is carried out on Eq. 4.9. It can be shown that

$$E(N^{1/2} | \Gamma_{max} = \gamma_{max}, \Gamma_{min} = \gamma_{min}, \Gamma = \gamma, \Sigma'_v = \sigma'_v) = -5.50116 + 0.36243\,\gamma + 0.00278\,\gamma\sigma'_v - 0.32280\,\gamma_{min} + 0.06053\,(\gamma_{max} - \gamma_{min}) \quad (4.10)$$

and

$$Var(N^{1/2} | \Gamma_{max}, \Gamma_{min}, \Gamma, \Sigma'_v) = \hat{\sigma}^2 = 0.183 \quad (4.11)$$

In Eq. 4.10, γ, γ_{max}, and γ_{min} are expressed in pcf units and σ'_v is expressed in ksf units. The coefficient of determination (r^2 - value) of Eq. 4.10 is found to be 0.9357. The predictability of Eq. 4.10 is expected to be very good.

For a site, the γ_{max} and γ_{min} vlaues can be easily calculated from samples obtained from the site, even using the material collected by the

split spoon sampler. Knowing these limiting densities and the N value, the corresponding Γ value can be calculated as:

$$E(\Gamma \mid N=n,\ \Gamma_{max} = \gamma_{max},\ \Gamma_{min} = \gamma_{min}, \Sigma_v' = \sigma_v') = \frac{5.50116 + n^{1/2} + 0.32280\ \gamma_{min} - 0.06053\ (\gamma_{max} - \gamma_{min})}{0.36243 + 0.00278\ \sigma_v'} \tag{4.12}$$

and

$$\text{Var}\ (\Gamma \mid N = n,\ \Gamma_{max} = \gamma_{max},\ \Gamma_{min} = \gamma_{min}, \Sigma_v' = \sigma_v') = \frac{0.183}{(0.36245 + 0.00278\sigma_v')^2} \tag{4.13}$$

In the proposed liquefaction model, the mean and COV of the relative density need to be known. They can be estimated at this stage in the following way:

$$E(D_r \mid N = n,\ \Gamma_{max} = \gamma_{max},\ \Gamma_{min} = \gamma_{min}, \Sigma_v' = \sigma_v') = \frac{\gamma_{max}}{E(\Gamma)} \times \frac{\left[E(\Gamma) - \gamma_{min}\right]}{\left[\gamma_{max} - \gamma_{min}\right]} \tag{4.14}$$

and

$$\delta_{D_r}^2 = E_3^2\ \Omega_\gamma^2 \tag{4.15}$$

where

$$E_3 = \left(\frac{\left[\frac{\gamma_{min}}{(\gamma_{max} - \gamma_{min})} + 1 \right]}{E(D_r)} \right) - 1 \tag{4.16}$$

$E(\Gamma)$, Ω_γ, and $E(D_r)$ can be calculated by using Eqs. 4.12, 4.13, and 4.14, respectively. Eq. 4.14 can be used to estimate the relative density indirectly in the laboratory. The superiority of this proposed laboratory relationship with respect to the presently available laboratory relationships will be discussed in Section 4.3.

4.2.4.2 Indirect Estimation of Relative Density in the Field

The laboratory relationship proposed in the previous section needs to be calibrated so that it can be used to estimate the relative density in the field conditions. In situ effects, such as age of the deposit, cementation, drainage, etc. may have a significant effect on the measured SPT values. The laboratory results failed to show these effects.

The prediction error of Eq. 4.14 in the field can be evaluated using field observations, where γ_{max}, γ_{min}, D_r, SPT value, and σ'_v are all measured and reported in the literature. After an extensive literature survey, only six such different sources of information (5, 55, 67, 84, 90, 92) could be located. The data reported by Wu (92) cannot be used since information on limiting densities is not available. Other sources can be used to improve the predictability of Eq. 4.14 in estimating the in situ relative density.

Before this calibration, Eq. 4.14 needs further modification. In the WES study, the standard penetration test was conducted with a hydraulically driven trip hammer; in the field, however, the hammer is raised and lowered by a rope and cathead system. Tokimatsu and Yoshimi (83) have shown that, on the average, the SPT value measured by the rope and cathead system may be greater by 2.7 blows than that measured by the trip hammer, particularly when SPT values are greater than 10 blows. In light of this observation, Eq. 4.14 or in essence Eq. 4.12 needs to be modified. It is proposed here that the value of N in Eq. 4.12 should be modified in the following way:

$$N = N_{th} = N_{rc}; \; N \leq 10 \tag{4.17}$$

and

$$N = N_{th} = N_{rc} - 2.7; \; N > 10 \tag{4.18}$$

where N_{th} is the SPT value as measured by the trip hammer system, and N_{rc}

is the SPT value as measured in the field with a rope and cathead system.

With this modification of Eqs. 4.12 and 4.14, the proposed laboratory model can be corrected for the field conditions considering all the available field test results mentioned earlier.

The values of D_r actually measured in the field versus the values of D_r predicted from Eq. 4.14 are plotted in Fig. 4.7. Theoretically, all points should lie on a 45° line if the reported data are reliable and the prediction equation is perfect. The plot shows considerable spread about the 45° line. However, no systematic bias can be observed from the plotting. Thus, Haldar and Miller's equations (Eqs. 4.12, 4.14, 4.17, and 4.18) can be used to adequately predict the mean relative density indirectly in the field. To consider the uncertainty associated with this prediction, an upper bound (Line A) and lower bound (Line B) are proposed in Fig. 4.7. Assuming a symmetrical triangular distribution between these bounds, and using Haldar and Miller's equations to predict mean value, the COV of the in situ relative desnity can be shown to be

$$\Delta^2_{D_r} = 0.95393 - 1.62679\ \bar{D}_r + 0.85357\ \bar{D}_r^2 \qquad (4.19)$$

Thus, the total uncertainty in the estimation of in situ relative density can be calculated as

$$\Omega^2_{D_r} = \delta^2_{D_r} + \Delta^2_{D_r} \qquad (4.20)$$

where δ_{D_r} and Δ_{D_r} can be calculated using Eqs. 4.15 and 4.19, respectively.

4.3 Comparison Among Haldar and Miller, Gibbs and Holtz, Bazaraa, and Wes Models

The stage is now set to compare the predictability of the most commonly used relationships, including the relationships proposed by Haldar

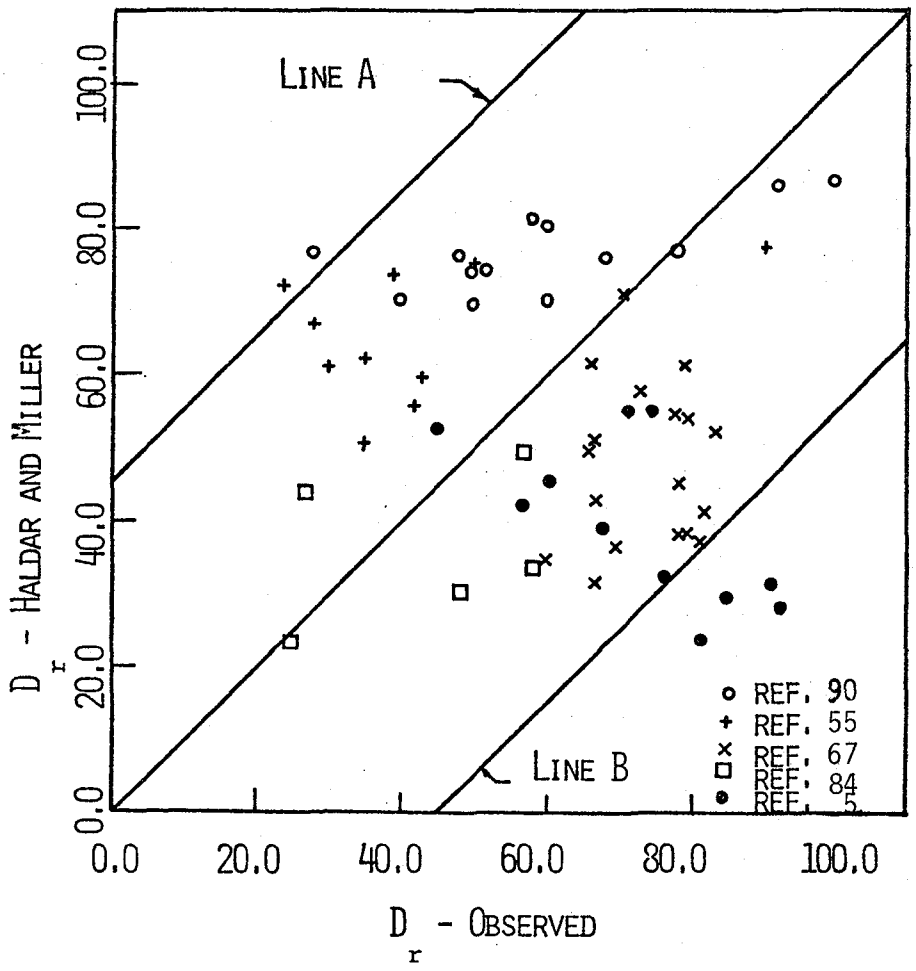

FIGURE 4.7 COMPARISON OF OBSERVED VS. PREDICTED D_r USING HALDAR AND MILLER'S RELATIONSHIP

and Miller, to indirectly predict the in situ relative density. This comparison can be made by considering all the available information on field observations of γ_{max}, γ_{min}, D_r, SPT value, and σ'_v as discussed in the previous section. The predictability of Haldar and Miller, Gibbs and Holtz, Bazaraa, and WES equations can be studied by introducing four factors F_1, F_2, F_3, and F_4, such that

$$F_1 = \frac{D_{r\ \text{Haldar and Miller}}}{D_{r\ \text{observed}}} \tag{4.21}$$

$$F_2 = \frac{D_{r\ \text{Gibbs and Holtz}}}{D_{r\ \text{observed}}} \tag{4.22}$$

$$F_3 = \frac{D_{r\ \text{Bazaraa}}}{D_{r\ \text{observed}}} \tag{4.23}$$

and

$$F_4 = \frac{D_{r\ \text{WES}}}{D_{r\ \text{observed}}} \tag{4.24}$$

The factors F_1, F_2, F_3, and F_3 are esentially ratios of predicted versus observed relative densities.

If an equation is perfect, the mean value of the F factor would be 1.0 and a COV of zero would be expected. Considering the available information on observed in situ relative density (5, 55, 67, 84, 90) and the corresponding predicted values using the four different models, the factors F_1, F_2, F_3, and F_4 are evaluated. The mean values of F_1, F_2, F_3, and F_4 are found to be 1.022, 1.388, 0.975, and 1.159, respectively, and the corresponding COV's are 0.582, 0.555, 0.571, and 0.512. From the above

statistics, it can be observed that the uncertainty associated with the prediction is about the same for all four models. However, the Haldar and Miller model will predict the in situ mean relative density most accurately. This study also confirms the general feeling among engineers that Gibbs and Holtz's equations overpredict the in situ relative density and Bazaraa's equations underpredict the in situ relative density. It is proposed here that in the future, Haldar and Miller's proposed equations should be used to indirectly predict the in situ relative density from the information on SPT values.

4.4 Scale of Fluctuation in Relative Density Field

The uncertainty associated with the point estimation of in situ relative density from information on SPT value has been discussed in Section 4.2. However, to develop a three-dimensional probabilistic model, the three-dimensional probabilistic characteristics of the relative density need to be known. As discussed in Section 3.7.3, for a statistically homogeneous soil deposit, the point mean can be considered as the spatial mean. However, the spatial variance needs to be calculated from the point variance using variance functions in the three directions. The variance function can be calculated from the information on the scale of fluctuation (Section 3.7.3). Thus it is necessary to estimate the scale of fluctuation in the relative density field.

At this stage, the primary data about the site under consideration are SPT results at a number of points. The objective here is to calculate the scale of fluctuation of relative density from the information on SPT values. This can be done in two ways: (1) a probabilistic model for SPT values can be developed from the field observation using techniques

developed in Section 3.7.2. This model then can be used to develop a probabilistic model in D_r field using the relationships developed in Section 4.2. (2) Field SPT values can be transformed to D_r values using the relationships mentioned above at the sampling points. These D_r values can then be used to estimate the scale of fluctuation in the D_r field. It can be shown that the two approaches are equivalent. From the discussion made in Section 3.7.2, it can also be stated that the scale of fluctuation in the SPT field may be identical to the scale of fluctuation in the D_r field. This area will be researched in subsequent studies in great detail considering an actual deposit.

The theory behind the development of a probabilistic model of three-dimensional soil deposit conditions has been developed in Chapter 3. In Chapter 6, numerical examples will be given to clarify the steps involved.

4.5 Shear Strength Parameter

The shear strength parameter, R, was introduced in Section 3.6.1 to estimate the in situ shear resistance mobilized by a saturated, cohesionless soil when subjected to earthquake-induced shear stresses. Much of the research to predict the in situ shear resistance has been done in the laboratory with disturbed or remolded soil samples. It is obvious that some of the factors that influence the shear resistance in the field can not be considered appropriately in the laboratory. Thus, the R parameter will be modeled in two stages: (1) a laboratory model will be developed to evaluate R using all the appropriate laboratory test results, and (2) this laboratory model will be corrected to consider the in situ field conditions. These will be discussed in Sections 4.5.2 and 4.5.3.

4.5.1 Failure Criterion

The degree of damage caused by earthquake-induced liquefaction is related to the amount of cyclic strain that the soil undergoes; hence, failure of the soil may be defined as the occurence of a certain level of strain. Typical failure criteria used in the literature may be initial liquefaction, 5%, 10%, or 20% double amplitude strain depending on the importance of the project, or the amount of permissible deformation.

For a saturated cohensionless soil subjected to cyclic shaking, initial liquefaction is defined as the point where the pore water pressure becomes equal to the total vertical stress; in other words, the point where the vertical effective stress is reduced to zero. The soil will undergo initial liquefaction before exhibiting 5%, 10% or 20% double amplitude strain; therefore it is conservative to choose initial liquefaction as the failure criterion. Moreover, the test results considered in this study correspond only to the initial liquefaction failure criterion. Thus, the soil resistance parameter cannot be developed for other failure criterion. However, Haldar (25) studied this area in great detail considering cyclic triaxial test results. He concluded that for the triaxial test, the value of the parameter R is different for each failure criterion, particularly when the equivalent number of uniform stress cycles, N_{eq}, is less than 50 cycles. For D_{50} = 0.2 mm and N_{eq} between 10 and 50 cycles, Haldar observed that the value of R for 5% double amplitude strain is about 12% greater than for the initial liquefaction failure cirterion, and about 7% less than for the 20% double amplitude strain failure criterion. In this study, the model to estimate the R parameter is developed considering the initial liquefaction failure criterion.

4.5.2 Laboratory Model for Shear Strength Parameter

As discussed in Section 2.2, using the simple shear tests to determine the shear resistance of a sand sample appears to be much more desirable than using the triaxial tests, as the former develop stress conditions much closer to the field conditions. An extensive literature survey was conducted to collect all the test results using the simple shear test apparatus. Thirteen major sources (12, 20, 21, 22, 23, 35, 36, 54, 61, 77, 96, 97, 98) were identified; eleven of the sources were reports of small-scale simple shear test (20, 21, 22, 23, 35, 36, 61, 77, 96, 97, 98) and two of the sources were reports of large-scale test (12, 54). In several small-scale tests, different types of simple shear devices were used. Properly conducted large-scale tests suffer from fewer shortcomings than small-scale tests and seem to reproduce in situ conditions more closely (see Sect. 2.2); therefore, only the data from the large-scale shaking table tests (12, 54) is considered for developing the shear resistance model.

De Alba et al. (12) and Mori et al. (54) performed large-scale shaking table tests on saturated samples of Monterey #0 sand prepared by dry pluvial deposition. The sand samples were subjected to an applied uniform cyclic shear stress, τ. The results were adjusted for the effect of compliance (see Sec. 2.4.2) and presented as the stress ratio $\frac{\tau}{\sigma'_v}$ versus the number of cycles to initial liquefaction, N_{eq}, where σ'_v is the vertical effective stress. Cases where N_{eq} was greater than 100 cycles or less than 2 cycles were regarded as irrelevant for a liquefaction study, since the number of equivalent uniform cycles produced by a strong motion earthquake is expected to be on the order of 10 to 30 cycles.

Information on the stress ratio (τ/σ'_v) can easily be transformed into

the shear strength parameter, $\hat{R}$, which is the predictor of R as defined in Eq. 3.37, considering the corresponding K_o and D_r values. The steps involved are described in detail in Section 3.6.1. The $\hat{R}$ parameter thus obtained is plotted against $Ln(N_{eq})$ in Fig. 4.8. The relationship appears to be linear; hence, the following regression model is proposed:

$$E(\hat{R}|N_{eq}) = a_o + a_1 \, Ln(n_{eq}) \tag{4.25}$$

where n_{eq} is the observed number of uniform stress cycles of intensity τ causing initial liquefaction. A regression analysis is carried out on data shown in Fig. 4.8 and the following regression equation results:

$$E(\hat{R}|N_{eq} = n_{eq}) = 0.68171 - 0.08778 \, Ln(n_{eq});$$

$$2 \leq N_{eq} \leq 63, \; D_{50} = 0.36mm \tag{4.26}$$

and

$$Var(\hat{R}|N_{eq} = n_{eq}) = 0.000384 \tag{4.27}$$

The corresponding r^2 value is found to be 0.939. This indicates that the predictability of Eq. 4.26 is very good. The same conclusion can be reached through residual analysis.

Eq. 4.26 is developed for a specific laboratory test condition. $\hat{R}$ could be different if different test conditions were used in some other test program. Thus, it is desirable to develop a laboratory relationship considering a standard set of test conditions. The parameters that need to be addressed at this stage are the system compliance effect, method of sample preparation, mean grain size effect, effect of multidirectional shaking, the frequency of the uniform cyclic stress applied, shape of the uniform cyclic load, grain size distribution, grain shape and other secondary factors. The effects of these parameters are discussed in the

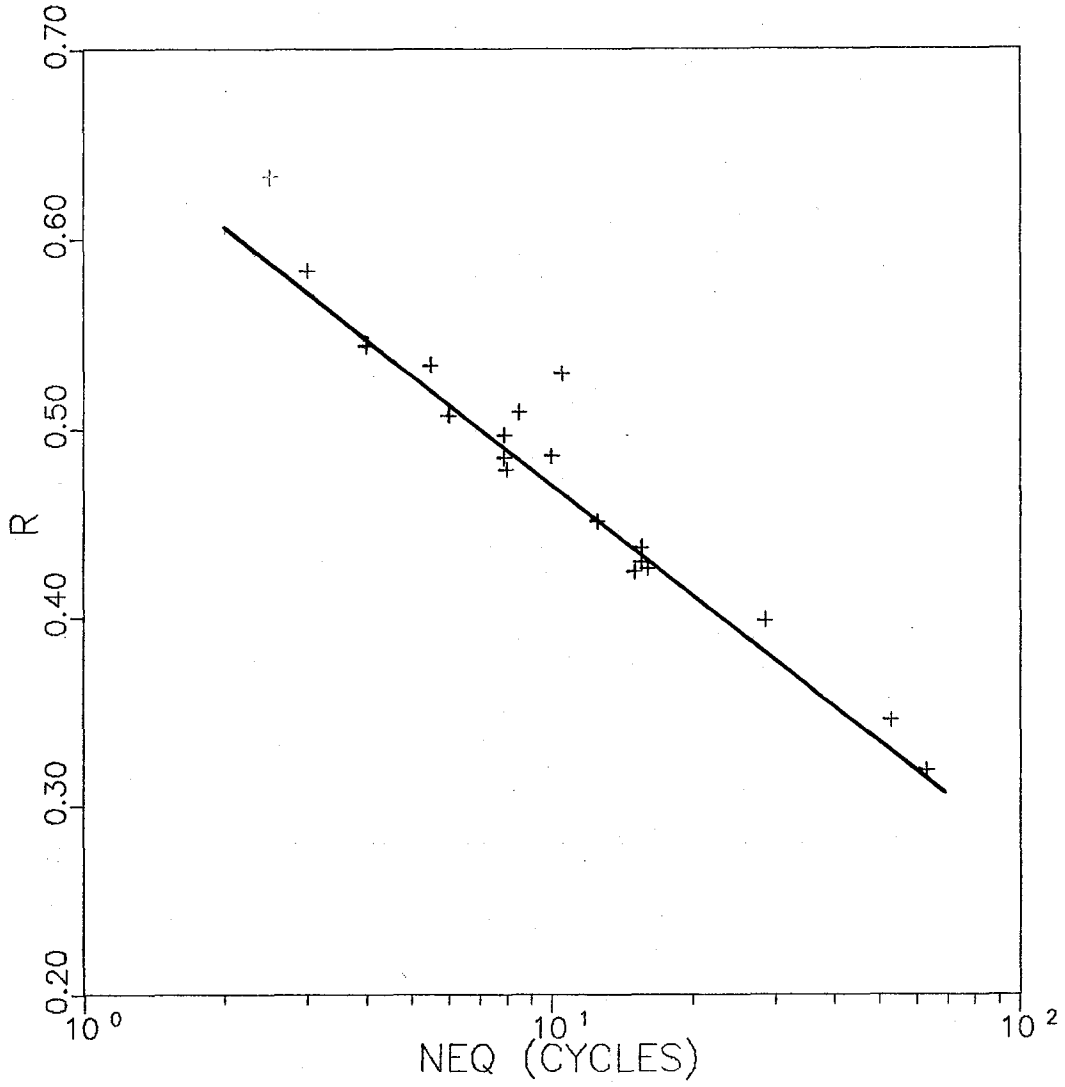

Fig. 4.8 Shear Strength Parameter, R, vs. the Number of Load Cycles to Initial Liquefaction, N_{eq}, for Monterey #0 Sand

following sections.

4.5.2.1 Effect of System Compliance

The test results reported by DeAlba et al. (12) and Mori et al. (54) were already corrected for the system compliance effect. Thus, no additional correction is necessary for this effect.

4.5.2.2 Effect of Sample Preparation

As briefly discussed in Section 2.4.1, the method by which the soil was deposited or how the samples were prepared in a laboratory has a significant effect on the liquefaction potential of that soil (43, 56, 70). Mulilis et al. (56) studied this effect by using the triaxial test to determine the shear resistances of saturated sand samples prepared by different deposition methods. From the results of tests on specimens prepared by pluviation through air and pluviation through water, the following regression model can be developed for each deposition method and are shown in Fig. 4.9.

$$E\left(\hat{R}_T \mid N_{eq} = n_{eq},\ D_{50} = 0.36,\ \text{Pluviation through air}\right) = 0.60873 - 0.06159 \cdot \text{Ln}(N_{eq}) \tag{4.28}$$

and

$$E\left(\hat{R}_T \mid N_{eq} = n_{eq},\ D_{50} = 0.36,\ \text{Pluviation through water}\right) = 0.65792 - 0.06159 \cdot \text{Ln}(n_{eq}) \tag{4.29}$$

where $\hat{R}_T$ = shear strength parameter as measured by the triaxial test. The difference in shear resistance of a sand prepared by pluviation through air and one prepared by pluviation through water, while all other parameters

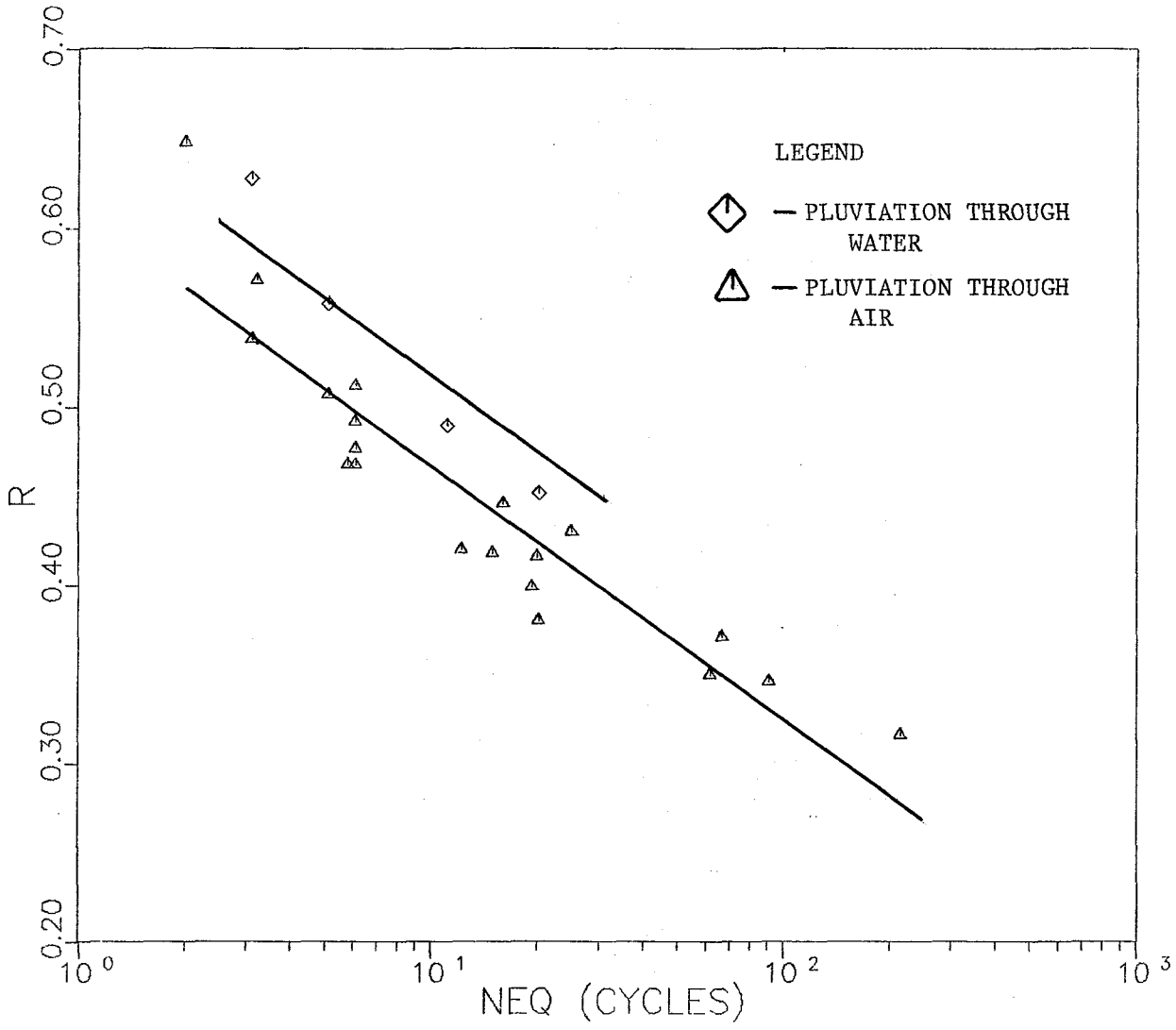

Fig. 4.9 Shear Resistances of Saturated Monterey #0 Sand Prepared by Different Deposition Methods

are identical, can be found by subtracting Eq. 4.28 from Eq. 4.29. The result can be expressed by

$$E\left(\Delta\hat{R}_{\text{water-air}}\right) = 0.65792 - 0.60873 = 0.04919 \tag{4.30}$$

The samples of sand used in the large shaking table tests that are considered to develop the laboratory model (Eq. 4.26), were prepared by dry pluviation through air. Most of the soil deposits in nature that are susceptible to earthquake-induced liquefaction are expected to be deposited by fluvial deposition. Thus, Eq. 4.26 needs to be modified to account for this effect.

If it is assumed that the effect of the deposition method on the parameter R will be the same for both the triaxial and the shaking table test results, the parameter $\Delta\hat{R}$ can be used to modify Eq. 4.26 as follows:

$$E(\hat{R} \mid N_{eq}, \text{water}) = E(\Delta\hat{R}) + E(\hat{R} \mid N_{eq}, \text{air})$$

$$= 0.7309 - 0.08778\ \text{Ln}(n_{eq}) \tag{4.31}$$

where $E(\hat{R} \mid N_{eq}, \text{air})$ is given by Eq. 4.26. Assuming the COV of $\Delta\hat{R}$ as 0.10, and errors are uncorrelated, Eq. 4.27 needs to be modified as

$$\text{Var}(\hat{R} \mid N_{eq} = n_{eq}, \text{water}) = 0.000384 + (0.10 \cdot 0.04919)^2$$

$$= 0.000408 \tag{4.32}$$

4.5.2.3 Effect of Mean Grain Size

The shear strength model, Eq. 4.26, is developed using results of one type of sand of mean grain size D_{50} = 0.36 mm. At this time large shaking table test results for sands with different D_{50} values are not available. However, the D_{50} size effect can be considered by introducing a corrective

factor, $N_{D_{50}}$, such that

$$E(\hat{R} \mid N_{eq} = n_{eq}, D_{50} = d_{50}) = N_{D_{50}} \cdot E(\hat{R} \mid N_{eq} = n_{eq}, D_{50} = 0.36 \text{ mm}) \quad (4.33)$$

$E(\hat{R} \mid N_{eq} = n_{eq}, D_{50} = 0.36 \text{ mm})$ can be estimated by Eq. 4.31.

It is perhaps sufficient at this time to assume that the effect of D_{50} on the parameter R will be the same for both the triaxial and the large scale shaking table tests. With this assumption, Haldar (25) and Haldar and Tang (29) suggested that the effect of D_{50} on the parameter R could be shown to be

$$E(\hat{R} \mid D_{50} = d_{50}) = 0.750 + 1.01\, d_{50} - 0.878\, d_{50}^2; \quad 0.06 \text{ mm} \leq D_{50} \leq 0.6 \text{ mm} \quad (4.34)$$

and

$$Var(\hat{R} \mid D_{50} = d_{50}) = 0.000202. \quad (4.35)$$

$E(R \mid D_{50} = 0.36)$ will be 1.0. Combining Eqs. 4.31 and 4.34, it can be shown that

$$E(\hat{R} \mid N_{eq} = n_{eq}, D_{50} = d_{50}) = \left(0.7309 - 0.08778 \text{ Ln } (n_{eq})\right) \times \left(0.750 + 1.01\, d_{50} - 0.878\, d_{50}^2\right)$$
$$2 \text{ cycles} \leq N_{eq} \leq 63 \text{ cycles}, \quad 0.06 \text{ mm} \leq D_{50} \leq 0.6 \text{ mm} \quad (4.36)$$

$$Var\,(\hat{R} \mid N_{eq} = n_{eq}, D_{50} = d_{50}) = 0.000408 + 0.000202 = 0.000610 \quad (4.37)$$

4.5.2.4 Effect of Multidirectional Shaking

During an earthquake, an element of soil is subjected to shaking in three directions. Therefore, in order to reproduce the in situ soil behavior in the laboratory, the soil samples must be subject to multi-

directional shaking. Nevertheless, most laboratory studies are conducted with only a unidirectional loading. Tests done by Pyke et al. (62) on soil samples subjected to multidirectional shaking indicate that the cyclic strength of a soil determined by unidirectional shaking tests should be reduced by 10% to account for the effects of multidirectional shaking. Hence, a multiplicative factor, N_{ms}, can be introduced in Eq. 4.36. The mean and COV of N_{ms} are considered to be 0.9 and 0.10, respectively in this study.

4.5.2.5 Effects of Secondary Factors

All the other factors mentioned in Section 4.5.2, namely, the frequency of the uniform cyclic load, shape of the cyclic load, grain size distribution, grain shape and other factors can be grouped as secondary factors. They all affect the liquefaction potential to some degree, but it is very difficult to quantify them due to limited research in these areas. Haldar (25) suggested that these effects are probably compensatory, i.e., no systematic trend in the mean of $\hat{R}$ is expected, but they do raise the level of uncertainty.

After examining the literature, Haldar (25) suggested that the additional uncertainty can be expressed in terms of the COV for each component effect as follows: The COV due to the frequency of the uniform cyclic load, shape of the uniform cyclic load, grain size distribution, grain shape, and all other secondary factors can be expressed as 0.058, 0.05, 0.05, 0.069, and 0.10, respectively. Therefore, a multiplicative factor, N_S, similar to $N_{D_{50}}$ can be introduced into Eq. 4.36 to consider the effects of secondary factors. The mean value of N_s can be considered as 1.0 and

COV of N_s can be shown to be

$$\Omega_{N_s} = \sqrt{0.058^2 + 0.05^2 + 0.05^2 + 0.69^2 + 0.10^2}$$
$$= 0.152 \qquad (4.38)$$

assuming the factors are statistically independent.

Considering all the corrective factors discussed in the previous sections, the mean value of the shear strength parameter in the laboratory can be shown to be

$$E(\hat{R} \mid N_{eq}, D_{50}) = 0.9 \times \left(0.7309 - 0.08778 \text{ Ln } (n_{eq})\right)$$
$$\times \left(0.750 + 1.01\, d_{50} - 0.878 \cdot d_{50}^2\right) ;$$
$$2 \leq N_{eq} \leq 63,\ 0.06 \leq D_{50} \leq 0.6, \qquad (4.39)$$

and

$$\text{Var } (\hat{R} \mid N_{eq}, D_{50}) = 0.000610 + (0.10^2 + 0.152^2)$$
$$\times\ E(\hat{R} \mid N_{eq}, D_{50})^2 \qquad (4.40)$$

4.5.3 In Situ Shear Strength Parameter

The shear strength parameter model developed for the laboratory conditions will be useful only if the test conditions correspond to the field loading and boundary conditions. As discussed previously, the laboratory model (Eq. 4.39) is expected to predict the in situ shear strength parameter very closely. However, it will fail to consider the site specific characteristics, e.g., cementation, age, seismic history of the deposit, etc. These are discussed in detail in Chapter 2. It is very difficult to make a general statement on the effect of these factors on the shear strength parameter for all deposits. In most cases, they increase the

shear resistance of the deposit. For a specific site, if the relevant information is available, it can be easily incorporated in Eq. 4.39. In the absence of any such information on the deposit, Eq. 4.39 is expected to give a very conservative estimate of the in situ shear strength parameter in most cases. Moreover, the effect of some of the aforementioned parameters will be indirectly considered in the SPT value obtained from the site.

In order to consider the site specific conditions a corrective factor, C_r, can be introduced in Eq. 4.39. The mean value of C_r can be considered very conservatively as 1.0. A COV of 0.10 for C_r is considered in this study.

It has been assumed so far that N_{eq}, the number of earthquake-induced uniform stress cycles, is known. However, as will be discussed in Section 5.3.4 a considerable amount of uncertainty is expected in the estimation of N_{eq} (Eq. 5.14).

Thus, considering the effects of all major factors, the mean in situ shear resistance parameter, R, of a deposit can be estimated as

$$E(R|N_{eq}, D_{50}) = E(\hat{R}|N_{eq}, D_{50}) \tag{4.41}$$

and

$$\begin{aligned} Var(R|N_{eq}, D_{50}) = {} & 0.000610 + (0.10^2 + 0.10^2 + 0.152^2) \\ & \times E(\hat{R}|N_{eq}, D_{50})^2 + \\ & + 0.08778^2 \times \Omega^2_{(N_{eq}|M)} \end{aligned} \tag{4.42}$$

where $E(\hat{R}|N_{eq}, D_{50})$ can be estimated from Eq. 4.39, and $\Omega_{(N_{eq}|M)}$ can be estimated from Eq. 5.14.

4.6 Effective Overburden Pressure

In order to assess the liquefaction potential of a saturated, cohesionless soil deposit, the vertical effective stress, σ'_v, must be estimated. In general, at a depth h, σ'_v can be computed from the following expression:

$$\sigma'_v = \gamma_s \cdot h - \gamma_W(h - h_{WT}) \tag{4.43}$$

in which γ_s is the saturated unit weight of the soil deposit, γ_W is the unit weight of water, and h_{WT} is the depth of the water table from the ground surface. For design purposes, h and γ_w are assumed to be known, but the determination of γ_s and h_{WT} may not be perfect; hence, σ'_v is uncertain. In this particular study, the uncertainty in γ_s and γ is assumed to be the same. Ω_{γ_s} is of the order of 0.01 (25). For this study $\Omega_{h_{WT}}$ is assumed to be 0.20.

Applying the first order approximation, the mean and variance of σ'_v can be estimated from the following equations:

$$\bar{\sigma}'_v = \bar{\gamma}_s h - \gamma_W(h - \bar{h}_{WT}) \tag{4.44}$$

and

$$\mathrm{Var}(\sigma'_v) = \mathrm{Var}\ (\gamma_s)\ h^2 + \mathrm{Var}(h_{WT})\ \gamma_W^2 \ . \tag{4.45}$$

In the proposed model, σ'_m, as defined by Eq. 3.39, needs to be considered. The mean and variance of σ'_m can be shown to be

$$\bar{\sigma}'_m = \frac{1 + 2K_o}{3}\,\bar{\sigma}'_v \tag{4.46}$$

and

$$\mathrm{Var}(\sigma'_m) = \left(\frac{1 + 2K_o}{3}\right)^2 \cdot \mathrm{Var}(\sigma'_v) \tag{4.47}$$

K_o is assumed to be a constant in Eqs. 4.46 and 4.47.

Chapter 5

UNCERTAINTY ANALYSIS OF LOAD PARAMETERS

5.1 Introduction

For a liquefaction study, the magnitude and duration of the future earthquake, as well as the maximum ground acceleration at a particular site within a specified time period, need to be estimated. It is well recognized that all these parameters are unpredictable. Available geological, seismological, and observed records at or around the region concerned may provide information for estimating these parameters. In the following sections, models and procedures for estimating the earthquake loading parameters are described.

5.2 Earthquake Magnitude

The objective of this section is to formulate a procedure for obtaining the probability distribution of the annual maximum earthquake magnitude. The distribution of magnitude M is needed to determine the distribution of the equivalent number of stress cycles N_{eq}.

The cumulative distribution function of magnitude can be derived by considering Richter's law of earthquake magnitude (63). This law states that, in a certain zone of the crust, the occurrence of earthquakes during a specified period of time can be approximated by the relationship

$$\text{Log}_{10}N(m) = a-bm \; ; \; m \geq 0 \tag{5.1}$$

where N(m) is the number of occurrences with magnitude m or greater, and a and b are constants. The procedure used to determine these constants will be discussed later in this section.

Equation 5.1 can be rewritten in the following form:

$$N(m) = \exp(\alpha-\beta m); \; m \geq 0 \tag{5.2}$$

where $\alpha = 2.3a$ and $\beta = 2.3b$

The distribution function of earthquake magnitude M can be determined in the following way:

$$F_M(m) = \frac{N(M\geq 0) - N(M\geq m)}{N(M\geq 0)} = 1-e^{-\beta m}; \; m \geq 0. \tag{5.3}$$

The occurrence of earthquakes in a region may be assumed to constitute a Poisson process (48, 65) with a mean occurrence rate of ν per year. Combining this assumption with Eq. 5.3, the probability distribution of the annual largest magnitude $F_{M_{max}}(m)$ becomes

$$F_{M_{max}}(m) = \sum_{n=0}^{\infty} \frac{e^{-\nu}(\nu)^n}{n!} [F_M(m)]^n$$

$$= \exp(-\nu e^{-\beta m}); \; m \geq 0 \tag{5.4}$$

The form of the cumulative distribution function expressed in Eq. 5.4 is also a "Type I" distribution of the largest values.

Recall the two constants a and b in Eq. 5.1. Lomnitz and Epstein (48) have shown that a and b can be expressed in terms of ν and β of Eq. 5.4. The relationships can be written in the following way:

$$a = \frac{\ell n \; \nu}{\ell n \; 10} \tag{5.5}$$

and

$$b = \frac{\beta}{\ell n\ 10} \tag{5.6}$$

The constants α and β of Eq. 5.2 can be written as

$$\alpha = \ell n\ \nu \tag{5.7}$$

and

$$\beta = 2.3\ b \tag{5.8}$$

The density function of the maximum annual earthquake can be obtained by differentiating the cumulative distribution function (Eq. 5.4). Assuming earthquakes with magnitudes smaller than m_o have no engineering importance, and that from a practical point of view the magnitude can not exceed an upper bound magnitude m_u, Eq. 5.4 can be normalized so that the area under the density curve of M_{max} between m_o and m_u is unity. Thus from Eq. 5.4 and introducing a factor C, the density function of M_{max} is found to be

$$\begin{aligned} f_{M_{max}}(m) &= C \cdot \frac{dF_{M_{max}}(m)}{dm} \\ &= C \cdot [\exp(-\nu e^{-\beta m})] \times [\nu\beta e^{-\beta m}]; \\ &\quad m_o \leq m \leq m_u \\ &= 0 \text{ elsewhere} \end{aligned} \tag{5.9}$$

where

$$C = \frac{1}{\exp(-\nu e^{-\beta m_u}) - \exp(-\nu e^{-\beta m_o})} \tag{5.10}$$

5.2.1 Evaluation of ν, β, m_o, and m_u

To solve Eq. 5.9 the values of ν, β, m_o, and m_u have to be known. The values of ν and β can be calculated from Eqs. 5.5 and 5.6, respectively if the values of a and b are known. Values of a and b can be determined for a geographical region by conducting a recurrence line for earthquake magnitude, as shown in Fig. 5.1. Basically, the recurrence line is a plot of the logarithm of the number of earthquakes with magnitude $\geq$ m per year versus the magnitude m. The recurrence line for the San Francisco Bay area, considering earthquakes within 100 kilometers of San Francisco from the year 1807 to 1969 with magnitude $\geq$ 4, is shown in Fig. 5.1. The value of b in this case is found to be 0.53 (14). The value of the parameter b may be assumed to be constant for a particular region, but it may vary from region to region (1, 34). Values of b ranging from 0.52 to 1.26 have been estimated for different regions of the world (14).

When b is known, the value of a can be evaluated using Eq. 5.1, in the following way. From Fig. 5.1, it is found that when $m \geq 4.0$, $N(m) = 1.570$ (14). Thus from Eq. 5.1, we get

$$a = 0.53 \times 4 + \text{Log}_{10}(1.57) = 2.3159$$

Thus, using Eqs, 5.5 and 5.6, the values of ν and β can be determined for known values of a and b, respectively.

Generally m_o and m_u are established based on engineering judgment. The lower bound magnitude should be determined considering two points: (i) an earthquake of magnitude smaller than m_o would not produce damaging intensities, and (ii) data collected from magnitudes as small as m_o are reliable. Generally, a value of $m_o = 4$ is appropriate (14). The upper

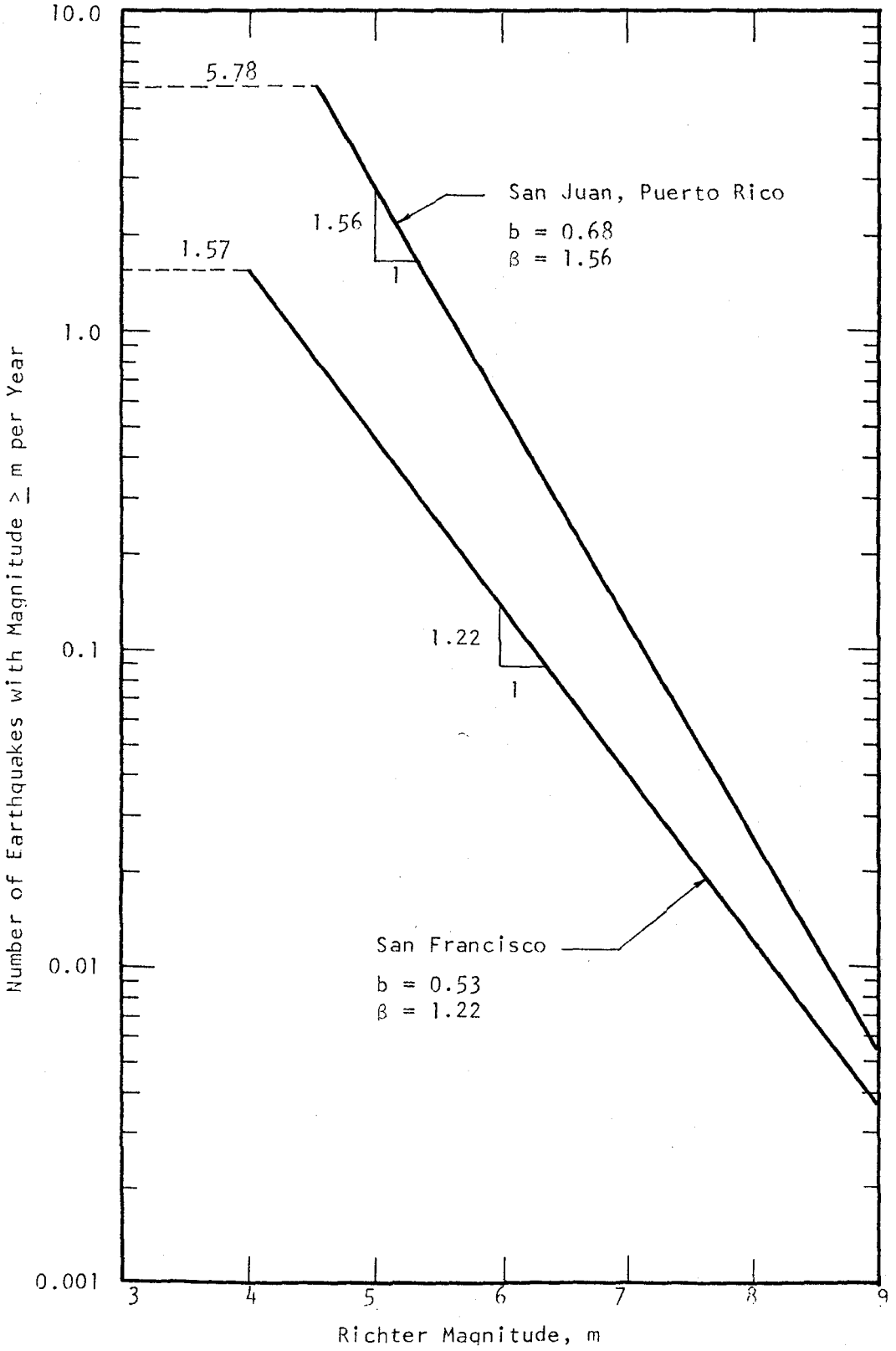

Fig. 5.1 Earthquake Magnitude Recurrence Lines for San Francisco and San Juan, Puerto Rico

bound magnitude m_u is generally estimated by considering the largest magnitude ever recorded for the region under consideration. DerKiureghian and Ang (14) considered $m_u = 8.5$ for the San Francisco area.

Thus, from all the above information, and using Eq. 5.9, the density function of $f_{M_{max}}(m)$ can be obtained.

5.3 Number of Equivalent Significant Cycles in Strong Motion Earthquake, N_{eq}

5.3.1 General Remarks

An earthquake loading pattern is extremely irregular. Ideally, to investigate the behavior of soil during earthquake shaking in the laboratory, the specimens should be tested under irregular-patterened loading like those actually generated during earthquakes. The use of the actual earthquake loading in the laboratory, however, may not be practical in many cases for the following reasons:

(i) The exact shear stress-time history of a future earthquake at a particular site is unknown.

(ii) Assuming a given time history of earthquake acceleration, the induced shear stress-time history may vary from site to site.

(iii) Even if a shear stress-time history is assumed, it is very difficult and expensive to duplicate this loading on a soil specimen in the laboratory.

Moreover, in the past a considerable number of laboratory investigations were carried out under uniform cyclic loading conditions to predict the in situ soil behavior under any dynamic loading, including earthquake

loading conditions. The past research results can be utilized properly only when a successful correlation between the two loading conditions can be found. The number of equivalent uniform cycles corresponding to an earthquake motion is one of the important parameters input to a liquefaction potential calculation. Thus, a reliable correlation between the two loading conditions is necessary in a liquefaction study. A statistical relationship between the irregular-patterned earthquake loading and the equivalent uniform stress cycles is proposed by Haldar (27) and Haldar and Tang (31). This is discussed briefly in the following sections.

5.3.2 Problem Description

The underlying principles of converting the irregular-patterned earthquake motions to the equivalent number of uniform cycles N_{eq} were well explained by Lee and Chan (44). According to Lee and Chan, "N_{eq} refers to that number of uniform cycles of stress intensity τ_{av}, which if applied to an element of soil in the field or a sample of the same soil in the laboratory, would have the same effect in terms of the soil strength or deformation as if the actual train of irregular cyclic shear stresses were applied." This concept of N_{eq} is essentially based on Miner's damage rule. In an earthquake engineering problem, it may be convenient to base N_{eq} calculations on acceleration rather than on stress-time histories because of the direct proportionality between acceleration, force and stress.

To estimate N_{eq} corresponding to an earthquake time history motion, the value of stress level S_L and soil strength curve must be available. The value of stress level S_L is usually referred to as a percentage of the

maximum stress. A soil strength curve can be described as a failure curve representing the relationship of the applied uniform stress and the number of cycles required to cause a soil specimen to fail. The steps involved in the estimation of N_{eq} for a given earthquake motion have been discussed in detail in the literature by Annaki and Lee (3) and Lee and Chan (44). The details of the steps involved will not be discussed here. However, the uncertainties associated with each parameter will be quantified in the following sections.

5.3.3 Assumptions in N_{eq} Concepts

When the uniform cycles of stress intensity concept was used in solving problems related to earthquake excitation, some implicit assumptions were made. They include (i) the ground motion is uniform at all sites in the same general area; (ii) the stress-time history at the depth of interest is directly proportional to the acceleration recorded at or near the ground surface; and (iii) for all soils, the laboratory liquefaction test data results can be represented by a single normalized curve relating stress ratio or stress level S_L to the number of cycles causing liquefaction.

These assumptions have been studied extensively by Annaki and Lee (3), Lee and Chan (44) and Haldar and Tang (31). Due to the tectonic nature of earthquake loads, the first assumption seems reasonable. The validity of the second assumption depends on the soil profile through which the acceleration has been propagated. To study these aspects related to N_{eq} evaluation, Lee and Chan (44) considered six different soil deposits. They concluded that "The value of N_{eq} computed from the surface or near

surface time history is appropriate for all other depths within the soil profile." They added that for routine work, it should not be necessary to determine N_{eq} rigorously for more than one location in a soil profile being analyzed. Regarding the third assumption, although a general trend can be established, a wide spread in the soil strength curve has been observed (Fig. 5.2). The reasons for this spread have been explored elsewhere by Haldar and Tang (31).

The general procedure for converting earthquake motions to uniform cyclic motion appears simple with the aforementioned assumptions. Yet, the study would be incomplete without answering the following questions: (i) would the value of N_{eq} be sensitive to the shape of the soil strength curve?, (ii) what stress level S_L should be used?, (iii) how would N_{eq} vary with the magnitude of the earthquake?, and (iv) if past earthquake records are used to find a relationship between N_{eq} and the earthquake magnitude, which one or both of the two horizontal records should be considered? In the following sections, attempts will be made to answer all these questions.

5.3.4 Statistical Evaluation

5.3.4.1 Uncertainties in the Soil Strength Curves

Haldar and Tang (31) explored the area of uncertainty associated with the soil strength curve extensively. It was observed that the soil strength curve depends on N_{eq}, the initial ambient pressure under which the sample was consolidated, relative density of the sample, and the mean grain size of the specimen D_{50}. When the soil strength curves are normalized properly (for details refer to Haldar and Tang (31)), they can be presented

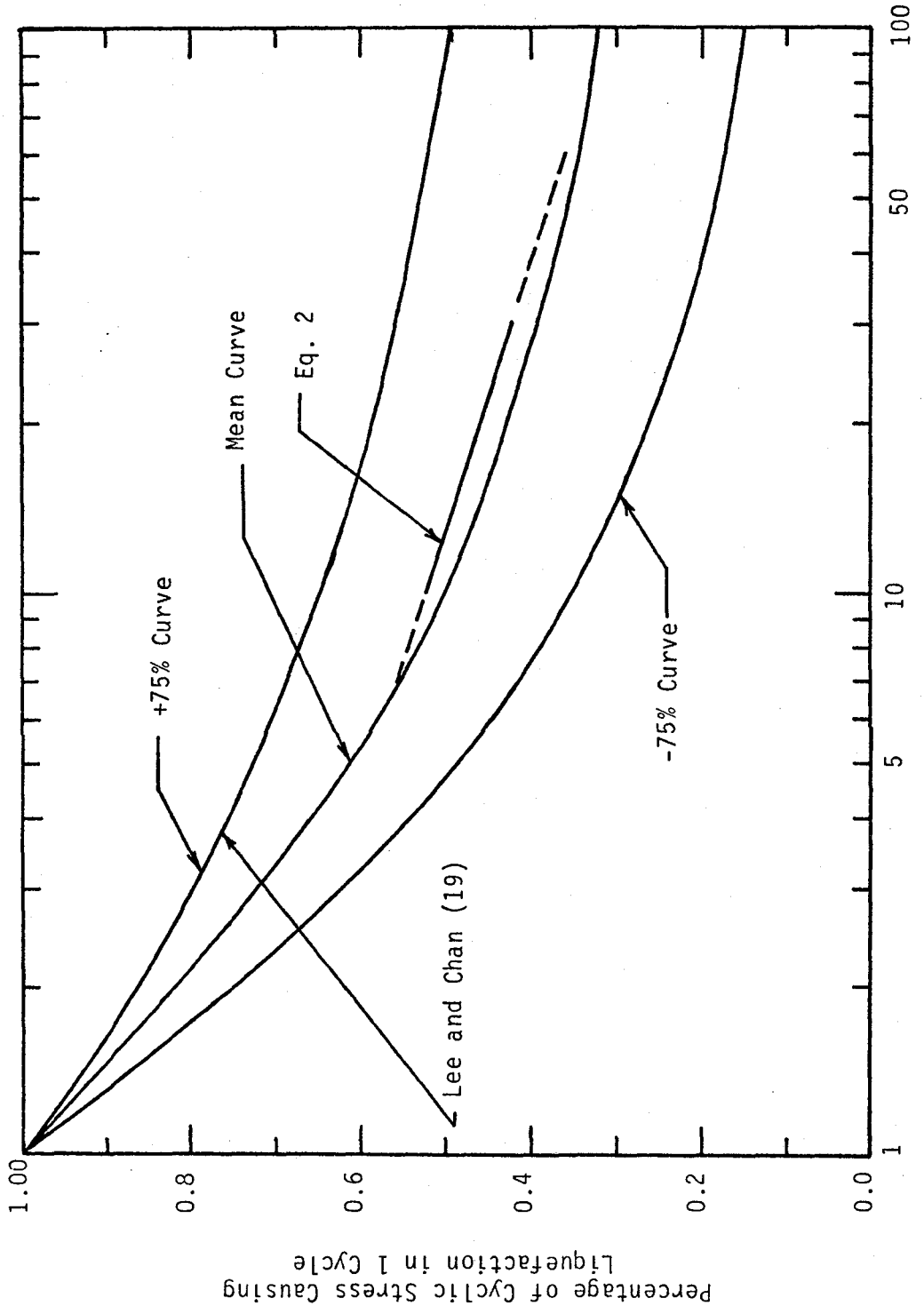

Fig. 5.2 Normalized Soil Strength Curves (From Ref. 31)

like the curves shown in Fig. 5.2. However, there is considerable scatter in the data. Observing this, Lee and Chan (44) proposed upper and lower 75 percentage ranges of the available data along with the mean curve as shown in Fig. 5.2. As discussed previously, for a given earthquake motion, a different value of N_{eq} will be obtained for each soil strength curve. This variation in N_{eq} values due to soil strength is not negligible and will be discussed in the subsequent section.

5.3.4.2 Earthquake Magnitude and N_{eq} Relationship

For a given S_L and soil strength curve, N_{eq} values can be calculated for past recorded earthquake motions. The values of N_{eq} thus obtained should be correlated with some other characteristic of the corresponding earthquake motions. It has been shown that larger magnitude earthquakes are associated with a longer duration of earth shaking (6). Since the number of equivalent uniform cycles varies with the duration of earth shaking, it is expected that some type of correlation would exist between N_{eq} and the earthquake magnitude. Earthquake magnitudes expressed in Richter's scale are considered for this discussion.

Lee and Chan (44) reported values of N_{eq} for 57 earthquakes recorded at or near the ground surface. They also included 12 artificially generated earthquakes in their study. Only earthquakes of magnitudes greater than 5.0 were considered. These data on N_{eq} and earthquake magnitude are used in the subsequent statistical studies.

Observing the trend of the data mentioned above, the relationship between N_{eq} (for a given S_L and soil strength curve) and magnitude M may be represented by the following regression equation:

$$E\,(N_{eq} \mid M = m) = A + B\,m + C\,m^2 \qquad (5.11)$$

in which A, B and C are regression coefficients. Eq. 5.11 will give an expected or mean value of N_{eq} for a given earthquake magnitude m. The scatter of the data about the mean curve is observed to be approximately constant. Thus, the variance of N_{eq} or Var $(N_{eq}|M=m)$ is assumed to be constant. The regression coefficients and variance are estimated later in this paper.

5.3.4.3 Stress Level S_L Selection

The choice of S_L is primarily subjective, based on literature review. Seed and Idriss (72) used $S_L = 0.65$ in their study. Intuitively, the choice of S_L could be based on the degree of sensitivity of the N_{eq} versus magnitude relationship to different soil strength curves. To find a suitable value for S_L, the data reported by Lee and Chan (44) are considered here. For S_L = 65%, 75% and 85% and considering the mean and $\pm$ 75% of data soil strength curves (Fig. 5.2), 9 sets of data on pairs of N_{eq} and M values are generated for each of the 69 earthquake time histories. Regression analysis is then performed on each set of data, thus obtaining 9 separate regression equations. The corresponding regression coefficients A, B and C and Var $(N_{eq}|M)$ of each regression equation are tabulated in Table 5.1. The results for S_L = 65%, 75%, and 85% are plotted in Figs. 5.3, 5.4 and 5.5. For comparison, the N_{eq} versus M relationships proposed by Seed and Idriss (72) are also plotted in these figures after appropriate modification. Seed and Idriss suggested that when $S_L = 0.65$, the number of equivalent cycles be 10, 20 and 30 cycles, corresponding to the earthquake magnitudes of 7.0, 7.5 and 8.0, respectively. The following observations can be made from these figures: (i) the effect of variation of

Table 5.1 Regression Equations Between N_{eq} and M, $M \geq 5.0$

$E(N_{eq} \mid M=m) = A+Bm+Cm^2$							
Equation No.	S_L	Soil Strength Curve	A	B	C	$VAR(N_{eq} \mid M)$	No. of Data Points
1	0.65	+75% of data	219.53	-74.40	6.821	162.82	69
2	0.65	Mean	174.56	-59.91	5.448	78.68	69
3	0.65	-75% of data	169.58	-58.52	5.301	66.10	69
4	0.75	+75% of data	91.95	-31.15	2.870	31.92	69
5	0.75	Mean	106.08	-36.42	3.312	29.05	69
6	0.75	-75% of data	120.02	-41.41	3.751	33.06	69
7	0.85	+75% of data	48.82	-16.54	1.517	8.07	69
8	0.85	Mean	66.39	-22.88	2.102	14.44	69
9	0.85	-75% of data	91.98	-31.72	2.872	19.27	69

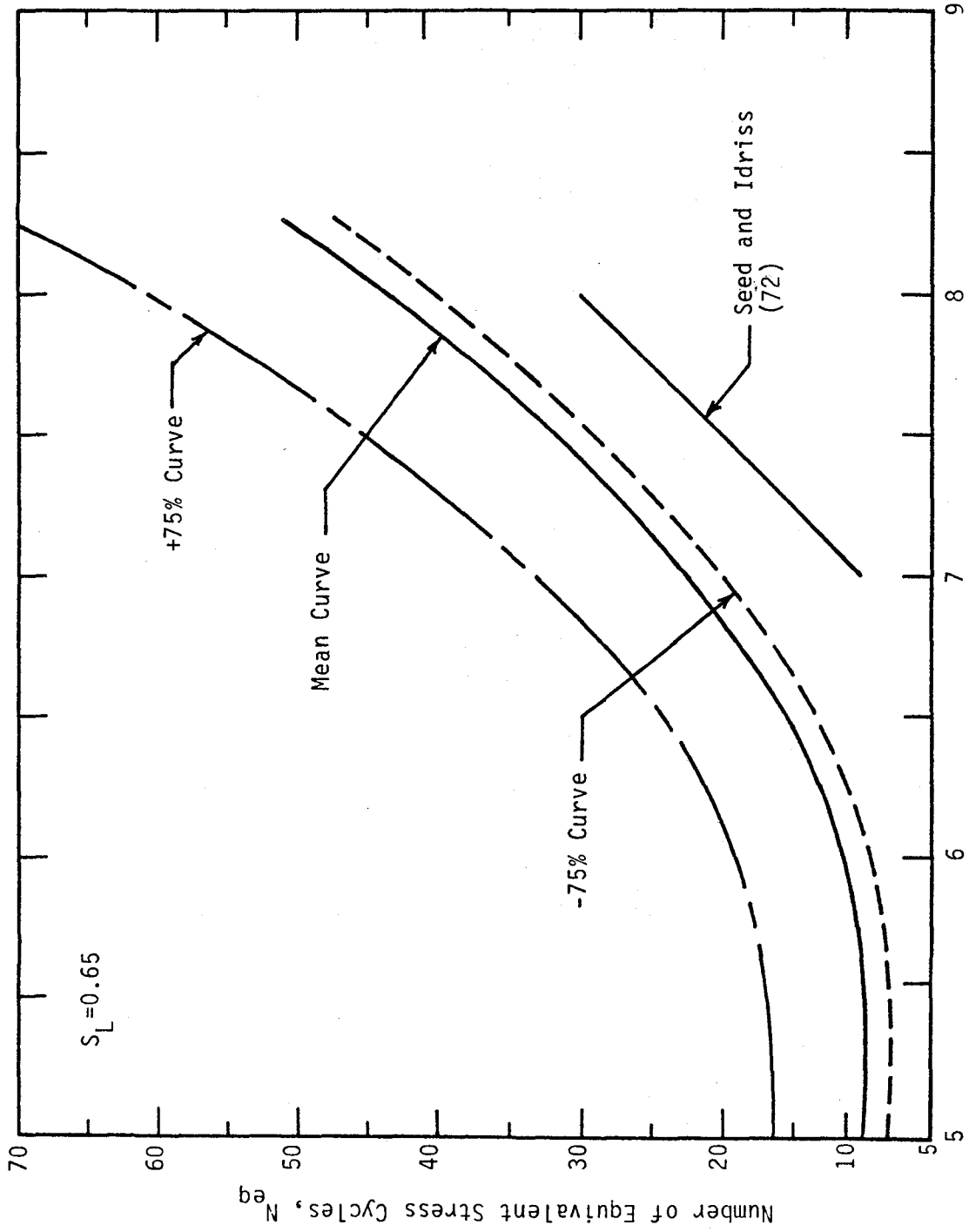

Fig. 5.3 Relationship Between N_{eq} and M, S_L = 0.65

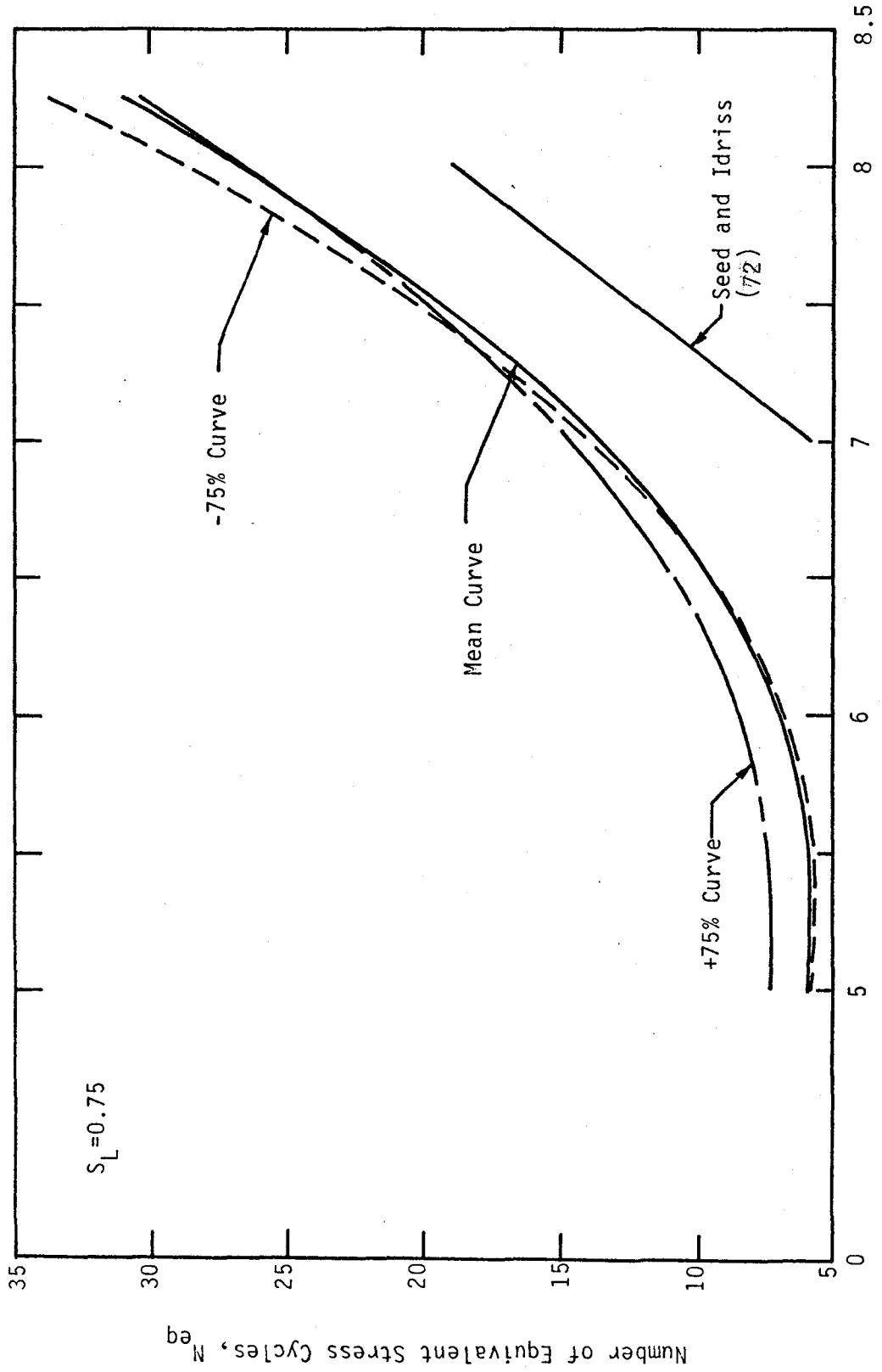

Fig. 5.4 Relationship Between N_{eq} amd M, S_L = 0.75

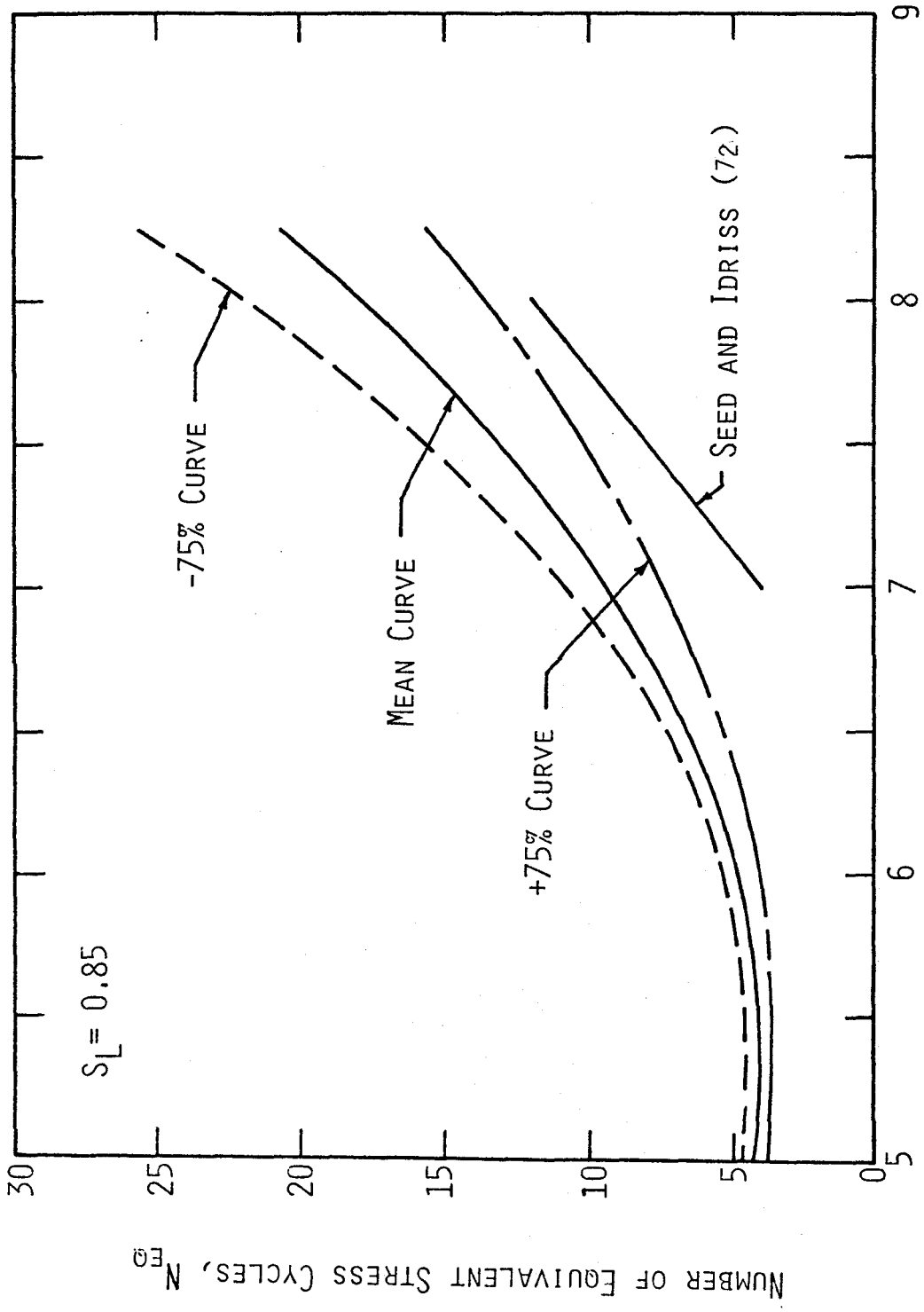

Fig. 5.5 Relationship Between N_{eq} and M, S_L = 0.85

the soil strength curves on the N_{eq} versus M relationship is minimum when $S_L = 0.75$, and (ii) Seed and Idriss' suggested relationship underestimates the value of N_{eq} for a given magnitude earthquake.

The first observation is very interesting. The closeness of the three curves in Fig. 5.4 indicates that the uncertainty in the soil strength curve would not have a significant effect on the N_{eq} versus M relationship, if the stress level chosen is 0.75. Thus, it is proposed here that Eq. 5 of Table 5.1 be considered as an acceptable relationship between N_{eq} and M. The relationship can be represented as

$$E\ (N_{eq} \mid M = m) = 106.08 - 36.42\ m + 3.312\ m^2;\ m \geq 5.0 \qquad (5.12)$$

and the corresponding $\text{Var}\ (N_{eq} \mid M) = 29.05$. When the earthquake magnitude is 7.0, the corresponding expected or mean value of N_{eq} will be about 13.4 cycles with $S_L = 0.75$; whereas there is about 70% probability that N_{eq} will be between 8 and 19 cycles. This scatter is considerable.

The second observation indicates that Seed and Idriss's suggested relationship underestimates the value of N_{eq} for a given magnitude earthquake. The implication of this observation may not be as significant as it appears to be. This will be discussed in further detail later.

5.3.4.4 Influence of Lower Bound Earthquake Magnitude on the N_{eq} versus M Relationship

The data sets used to obtain the regression equations given in Table 5.1 include the earthquakes of magnitudes between 5.0 and 8.25. In many engineering problems, where strong motion earthquakes are of primary concern, earthquakes with magnitudes less than 6 may not be relevant. To study the significance of the lower bound earthquake magnitude on the

N_{eq} versus M relationship, another set of data where M is greater than 6.0 is considered. Again, 9 sets of data on pairs of N_{eq} and M values can be generated for this reduced sample of 49 earthquakes, considering S_L = 0.65, 0.75, and 0.85, and the average and $\pm$ 75% of data soil strength curves. The regression analysis given by Eq. 5.11 is performed on each set of data. The results are presented in Table 5.2.

The regression curves thus obtained can be plotted similar to Figs. 5.3, 5.4 and 5.5. When plotted, they exhibit the same characteristics as mentioned in the previous two sections and are not presented here. In Fig. 5.6, the N_{eq} versus M relationships based on the mean soil strength curve and S_L = 75% are plotted for the cases $M \geq 6.0$. The proximity of the two curves suggests that the N_{eq} versus M relationship for mean soil strength curve and S_L = 75%, shown in Fig. 5.4 could be used for all practical purposes.

5.3.4.5 $N_{eq_{max}}$ versus M Relationship

The N_{eq} value for the two horizontal accelerograms can be calculated in two ways: (i) by considering the accelerogram containing the maximum acceleration a_{max}, or (ii) by considering the accelerogram giving the maximum value of N_{eq}. All discussions made so far were based on alternative (i). To study alternative (ii), the larger of the two values is designated $N_{eq_{max}}$, and a regression analysis (Eq. 5.11) is performed. The relationship between $N_{eq_{max}}$ and M based on the mean soil strength curve and S_L = 0.75 is plotted in Fig. 5.6, along with two other curves for comparison. The difference is not significant, especially in view of the large values of var (N_{eq} | M=m). Since a_{max} is the main design input parameter in the evaluation of liquefaction potential, it is perhaps satisfactory

Table 5.2 Regression Equations Between N_{eq} and M, $M \geq 6.0$

$E(N_{eq} \mid M=m) = A+Bm+Cm^2$							
Equation No.	S_L	Soil Strength Curve	A	B	C	$VAR(N_{eq} \mid M)$	No. of data Points
1	0.65	+75% of data	277.64	-91.15	8.017	187.14	49
2	0.65	Mean	271.16	-87.35	7.379	88.74	49
3	0.65	-75% of data	283.17	-90.71	7.562	73.62	49
4	0.75	+75% of data	108.96	-36.13	3.230	36.48	49
5	0.75	Mean	164.32	-52.96	4.476	32.83	49
6	0.75	-75% of data	200.15	-64.12	5.346	36.84	49
7	0.85	+75% of data	62.18	-20.40	1.791	9.24	49
8	0.85	Mean	85.18	-28.31	2.490	16.48	49
9	0.85	-75% of data	152.83	-48.97	4.083	21.53	49

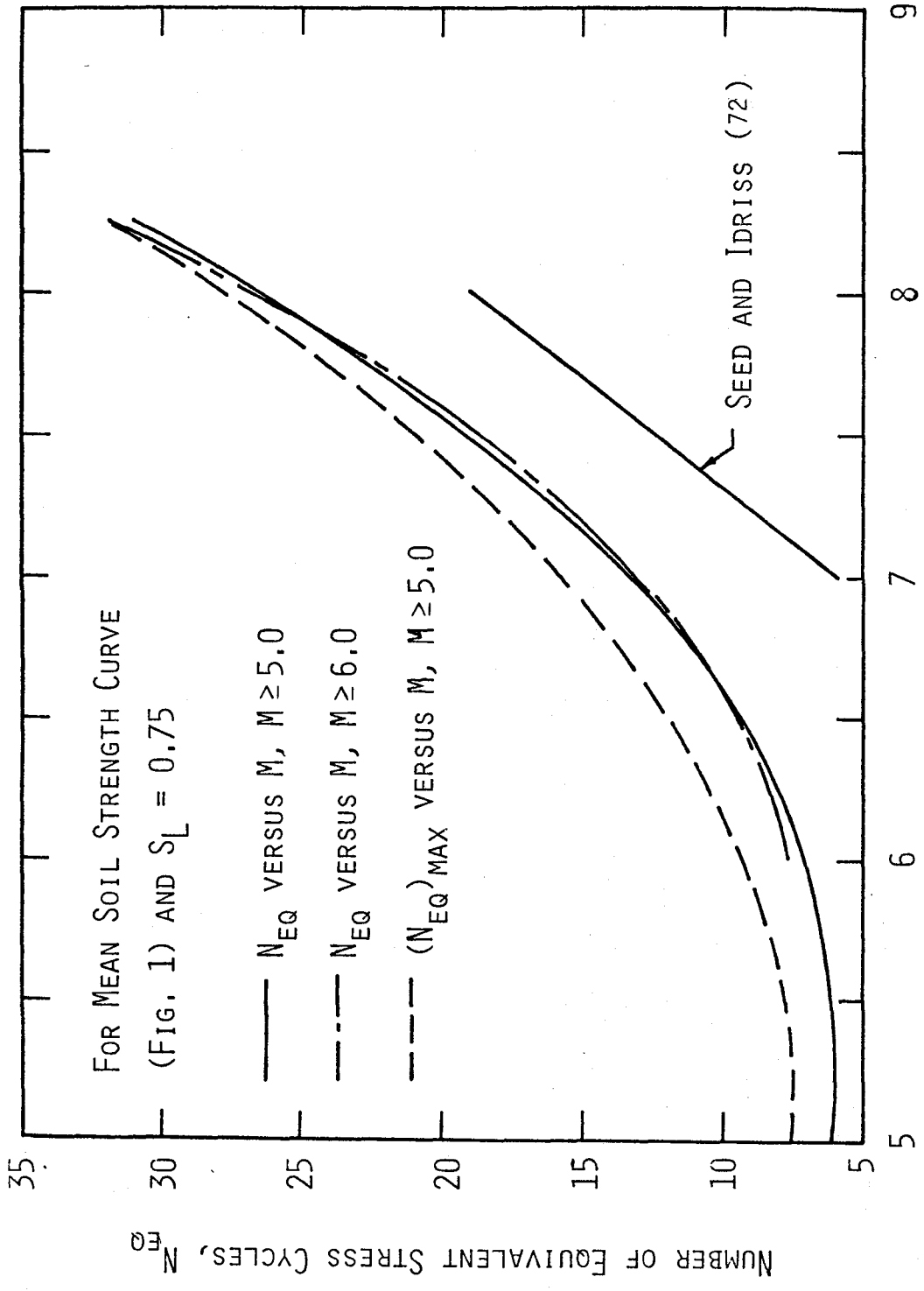

Fig. 5.6 Comparison of N_{eq} Versus M Relationship for Various Criteria, S_L = 0.75

to compute N_{eq} considering the accelerogram containing a_{max}.

5.3.4.6 Conclusion

It is proposed here that the intensity of the uniform stress should be taken as 75% of the maximum stress. It is also shown that N_{eq} could be estimated adequately by considering the component of excitation containing the peak acceleration. The expected number of cycles $E(N_{eq} \mid M)$ can be found from the following regression equation for a given design magnitude of earthquake:

$$E(N_{eq} \mid M=m) = 106.08-36.42m + 3.312\ m^2$$

$$5.0 \leq M \leq 8.25 \qquad (5.13)$$

and the corresponding $Var(N_{eq} \mid M) = 29.05$. When M is less than 5.0, N_{eq} is assumed to be 6.0 cycles.

For the sake of completeness, a corrective factor N_m of mean 1.0 and COV of 0.05 may be introduced to represent any prediction error associated with the form of equation assumed in Eq. 5.11. It can be shown that $E(N_{eq} \mid M=m)$ is still given by Eq. 5.13. The uncertainty in N_{eq} for a given value of m can be calculated in the following way:

$$\Omega_{N_{eq}|M=m} = \sqrt{0.05^2 + \frac{29.05}{[E(N_{eq} \mid M=m)]^2}} \qquad (5.14)$$

5.3.5 Density Function of N_{eq}

For a given value of an earthquake magnitude, say m, the expected

value of N_{eq}, say n_{eq}, can be obtained from Eq. 5.13. Eq. 5.13 can be rewritten as

$$m = 5.5 + \frac{1}{2}\sqrt{1.21n_{eq} - 7.20} \tag{5.15}$$

If the density function of M is known, the density function of N_{eq} can be determined by the following equation (2):

$$f_{N_{eq}}(n_{eq}) = f_{M_{max}}(m)\left|\frac{dm}{dn_{eq}}\right| \tag{5.16}$$

where $f_{M_{max}}(m)$ can be evaluated from Eqs. 5.9 and 5.15, and

$$\left|\frac{dm}{dn_{eq}}\right| = \frac{1.21}{4}(1.21n_{eq} - 7.20)^{-\frac{1}{2}};\ n_{eq} \geq 6.0 \tag{5.17}$$

Thus, combining Eqs. 5.9, 5.15, and 5.17, Eq. 5.16 can be rewritten as

$$f_{N_{eq}}(n_{eq}) = C\left[\exp\left\{-\nu \exp[-\beta(5.5 + \frac{1}{2}\sqrt{1.21n_{eq} - 7.20})]\right\}\right]$$
$$\times \left[\nu\beta \exp\left\{-\beta(5.5 + \frac{1}{2}\sqrt{1.21n_{eq} - 7.20})\right\}\right]$$
$$\times \left[\frac{1.21}{4}(1.21n_{eq} - 7.20)^{-\frac{1}{2}}\right];\ n_{eq} \geq 6.0 \tag{5.18}$$

5.4 Maximum Acceleration

The maximum acceleration a_{max} at a particular site may be estimated by identifying all potential sources of earthquakes in the vicinity of the site. Consideration should be given to the earthquake magnitude, the distance of each source of earthquakes from the site, the direction of fault slip, if any, and the attenuation equation applicable for the region under consideration. The objective of this section is to determine the maximum acceleration a_{max} such that the probability of exceeding this intensity at the site is within a specified limit.

Suppose an earthquake has occurred in a potential source. The magnitude and location of this earthquake is not necessarily known. Several researchers (10, 14) have studied this problem. Anlaytical models were proposed by Cornell (10) and by DerKiureghian and Ang (14), considering different types of sources (i.e., fault lines, areal sources, and point sources), each having the magnitude distribution and activity rate assessed based on statistical data. They also used an attenuation equation to relate site intensity to magnitude and focal distance. Cornell's model does not consider that tectonic earthquakes are caused by the sudden release of built-up elastic strain in the earth's crust and originate as slips along geologic faults. He assumed that the energy released during an earthquake is concentrated at a point. DerKiureghian and Ang's model instead assumed that the slip length for a large earthquake may be several hundred kilometers, and the greatest contribution to the intensity at the site might be caused by the slip that was closest to the site. Since DerKiureghian and Ang's model (line source model) is more general, and Cornell's model (point source model) is a special case of the line source model, the former is chosen for this reliability study. Section 5.4.1 summarizes the concepts and results presented in DerKiureghian and Ang's (14) report that are pertinent to the present liquefaction study. For details, their report should be referred to.

5.4.1 Line Source Model, Distribution Function of A_{max}

The potential sources of earthquakes can be divided into three types:

(i) Type 1 source; this type of source is a recognized, well-defined fault. The length, direction, and position of the fault relative to the

site are known.

(ii) Type 2 source; in this category, only the fault direction is known. The exact location of the fault relative to the site is unknown.

(iii) Type 3 source; the fault locations as well as their directions are unknown in this type of source.

The seismic risk analysis for each type of source will be different. However, the general mathematical formulation for seismic risk analysis for all three types of sources is summarized as follows.

Assume there are n potential earthquake sources around a given site. Let ν_i be the average number of earthquakes per year with magnitudes greater than or equal to m_o. Then the average number of earthquakes in a year for the entire region would be:

$$\nu = \sum_{i=1}^{n} \nu_i \tag{5.19}$$

If an earthquake occurs somewhere in the region, the probability that the random intensity of the acceleration A_{max} at the site will exceed some value a_{max} is then

$$P(A_{max} > a_{max}) = \sum_{i=1}^{n} P(A_{max} > a_{max} \mid E_i)\, P(E_i) \tag{5.20}$$

where E_i is the occurrence of the earthquake in source i.

Assuming the average occurrence rate in source i relative to the rate of the whole region remains constant with time, $P(E_i)$ can be determined as follows:

$$P(E_i) = \frac{\nu_i}{\nu} \tag{5.21}$$

It is also assumed that the occurrence of earthquakes in the region constitutes a Poisson process, with the average occurrence rate ν per year. Considering that in any given year, there could be any number of

earthquakes in the region, the cumulative distribution of the annual maximum acceleration A_{max} can be expressed as:

$$F_{A_{max}}(a_{max}) = \sum_{j=1}^{\infty} P(A_{max}<a_{max} \mid j \text{ earthquakes}) \times P(j \text{ earthquakes}) \tag{5.22}$$

where

$$P(A_{max}<a_{max} \mid j \text{ earthquakes}) = [1-P(A>a_{max})]^j \tag{5.23}$$

and

$$P(j \text{ earthquakes}) = \frac{\nu^j e^{-\nu}}{j!} \tag{5.24}$$

Therefore,

$$F_{A_{max}}(a_{max}) = \sum_{j=1}^{\infty} [1-P(A_{max}>a_{max})]^j \frac{\nu^j e^{-\nu}}{j!}$$

$$= \exp[-\nu P(A_{max}>a_{max})] \tag{5.25}$$

Now, combining Eqs. 5.20, 5.21, and 5.25

$$F_{A_{max}}(a_{max}) = \exp\left[-\sum_{i=1}^{n} P(A_{max}>a_{max} \mid E_i)\nu_i\right] \tag{5.26}$$

Hence, the probability of the intensity exceeding a_{max} in a year is

$$P(A_{max}>a_{max}) = 1-\exp\left[-\sum_{i=1}^{n} P(A_{max}>a_{max} \mid E_i)\nu_i\right] \tag{5.27}$$

The corresponding return period would be

$$T_{a_{max}} = \left\{1-\exp\left[-\sum_{i=1}^{n} P(A_{max}>a_{max} \mid E_i)\nu_i\right]\right\}^{-1} \tag{5.28}$$

The probability $P(A_{max}>a_{max} \mid E_i)$ in Eqs. 5.20 through 5.28 can be determined for each type of source, with the following assumptions:

(i) The relative frequency of earthquake magnitudes in a region follows Richter's law of mangitudes. Hence, the distribution function of the magnitude of a given earthquake can be derived from Eq. 5.3 and shown to be

$$F_M(m) = \frac{1-e^{-\beta(m-m_o)}}{1-e^{-\beta(m_u-m_o)}} \; ; \; m_o < m < m_u \tag{5.29}$$

(ii) The distribution of the focal location is uniform over the source (either a fault line or an area).

(iii) An earthquake originates as a slip propagating symmetrically on each side of the focus along the fault, and the slip length is a function of the earthquake magnitude. The length of the slip on each side of the focus can be estimated from the following expression:

$$S = \frac{1}{2} \exp(aM-b) \tag{5.30}$$

where S is one-half of the slip length, M is the magnitude of the earthquake, and a and b are constants.

(iv) The attenuation formula is assumed to have the general form $y = f_1(m,r)$, in which m is the magnitude and r is the shortest distance from the site to the slip. The form of equation generally used, as summarized in Table 5.3, can be represented by:

$$Y = b_1 e^{b_2 m} (r+25)^{-b_3} \tag{5.31}$$

it is also assumed that the inverse functions $m = f_2(y, r)$ and $r = f_3(y,m)$ are available.

(v) The average depth of the focus may vary from source to source, but it is assumed to be known in an area.

Table 5.3 Ground Motion Attenuation Equations (from Ref. 25)

Eq.	Ref.	Author	$y=f(m,r)$	$m=g_1(y,r)$	$r=g_2(y,m)$	δ_1	σ
1	102	Donovan	$a=1320e^{0.58m}(r+25)^{-1.52}$	$m=1.72\ln\frac{a(r+25)^{1.52}}{1320}$	$r=113a^{-0.66}e^{038m}-25$	0.84	0.894
2	103	Donovan	$a=1080e^{0.50m}(r+25)^{-1.32}$	$m=2.0\ln\frac{a(r+25)^{1.32}}{1080}$	$r=197a^{-0.76}e^{0.38m}-25$	0.707	0.755
3	104	McGuire	$a=472.3e^{0.64m}(r+25)^{-1.301}$	$m=1.56\ln\frac{a(r+25)^{1.301}}{472.3}$	$r=114a^{-0.77}e^{0.49m}-25$	0.51	0.573
4	104	McGuire	$v=5.64e^{0.924m}(r+25)^{-1.202}$	$m=1.08\ln\frac{v(r+25)^{1.202}}{5.64}$	$r=4.21v^{-0.83}e^{0.77m}-25$	0.63	0.674
5	104	McGuire	$d=0.393e^{m}(r+25)^{-0.885}$	$m=\ln\frac{d(r+25)^{0.885}}{0.393}$	$r=0.348d^{-1.13}e^{1.13m}-25$	0.76	0.780

y = intensity

a = maximum ground acceleration, cm/sec^2

v = maximum ground velocity, cm/sec

d = maximum ground displacement, cm

m = earthquake magnitude in Richter scale

r = shortest distance of site to slipped area

δ_1 = standard deviation of $\ln X_1$ (representing the uncertainty in the attenuation equation)

σ = standard deviation of Z (representing the uncertainty in both the attenuation equation and slip length equation)

Using the aforementioned information, Eq. 5.22 can be solved for each type of source. This will give the annual probability distribution function of A_{max}, i.e., it will give the annual probability that A_{max} will be less than a_{max}.

5.4.2 Density Function of A_{max}

A typical result from the study mentioned in Section 5.4.1 would be acceleration in terms of return period or annual probability of exceedence of the given acceleration as shown in Fig. 5.7. Fig. 5.7 is developed for the San Francisco Bay Area, California. DerKiureghian and Ang (14) summarized all the information necessary to develop the figure. Similar curves can be obtained for other sites.

Fig. 5.7 is essentially a graphical representation of Eq. 5.27 for the San Francisco Bay area. For the simplicity of the discussion, the relationship shown in Fig. 5.7 can be expressed mathematically as

$$\ell n[P(A_{max} > a_{max})] = - 0.12202 - 18.013a_{max} = 24.291a_{max}^2 - 13.703a_{max}^3 \quad (5.32)$$

Thus, the density function of A_{max} can be obtained from Eq. 5.32 as

$$f_{A_{max}}(a_{max}) = [\exp(-0.12202 - 18.013a_{max} + 24.291a_{max}^2 - 13.703a_{max}^3)][+ 18.013 - 2 \times 24.291a_{max} + 3 \times 13.703 \cdot a_{max}^2] \quad (5.33)$$

Since Eq. 5.32 represents only a best fit curve, Eqs. 5.32 and 5.33 should be multiplied by a factor of [1.0/exp(-0.12202)] to make the area under the density curve of A_{max} unity. Thus, for all practical purposes

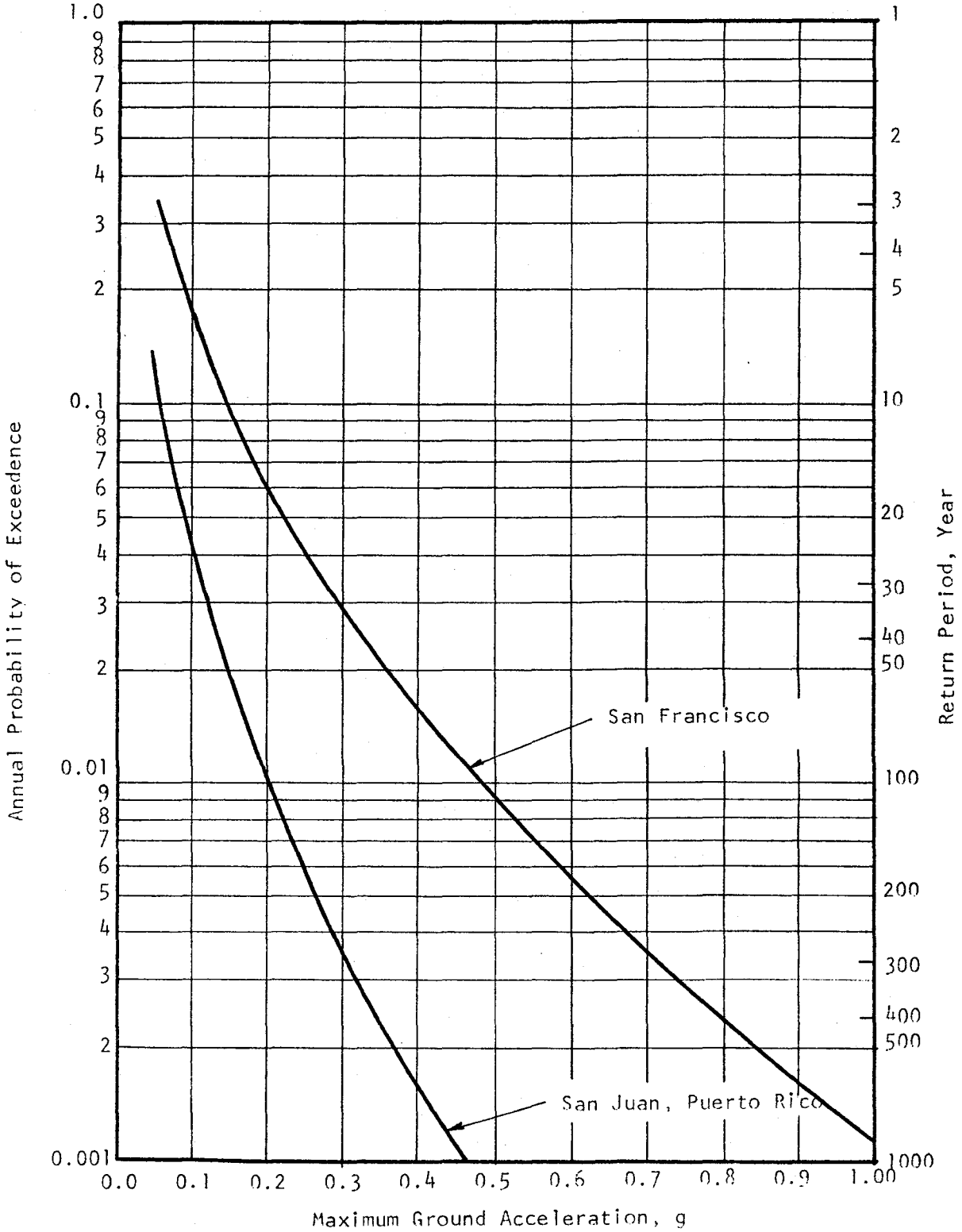

Fig. 5.7 Estimated Risks for Maximum Ground Acceleration for San Francisco and San Juan, Puerto Rico (from Ref. 25)

purposes, the density function of A_{max} for the San Francisco Bay area can be expressed as

$$f_{A_{max}}(a_{max}) = [\exp(0.12202)]\,[\exp(-0.12202 - 18.013a_{max} + 24.291a_{max}^2 - 13.703a_{max}^3)]\,[+18.013 - 48.582a_{max} + 41.109a_{max}^2] \quad (5.34)$$

5.5 Stress Reduction Coefficient r_d

In Chapter 3, Eq. 3.35, the stress reduction coefficient r_d was introduced. Seed and Idriss (72) reported a range of values of r_d, calculated for a wide variety of earthquake motions and soil conditions having sand in the upper 50 ft. This result has been reproduced in Fig. 5.8. The maximum value of r_d is 1.0 at the ground surface. At other depths, the value of r_d is less than 1.0. The average values of r_d are shown as a dotted line in Fig. 5.8, for depths of up to 50 ft. The average curve can be mathematically represented by the following equation:

$$\mu_{r_d} = 10^{-4}(9995.7 - 22.857h + 0.707h^2 - 0.025h^3) \quad (5.35)$$

where h is the depth under consideration in feet.

The uncertainties in r_d values can be estimated by considering the upper and lower bounds of r_d values at a particular depth. From Fig. 5.8 it is seen that the values of r_d vary between 0.985 and 0.94, with mean = 0.963 at a depth of 20 ft. Assuming a uniform distribution of r_d between the two bounds, the standard deviation of r_d at a depth of 20 ft. is found to be about 0.0058. Similarly, the standard deviations of r_d at other depths can be calculated. The following equation represents the change of σ_{r_d} as a function of depth h:

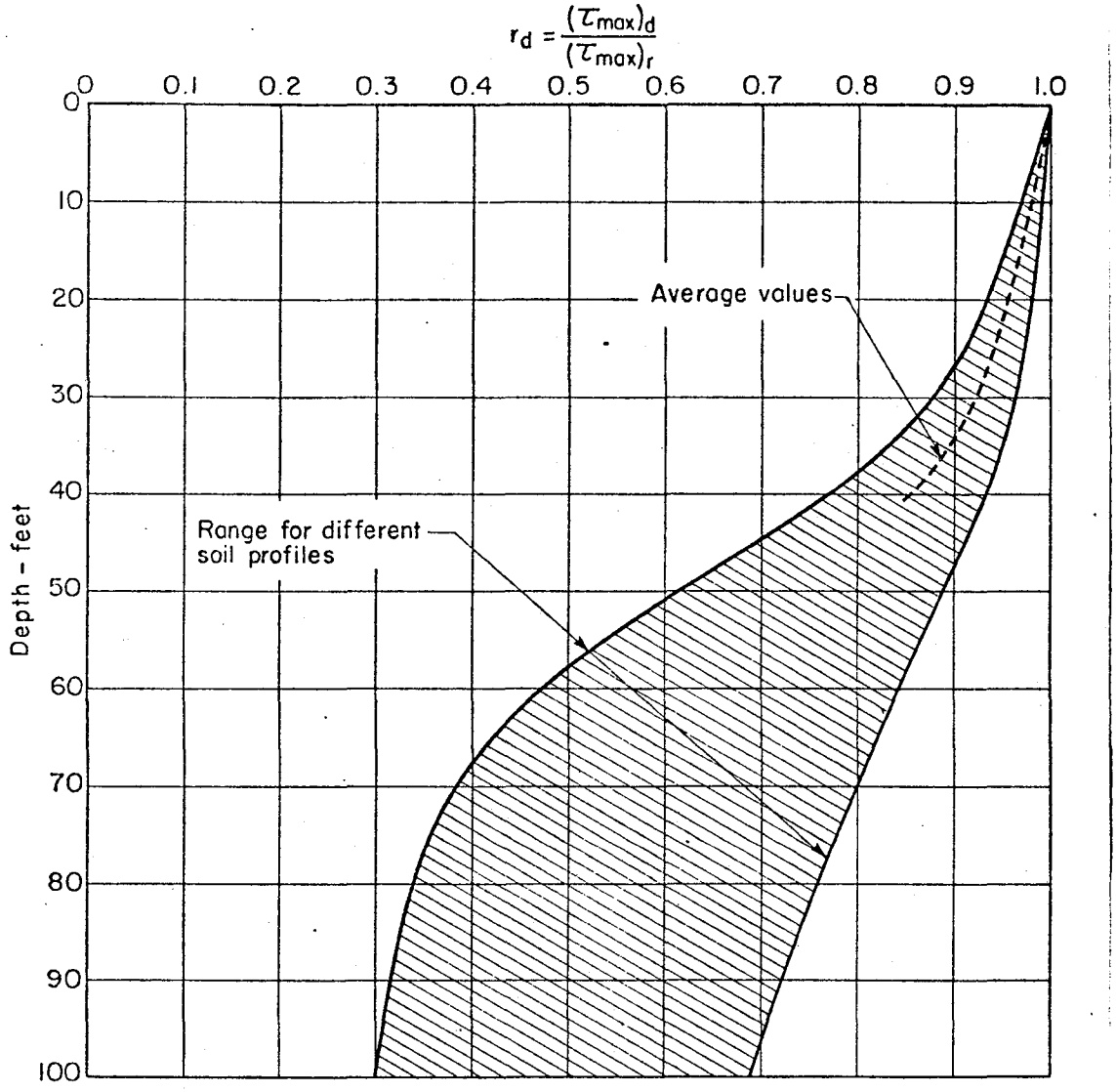

Fig. 5.8 Range of r_d for Different Soil Profiles (from Ref. 72)

$$\sigma_{r_d} = \exp\left(\frac{h-84}{14.5}\right) \tag{5.36}$$

In short, the mean value and the standard deviation of r_d at any given depth can be calculated from Eqs. 5.35 and 5.36, respectively.

Chapter 6

PROBABILISTIC DESIGN PROCEDURES

6.1 General Remarks

The results of the analysis of uncertainties on the relevant parameters from Chapters 4 and 5 can be incorporated into the reliability model developed in Chapter 3 to evaluate the probability of liquefaction of a soil stratum. In the following sections, the probability of liquefaction of a site at a particular depth will be estimated by first calculating the relative density from SPT-values. Since the relationship proposed by Haldar and Miller to indirectly estimate the relative density from SPT-values is valid for a normally consolidated homogeneous soil deposit, the procedure outlined here should not be used for over-consolidated soil. If it is found from this preliminary study that the site is susceptible to liquefaction, the direct method discussed in Section 4.2.2 should be performed to estimate the in situ relative density. Furthermore, it is also desirable that the Haldar-Miller relationship be calibrated whenever possible to consider the site-specific characteristics from the information on direct in-place measurements of dry unit weight.

To estimate the liquefaction potential of a volume of soil, the scales of fluctuation in the three directions need to be known. They are assumed to be known in this study. However, they will be studied in detail in the subsequent study.

Information on the maximum and minimum dry unit weights of the deposit need to be known to use the proposed model. Although cases of

liquefaction or no-liquefaction are reported in the literature (25, 29, 72), the information on limiting densities are not available in most cases. This limitation makes verification of the proposed model difficult. The proposed model will be verified in detail in the subsequent study. In the following section, an example is given to elaborate the steps involved in the proposed liquefaction model. A general design procedure for finding the probability of liquefaction of a site located in the San Francisco Bay area is developed and illustrated in Section 6.4.

6.2 Probability of Liquefaction, a_{max} and M are Known

A site in Niigata, Japan which liquefied during the 1964 earthquake is considered here. The magnitude of the earthquake was 7.5 and the site experienced 0.16 g maximum ground accelaration (72). The SPT-value of 6 was measured at the critical depth 25 ft. The depth of the water table was 3 ft. from the ground surface. The saturated unit weight and the mean grain size, D_{50}, were considered to be 120 pcf and 0.26 mm, respectively (25). The maximum and minimum dry densities of the deposit are considered to be 102.7 pcf and 81.5 pcf, respectively from indirect information. The scales of fluctuation, Θ_x, Θ_y, and Θ_z cannot be estimated for the site. The scales of fluctuation in the two horizontal directions are assumed to be the same. Θ_x, Θ_y, and Θ_z are considered to be 120 ft., 120 ft., and 7 ft., repsectively. The volume of the liquefied sand is assumed to be 200 ft. x 200 ft. x 5 ft. The COV of γ_s and h_{WT} can be taken as 0.01 and 0.20, respectively. The following summarizes the steps in the computation procedure.

(i) Effective Vertical Stress, σ'_v

Using Eqs. 4.44 and 4.45,

$$\bar{\sigma}'_v = 120x25 - 62.5(25-3) = 1625 \text{ psf.}$$

and

$$\Omega_{\sigma'_v} = \frac{\sqrt{25^2 x(0.01x120)^2 + (0.20x3)^2 x62.5^2}}{1625} = 0.0296$$

(ii) Mean Effective Stress, σ'_m

Using Eq. 4.46,

$$\sigma'_m = \frac{(1 + 2 \times 0.4)}{3} \times 1625 = 975 \text{ psf}$$

and

$$\Omega_{\sigma'_m} = 0.0296$$

(iii) In-Place Dry Density, γ

For N = 6 blows/ft., $\gamma_{max} = 102.7$ pcf, $\gamma_{min} = 81.5$ pcf, and $\bar{\sigma}'_v = 1.625$ ksf, using Eq. 4.12,

$$\bar{\gamma} = \frac{5.50116 + 6^{1/2} + 0.3228 \times 81.5 - 0.06053x(102.7-81.5)}{0.36243 + 0.00278 \times 1.625} = 89.9 \text{ pcf}$$

Eq. 4.13 yields

$$\text{Var } (\gamma) = \frac{0.183}{(0.36243 + 0.00278 \times 1.625)^2} = 1.359$$

Thus,

$$\Omega_\gamma = \frac{\sqrt{1.359}}{89.9} = 0.01297$$

(iv) Relative Density, D_r

Using Eq. 4.14,

$$\bar{D}_r = \frac{102.7}{89.9} \times \frac{(89.9 - 81.5)}{(102.7 - 81.5)} = 0.453$$

From Eq. 4.16,

$$E_3 = \left[\frac{\frac{81.5}{102.7 - 81.5} + 1}{0.453} \right] - 1.0$$

$$= 9.694$$

Using Eqs. 4.15 and 4.19,

$$\delta_{D_r} = 9.694 \times 0.01297 = 0.1257$$

and

$$\Delta_{D_r} = 0.95393 - 1.62679 \times 0.453 + 0.85357 \times 0.453^2$$

$$= 0.3922$$

$$\Omega_{D_r} = \sqrt{0.1257^2 + 0.3922^2} = 0.412 \text{ (point estimation)}$$

(v) Variance Reduction Factor

Using Eq. 3.56,

$$\Gamma^2(\Delta x) = \Gamma^2(\Delta y) = 120/200 = 0.60$$

$$\Gamma^2(\Delta z) = 7/5 = 1.0$$

$$\Gamma^2(\Delta v) = 0.6 \times 0.6 \times 1.0 = 0.36$$

$$\Gamma(\Delta v) = 0.6$$

(vi) Statistics of D_r in a volume

$$\bar{D}_r = 0.453$$

$$\Omega_{D_r} = 0.6 \times 0.412 = 0.247$$

(vii) N_{eq} Corresponding to $S_L = 0.75$

Using Eqs. 5.13 and 5.14,

$$E(N_{eq} \mid M = 7.5) = 106.08 - 36.42 \times 7.5 + 3.312 \times 7.5^2 = 19.23$$

$$\Omega_{(N_{eq} \mid M = 7.5)} = \sqrt{0.05^2 + \frac{29.05}{19.23^2}} = 0.2847$$

(viii) R Parameter

Using Eq. 4.39,

$$E(R \mid N_{eq}, D_{50}) = 0.9 \times \left[0.7309 - 0.08778 \, Ln(19.23)\right]$$

$$\times(0.750 + 1.01 \times 0.26 - 0.878 \times 0.26^2) = 0.4044$$

and from Eq. 4.42,

$$Var(R \mid N_{eq}, D_{50}) = 0.000610 + (0.10^2 + 0.10^2 + 0.152^2) \times 0.4044^2 +$$

$$0.08778^2 \times 0.2847^2 = 0.00828$$

$$\Omega_{(R \mid N_{eq}, D_{50})} = \frac{\sqrt{0.00828}}{0.4044} = 0.225$$

(ix) Variable r_d

Using Eqs. 5.35 and 5.36,

$$\bar{r}_d = 10^{-4}(9995.7 - 22.857 \times 25 + 0.707 \times 25^2 - 0.025 \times 25^3 = 0.948$$

and

$$\Omega_{r_d} = \frac{\exp\left(\frac{25-84}{14.5}\right)}{0.948} = 0.018$$

(x) Estimation of μ_{τ_R} and Ω_{τ_R}

Using Eqs. 3.45 and 3.46,

$$\mu_{\tau_R \mid N = 19.23} = 1.0 \times 1.0 \times 0.4044 \times \frac{975}{1000} \times 0.453 = 0.1786 \text{ ksf.}$$

and

$$\Omega^2_{\tau_R} = 0.1^2 + 0.225^2 + 0.0296^2 + 0.247^2 = 0.12251$$

(xi) Estimation of μ_{τ_A} and Ω_{τ_A}

In this particular case, $\Omega_{a_{max}} = 0.0$. Thus, using Eqs. 3.42 and 3.43,

$$\mu_{\tau_A} = 0.75 \times 0.948 \times 0.120 \times 25 \times 0.16 = 0.3413 \text{ ksf}$$

and

$$\Omega^2_{\tau_A} = 0.018^2 + 0.01^2 = 0.000424$$

(xii) Risk of Liquefaction

The probability of liquefaction of the critical volume can be shown to be

$$p_f = 1.0 - \Phi \left[\frac{\text{Ln}\left(\frac{0.1786}{0.3413}, \sqrt{\frac{1 + 0.000424}{1 + 0.12251}}\right)}{\sqrt{\text{Ln}\left[(1 + 0.12251)\ (1 + 0.000424)\right]}} \right]$$

$$= 1.0 - \Phi\ (-2.07) = \phi\ (2.07)$$

$$= 0.980774$$

(xiii) Risk of Liquefaction at a Point

All parameters except the COV of τ_R will be the same. In this case

$$\Omega^2_{\tau_R} = 0.1^2 + 0.225^2 + 0.0296^2 + 0.412^2$$

$$= 0.23125$$

The corresponding risk of liquefaction can be shown to be

$$p_f = 1.0 - \Phi \left[\frac{\text{Ln}\left(\frac{0.1786}{0.3413} \sqrt{\frac{1 + 0.000424}{1 + 0.23125}}\right)}{\sqrt{\text{Ln}\left[(1 + 0.23125)\ (1 + 0.000424)\right]}} \right]$$

$$= 1.0 - \Phi(-1.65) = \Phi\ (1.65) = 0.950529$$

6.3 Probability of Liquefaction, M is Known, a_{max} is Estimated

The assumption that both M and a_{max} are known at a particular site, as discussed in Section 6.2, is not justifiable. Even if it is assumed that an upper bound magnitude of m_u has occurred in the region under consideration, it will perhaps be very difficult to estimate the intensity of a_{max} at a particular site. Generally, when the magnitude and the distance of the site from the source are known, the intensity of the acceleration at the site is evaluated with the help of some kind of attenuation equation (see Table 5.3) (10, 14). This is the main source of uncertainty in the estimation of τ_A. It can be shown that the logarithm of the ratio ℓn(a_{max} measured at the site/a_{max} estimated from the attenuation equation) is normally distributed. Considering the uncertainty in the attenuation equation (Eq. 5.31) and the slip length equation (Eq. 5.30), the standard deviation of the logarithm of the above ratio could be between 0.573 and 0.894 (see Table 5.3). Thus, the COV of a_{max} estimated from an attenuation equation could be between 0.62 and 1.11. When a_{max} is estimated, the minimum value of COV of a_{max} may be taken as 0.60, assuming the attenuation equation used is as good as that suggested by McGuire. The methodology developed in Section 6.2 could be used in this case, except that in the calculation of Ω_{τ_A}, $\Omega_{a_{max}} = 0.60$ has to be added. If the uncertainty in a_{max} is added in the example given in Section 6.2, then

$$\Omega_{\tau_A} = 0.000424 + 0.6^2 = 0.360424$$

Thus, when a_{max} is estimated, the revised probability of failure for the given volume of sand will be

$$p_f = 1.0 - \Phi \left[\frac{\text{Ln}\left(\frac{0.1786}{0.3413} \sqrt{\frac{1 + 0.360424}{1 + 0.12251}} \right)}{\sqrt{\text{Ln}\left[(1 + 0.12251)\ (1 + 0.360424 \right]}} \right]$$

$$= 1.0 - \Phi\ (-0.85) = \Phi\ (0.85)$$

$$= 0.802337$$

6.4 Suggested Design Procedure and Application

6.4.1 General Remarks

A probabilistic design procedure should consider the probability of failure given an event has occurred as well as the probability of the occurrence of that event. The procedure described in Section 6.2, where a_{max} and M are assumed to be known, does not consider the probability of occurrence of a_{max} and M. Statistically speaking, the probability of an earthquake of magnitude M producing ground acceleration of a_{max} at a particular site under consideration is small. The following sections describe procedures for incorporating the uncertainties of these parameters into design against liquefaction.

6.4.2 Probabilistic Design Procedure

For given values of a_{max} and N_{eq}, the probability of failure at a site can be estimated (see Section 6.2). Using the theorem of total probability, the probability of failure of a site is obtained as

$$P_f = \int_{(n_{eq})_o}^{(n_{eq})_u} \int_0^{a_{max}} (P_f \mid a_{max}, n_{eq})\ f_{A_{max}, N_{eq}}\ (a_{max}, n_{eq})\ da_{max} dn_{eq} \qquad (6.1)$$

where $f_{A_{max}, N_{eq}}(a_{max}, n_{eq})$ is the joint density function of A_{max} and N_{eq}, and $(n_{eq})_u$ and $(n_{eq})_o$ are the values of N_{eq} corresponding to the upper and lower bound magnitudes of the earthquake. $(P_f | a_{max}, n_{eq})$ can be estimated from Section 6.2. The correlation coefficient of N_{eq} and A_{max} is found to be 0.093 (25). So for all practical purposes, they can be assumed to be statistically independent. With the above observation, Eq. 6.1 can be simplified as

$$P_f = \int_{(n_{eq})_o}^{(n_{eq})_u} \int_0^{a_{max}} (P_f | a_{max}, n_{eq}) f_{A_{max}}(a_{max}) f_{N_{eq}}(n_{eq}) da_{max} dn_{eq} \quad (6.2)$$

$f_{A_{max}}(a_{max})$ and $f_{N_{eq}}(n_{eq})$ can be evaluated using Eqs. 5.34 and 5.18, respectively.

6.4.3 Design Example

The concepts developed in Section 6.4.2 can be better explained by the following illustrations.

A site in the San Francisco Bay Area is considered here. Considering all the available information, the seismic risk of the San Francisco Bay area can be estimated from Eq. 5.34. Assuming the site conditions in this hypothetical site are similar to those considered in Section 6.2, the probability of failure of the site can be estimated for different SPT-values as shown in Fig. 6.1. The figure clearly indicates that the probability of liquefaction decreases as the SPT-values increase.

In addition to the San Francisco site, two other sites are considered. One is a site in San Juan, Puerto Rico which has the same soil conditions as the site in San Francisco. The other is a site designed against lique-

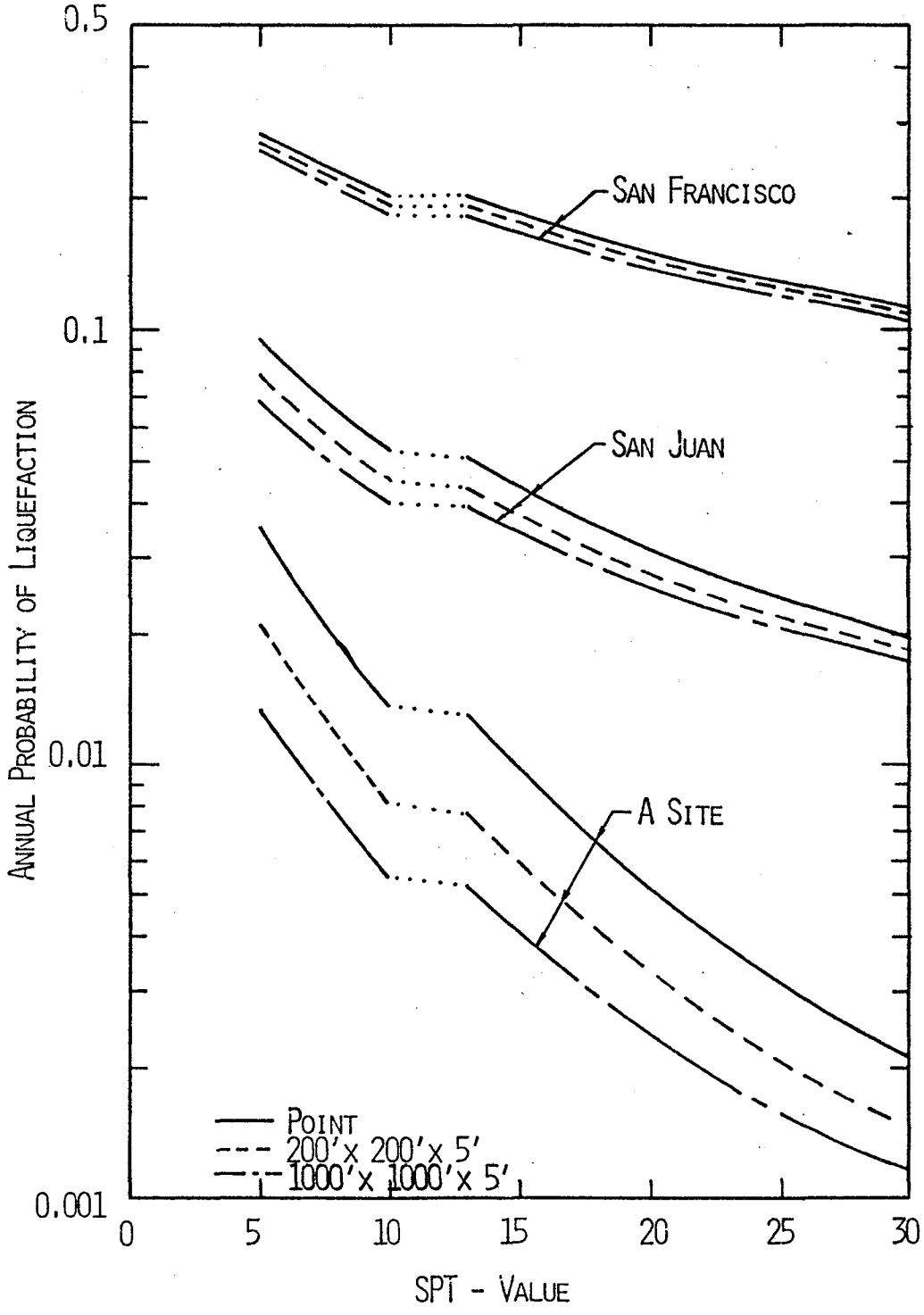

FIGURE 6.1 ESTIMATED ANNUAL PROBABILITY OF LIQUEFACTION

faction. In Fig. 6.1 the annual probabilities of liquefaction for both of these sites are plotted versus SPT-values for various soil volumes. Fig. 6.1 shows that the site in San Juan has a smaller annual risk of liquefaction than the site with the same soil conditions in San Francisco. This result is due to the different seismicities of the two areas. Furthermore, for all three sites, Fig. 6.1 shows that the annual risk of liquefaction decreases with larger liquefiable volumes. The effect of the size of the liquefiable volume of sand on the annual risk of liquefaction is considerable for sites with a small annual risk of liquefaction such as the site designed against liquefaction. This subject will be studied in more detail in the subsequent study.

Chapter 7

SUMMARY AND CONCLUSION

7.1 Summary

The damage associated with earthquake-induced liquefaction needs better understanding, since liquefaction can result in damage to property and the environment and suffering and loss of human life. A probabilistic model is proposed here considering the damage aspect of the problem. Probabilistic and statistical methods are used in this study to develop a simple but efficient and practical probabilistic model by which the risk of liquefaction at a site can be systematically analyzed.

To have a noticeable amount of damage at a referenced location, a minimum volume of sand needs to undergo a considerable amount of strain due to liquefaction. This minimum volume will be studied in detail in the subsequent study. In this study, the soil properties affecting liquefaction potential in a given volume of sand are modeled probabilistically in three dimensions.

The applicability of the proposed probabilistic procedures are limited to normally consolidated, homogeneous soil deposits. Estimation of the probability of liquefaction of an over-consolidated soil deposit is beyond the scope of this study.

The estimation of in situ relative density is an important parameter in the proposed model. In the initial stage of a project, the SPT-value can be used to estimate the in situ D_r value. D_r is an error-prone parameter. Any correlation between D_r and the SPT-value may also be error-

prone. A new relationship, designated as the Haldar and Miller relationship, is proposed here between the SPT-value, in place dry density, limiting densities and effective overburden pressure. The predictability of the Haldar and Miller relationship is superior to other presently available relationships that are commonly used.

The in situ shear resistance of a soil deposit is evaluated here by introducing a parameter R. This parameter is first evaluated using large-scale shaking table test results. Subsequently, the relationship is corrected for the compliance effect, sample preparation methods, mean grain size, multidirectional shaking and for some other secondary factors. The R parameter evaluated in this study is expected to be quite reliable.

The probabilistic characteristics of all other parameters required for the development of the model are evaluated using information available in the literature.

A comprehensive seismic risk analysis of a site is carried out here considering a regional seismicity parameter (β), lower and upper bound magnitudes, average occurrence rates (γ), a ground motion attenuation equation, a slip length magnitude relationship, and the geometric parameters that describe the idealization of the potential sources into one or more types of line sources.

Typical design procedures are illustrated by determining the liquefaction risk of an idealized site in San Francisco, California.

7.2 Principal Results and Conclusions

On the basis of the results obtained from this study, the following

major conclusions can be reached:

(i) The risk of liquefaction at a site needs to be estimated considering the damage aspect of the problem. It is necessary to consider the minimum soil volume that will produce a noticeable amount of damage at the referenced point when it liquefies. Soil properties in that soil volume need to be modeled probabilistically in three dimensions.

(ii) Relative density is one of the important parameters in the proposed model. However, it is an error-prone parameter. A considerable amount of uncertainty is expected in the determination of the in situ relative density. Haldar and Miller's proposed relationship should be used to estimate the in situ relative density indirectly from the SPT-value. The predictability of the Haldar and Miller relationship is superior to other presently available relationships. For sites which are susceptible to liquefaction, a direct determination of the in situ dry density is desirable. This will also help to calibrate the Haldar and Miller relationship considering the site's specific characteristics.

(iii) Uncertainty in the determination of the parameter R, which indicates the normalized shear strength of the soil deposit under cyclic loads, is also high. Additional laboratory test results will be helpful in reducing the prediction error in this parameter. The relationship proposed in this study after considering the effects of compliance, mean grain size, sample preparation, multidirectional shaking, and other secondary factors, is expected to be quite reliable.

(iv) The effects of the secondary factors discussed in Chapter 4 on the laboratory determination of the parameter R need further consideration. Further research is needed in this area.

(v) In the evaluation of the liquefaction potential of a site, it is found that the uncertainties in the load parameters could be higher than those in the resistance parameters. Hence, seismic activity of the region should be given serious consideration in a liquefaction study.

(vi) When selecting the stress level of the equivalent uniform stress cycles, the value of the stress ratio is 0.75 instead of 0.65 as suggested by Seed and Idriss. At this level, the sensitivity effect of different soil strength curves will be minimum.

(vii) The proposed probabilistic model provides information on the relative risk of liquefaction between various design alternatives. This information will be valuable to designers in selecting the appropriate design alternative.

LIST OF REFERENCES

1. Allen, C. R., Nordquist, J. M., Richter, C. F. and Amand, P. St., "Relationship Between Seismicity and Geologic Structure in the Southern California Region," Bulletin of Seismological Society of America, Vol. 55, 1965.

2. Ang, A. H-S, and Tang, W. H., Probability Concepts in Engineering Planning and Design, Vol. 1 - Basic Principles, John Wiley & Sons, Inc., New York, New York, 1975.

3. Annaki, M. and Lee, K. L., "Equivalent Uniform Cycle Concept for Soil Dynamics," Journal of the Geortechnical Engineering Division, ASCE, Vol. 103, No. GT6, Proc. Paper 12991, June 1977, pp. 549-564.

4. ASTM Standard D1586-67, "Penetration Test and Split-Barrell Sampling of Soils."

5. Basore, C. E. and Boitano, J. D., "Sand Densification by Piles and Vibroflotation," Journal of the Soil Mechanics and Foundations Division, ASCE, Vol. 95, No. SM6, November 1969, pp. 1303-1323.

6. Bolt, B. A., "Duration of Strong Ground Motion," Proceedings, Fifth World Conference on Earthquake Engineering, Rome, 1973.

7. Castro, G., "Liquefaction and Cyclic Mobility of Saturated Sands," Journal of the Geotechnical Engineering Division, ASCE, Vol. 101, No. GT6, Proc. Paper 11388, June 1975, pp. 551-569.

8. Castro, G. and Poulos, S. J., "Factors Affecting Liquefaction and Cyclic Mobility," Journal of the Geotechnical Engineering Division, ASCE, Vol. 103, No. GT6, Proc. Paper 12994, June 1977, pp. 501-516.

9. Christian, J. T. and Swiger, W. F., "Statistics of Liquefaction and SPT Results," Journal of the Geotechnical Engineering Division, ASCE, Vol. 101, No. GT11, Proc. Paper 11701, November 1975, pp. 1135-1150.

10. Cornell, C. A., "Engineering Seismic Risk Analysis," Bulletin of Seismological Society of America, Vol. 58, No. 5, October 1968, pp. 1583-1606.

11. Coulter, H. W. and Migliaccio, R. R., "Effects of the Earthquake of March 27, 1964 at Valdez, Alaska," Geological Survey Professional Paper 542-C, U. S. Department of the Interior, 1966.

12. DeAlba, P., Chan, C. K. and Seed, H. B., "Determination of Soil Liquefaction Characteristics by Large-Scale Laboratory Tests," Earthquake Engineering Research Center Report No. EERC 75-14, Universtiy of California, Berkeley, May 1975.

13. deMello, Victor F. B., "The Standard Penetration Test," Proceedings, Fourth Pan-American Conference on Soil Mechanics and Foundation Engineering, San Juan, Puerto Rico, 1971, pp. 1-86.

14. DerKiureghian, A. and Ang, A. H-S., "Fault-Rupture Model for Seismic Risk

Analysis," Bulletin of Seismological Society of America, Vol. 67, No. 4, August 1977, pp. 1173-1194.

15. Donovan, N. C., "A Stochastic Approach to the Seismic Liquefaction Problem," Proceedings, Conference on Statistics and Probability in Soil and Structural Engineering, Hong Kong, September 1971, pp. 513-535.

16. Drnevich, V. P., "Undrained Cyclic Shear of Saturated Sand," Journal of the Soil Mechanics and Foundations Division, ASCE, Vol. 98, No. SM8, Proc. Paper 9134, August 1972, pp. 807-825.

17. Faccioli, E., "A Stochastic Model for Predicting Seismic Failure in a Soil Deposit," Earthquake Engineering and Structural Dynamics, Vol. 1, 1973, pp. 293-307.

18. Fardis, M. N. and Veneziano, D., "Probabilistic Liquefaction of Sands During Earthquakes," Report No. R79-14, Massachusetts Institute of Technology, Cambridge, Mass., March 1979.

19. Feld, J., "The Factor of Safety in Soil and Rock Mechanics," Proceedings, Sixth Int. Conference on Soil Mechanics and Foundation Engineering, Montreal, Vol. 3, 1965.

20. Finn, W. D. L., Bransby, P. L. and Pickering, D. J., "Effect of Strain History on Liquefaction of Sands," Journal of the Soil Mechanics and Foundations Division, ASCE, Vol. 96, No. SM6, Proc. Paper 7670, June 1970, pp. 1917-1934.

21. Finn, W. D. L., Lee, K. W. and Martin, G. R., "An Effective Stress Model for Liquefaction," Journal of the Geotechnical Engineering Division, ASCE, Vol. 103, No. GT6, Proc. Paper 13008, June 1977, pp. 517-533.

22. Finn, W. D. L., Pickering, D. J. and Bransby, P. L., "Sand Liquefaction in Triaxial and Simple Shear Tests," Journal of the Soil Mechanics and Foundations Division, ASCE, Vol. 97, No. SM4, April 1971, pp. 639-659.

23. Finn, W. D. L. and Vaid, Y. P., "Liquefaction Potential From Drained Constant Volume Cyclic Simple Shear Tests," Proceedings, Sixth World Conference on Earthquake Engineering, Vol. 6, New Delhi, India, January 1977, pp. 2157-2162.

24. Gibbs, H. J. and Holtz, W. G., "Research of Determining the Density of Sand by Spoon Penetration Test," Proceedings, Fourth International Conference on Soil Mechanics and Foundations Engineering, Vol. 1, 1957, pp. 35-39.

25. Haldar, A., "Probabilistic Evaluation of Liquefaction of Sand Under Earthquake Motions," thesis presented to the University of Illinois at Urbana, Illinois in 1976, in partial fulfillment of the requirements for the degree of Doctor of Philosophy.

26. Haldar, A., "Liquefaction Study - A Decision Analysis Framework," Journal of the Geotechnical Engineering Division, ASCE, Vol. 106, No. GT12, Proc. Paper 15925, December 1980, pp. 1297-1312.

27. Haldar, A., "Uniform Cycles in Earthquakes: A Statistical Study," Proceedings, International Conference on Recent Advances in Geotechnical Earthquake Engineering and Soil Dynamics, St. Louis, Mo., Vol. I, May 1981, pp. 195-198.

28. Haldar, A., "Statistical and Probabilistic Methods in Geomechanics," NATO - Advanced Study Institute, Lisbon, Portugal, September 1981.

29. Haldar, A. and Tang, W. H., "Probabilistic Evaluation of Liquefaction Potential," Journal of the Geotechnical Engineering Division, ASCE, Vol. 105, No. GT2, Proc. Paper 14374, February 1979, pp. 145-163.

30. Haldar, A. and Tang, W. H., "Uncertainty Analysis of Relative Density," Journal of the Geotechnical Engineering Division, ASCE, Vol. 105, No. GT7, Proc. Paper 14665, July 1979, pp. 899-904.

31. Haldar, A. and Tang, W. H., "Statistical Study of Uniform Cycles in Earthquake Motions," Journal of the Geotechnical Engineering Division, ASCE, Vol. 107, No. GT5, Proc. Paper 16239, May 1981, pp. 577-589.

32. Hoel, P. G., Port, S. C. and Stone, C. J., Introduction to Statistical Theory, Houghton Mifflin Company, Boston, Mass., 1971.

33. Housner, G. W., "Intensity of Ground Shaking Near the Causative Fault," Proceedings, Third World Conference on Earthquake Engineering, Vol. 1, New Zealand, 1965.

34. Isacks, B. and Oliver, J., "Seismic Waves with Frequencies from 1 to 100 Cycles per Second Recorded in a Deep Mine in Northern New Jersey," Bulletin of Seismological Society of America, Vol. 54, 1964.

35. Ishibashi, I. and Sherif, M. A., "Soil Liquefaction by Torsional Simple Shear Device," Journal of the Geotechnical Division, ASCE, Vol. 100, No. GT8, August 1974, pp. 871-888.

36. Ishihara, K. and Li, Sang-Il, "Liquefaction of Saturated Sand in Triaxial Torsion Shear Test," Soils and Foundations, Vol. 12, No. 3, June 1972.

37. Ishihara, K. and Takatsu, H., "Effects of Overconsolidation and K_o Conditions on the Liquefaction of Sands," Soils and Foundations, Vol. 19, No. 4, December 1979, pp. 59-68.

38. Ishihara, K. and Yamazaki, F., "Cyclic Simple Shear Tests on Saturated Sand in Multi-Directional Loading," Soils and Foundations, Vol. 20, No. 1, Tokyo, Japan, March 1980, pp. 47-59.

39. Ishihara, K. and Yasuda, S., "Sand Liquefaction Due to Irregular Excitation," Soils and Foundations, Vol. 12, No. 4, December 1972.

40. Ishihara, K. and Yasuda, S., "Sand Liquefaction Under Random Earthquake Loading Condition," Proceedings, Fifth World Conference on Earthquake Engineering, Rome, Italy, 1973.

41. Ishihara, K. and Yasuda, S., "Sand Liquefaction in Hollow Cylinder Torsion Under Irregular Excitation," Soils and Foundations, Vol. 15, No. 1, Tokyo, Japan, March 1975, pp. 45-59.

42. Kishida, H., "Characteristics of Liquefied Sands During Mino-Owari, Tohnankai, and Fukui Earthquake," Soils and Foundations, Vol. 9, No. 1, 1969, pp. 76-92.

43. Ladd, R. S., "Specimen Preparation and Cyclic Stability of Sands," Journal of the Geotechnical Engineering Division, ASCE, Vol. 103, No. GT6, Proc. Paper 13014, June 1977, pp. 535-547.

44. Lee, K. L. and Chan, K., "Number of Equivalent Significant Cycles in Strong Motion Earthquakes," Proceedings, International Conference on Microzonation, Seattle, Washington, November 1972.

45. Lee, K. L. and Fitton, J. A., "Factors Affecting the Cyclic Loading Strengths of Soil," Vibration Effects of Earthquakes on Soils and Foundation, STP 450, American Society for Testing and Materials, 1969, pp. 71-95.

46. Lee, K. L. and Seed, H. B., "Cyclic Stress Conditions Causing Liquefaction of Sand," Journal of the Soil Mechanics and Foundations Division, ASCE, Vol. 93, No. SM1, Proc. Paper 5058, January 1967, pp. 47-70.

47. Liou, C. P., Streeter, V. L. and Richart, F. E., Jr., "Numerical Model for Liquefaction," Journal of the Geotechnical Engineering Division, ASCE, Vol. 103, No. GT6, Proc. Paper 12998, June 1977 pp. 589-606.

48. Lomnitz, C. and Epstein, B., "A Model for Occurrences of Large Earthquakes," Nature, Vol. 211, August 27, 1966.

49. Lumb, P., "The Variability of Natural Soils," Canadian Geotechnical Journal, Vol. 3, No. 2, 1966.

50. Marcuson, W. F. and Bieganousky, W. A., "Laboratory Standard Penetration Tests on Fine Sand," Journal of the Geotechnical Engineering Division, ASCE, Vol. 103, No. GT6, Proc. Paper 12987, June 1977, pp. 565-588.

51. Marcuson, W. F. and Bieganousky, W. A., "SPT and Relative Density in Coarse Sands," Journal of the Geotechnical Engineering Division, ASCE, Vol. 103, No. GT11, Proc. Paper 13350, November 1977, pp. 1295-1309.

52. Martin, G. R., Finn, W. D. L. and Seed, H. B., "Effects of System Compliance on Liquefaction Tests," Journal of the Geotechnical Engineering Division, ASCE, Vol. 104, No. GT4, Proc. Paper 13667, April 1978, pp. 463-479.

53. Montgomery, D.C. and Peck, E. A., Introduction to Regression Analysis, John Wiley & Sons, Inc., 1981 (in press).

54. Mori, K., Seed, H. B. and Chan, C. K., "Influence of Sample Disturbance on Sand Response to Cyclic Loading," Report No. EERC 77-03, Earthquake Engineering Research Center, University of California, Berkeley, California, January 1977.

55. Morreto, O., "Subsoil Exploration for a Bridge Over the Parana River, Argentina," Geotechnique, Vol. 4, No.4, 1954, pp. 137-142.

56. Mulilis, J. P., Seed, H. B., Chan, C. K., Mitchell, J. K., and Arulanandan, K., "Effects of Sample Preparation on Sand Liquefaction," Journal of the Geotechnical Engineering Division, ASCE, Vol. 103, No. GT2, Proc. Paper 12760, February 1977, pp. 91-108.

57. Ohsaki, Y., "The Effects of Local Soil Conditions upon Earthquake Damage," Proceedings, Seventh International Conference on Soil Mechanics and Foundation Engineering, Mexico City, Mexico, 1969.

58. Ohsaki, Y., "Effects of Sand Compaction on Liquefaction During the Tokachioki Earthquake," Soils and Foundations, Vol. 10, No. 2, June 1970, pp. 112-128.

59. Padilla, J. D. and Vanmarcke, E. H., "Settlement of Structures on Shallow Foundations: A Probabilistic Analysis," Soils Publication No. 334, Department of Civil Engineering, M.I.T., January 1974.

60. Papoulis, A., Probability, Random Variables and Stochastic Processes, McGraw-Hill Book Company, New York, New York, 1965.

61. Peacock, W. H. and Seed, H. B., "Sand Liquefaction Under Cyclic Loading Simple Shear Conditions," Journal of the Soil Mechanics and Foundation Division, ASCE, Vol. 94, No. SM3, Proc. Paper 5957, May 1968, pp. 689-708.

62. Pyke, R. M., Chan, C. K. and Seed, H. B., "Settlement and Liquefaction of Sands under Multi-Directional Shaking," Report No. EERC 74-2, Earthquake Engineering Research Center, University of California, Berkeley, California, February 1974.

63. Richter, C. F., Elementary Seismology, W. H. Freeman and Company, San Francisco, 1958.

64. Roscoe, K. H., "An Apparatus for the Application of Simple Shear to Soil Samples," Proceedings, Third International Conference on Soil Mechanics and Foundation Engineering, Zurich, Vol. 1, 1953.

65. Rosenblueth, E., "Analysis of Risk," Proceedings, Fifth World Conference on Earthquake Engineering, Rome, Italy, 1973.

66. Ross, G. A., Seed, H. B., and Migliaccio, R. R., "Bridge Foundation Behavior in Alaska Earthquake," Journal of the Soil Mechanics and Foundations Division, ASCE, Vol 95, No. SM4, Proc. Paper 6664, July 1969, pp. 1007-1036.

67. Schmertmann, J. H., Discussion on "Standard Penetration Test: Its Uses and Abuses," Journal of the Soil Mechanics and Foundations Division, ASCE, Vol. 92, September 1966, pp. 130-133.

68. Schmertmann, J. H., Discussion on "Simplified Procedure for Evaluating Soil Liquefaction Potential," Journal of the Soil Mechanics and Foundations Division, ASCE Vol. 98, No. SM4, Proc. Paper 8371, April 1972, pp. 430-433.

69. Schnabel, P. B., Lysmer, J. and Seed, H. B., "SHAKE: A Computer Program

for Earthquake Response Analysis of Horizontally Layered Sites," Report No. EERC 72-12, Earthquake Engineering Research Center, University of California, Berkeley, California, December 1972.

70. Seed, H. B., "Soil Liquefaction and Cyclic Mobility Evaluation for Level Ground During Earthquakes," Journal of the Geotechnical Engineering Division, ASCE, Vol. 105, No. GT2, Proc. Paper 14380, February 1979, pp. 201-255.

71. Seed, H. B. and Idriss, I. M., "Soil Liquefaction in the Niigata Earth quake," Journal of the Soil Mechanics and Foundations Division, ASCE, Vol. 93, No. SM3, Proc. Paper 5233, May 1967, pp. 83-108.

72. Seed, H. B. and Idriss, I. M., "Simplified Procedure for Evaluating Soil Liquefaction Potential," Journal of the Soil Mechanics and Foundations Division, ASCE, Vol. 97, No. SM9, Proc. Paper 9371, September 1971, pp. 1249-1273.

73. Seed, H. B. and Lee, K. L., "Liquefaction of Saturated Sands During Cyclic Loading," Journal of the Soil Mechanics and Foundations Division, ASCE, Vol. 92, No. SM6, November 1966, pp. 105-134.

74. Seed, H. B., Mori, K. and Chan, C. K., "Influence of Seismic History on Liquefaction of Sands," Journal of the Geotechnical Engineering Division, ASCE, Vol. 103, No. GT4, Proc. Paper 12841, April 1977, pp. 246-270.

75. Seed, H. B. and Peacock, W. H., "Test Procedures for Measuring Soil Liquefaction Characteristics," Journal of the Soil Mechanics and Foundations Division, ASCE, Vol. 97, No. SM8, Proc. Paper 8330, August 1971, pp. 1099-1119.

76. Seed, H. B., Pyke, R. and Martin, G. R., "Analysis of the Effect of Multidirectional Shaking on the Liquefaction Characteristics of Sands," Report No. EERC 75-41, Earthquake Engineering Research Center, University of Calfornia, Berkely, California, December 1975.

77. Sherif, M.A., Ishibashi, I. and Tsuchiya, C., "Saturation Effects on Initial Soil Liquefaction," Journal of the Geotechnical Engineering Division, ASCE, Vol. 103, No. GT8, August 1977, pp. 914-917.

78. Shibata, T., Yukitomo, H. and Miyoshi, M., "Liquefaction Process of Sand During Cyclic Loading," Soils and Foundations, Vol. 12, No. 1, Tokyo, Japan, March 1972.

79. Silver, M. L. and Park, T. K., "Liquefaction Potential Evaluation from Cyclic Strain-Controlled Properties Tests on Sands," Soils and Foundations, Vol. 16, No. 3, September 1976, pp. 51-65.

80. Singh, A. and Lee, K. L., "Variability in Soil Parameters," Proceedings, Eighth Annual Conference on Geological and Soil Engineering, Idaho, 1970.

81. Tang, W. H. and Ang, A. H-S., "Modeling Analysis and Updating of Uncertainties," Preprint No. 2016, ASCE National Structural Engineering Meeting, San Francisco, April 1973.

82. Tavenas, F. A., Ladd, R. S. and LaRochelle, P., "The Accuracy of Relative Density Measurements: Results of a Comparative Test Program," Relative Density Involving Cohesionless Soils, STP 523, American Society for Testing and Materials, 1972, pp. 18-60.

83. Tokimatsu, K. and Yoshimi, Y., "Field Correlation of Soil Liquefaction with SPT and Grain Size," Proceedings, International Conference on Recent Advances in Geotechnical Earthquake Engineering and Soil Dynamics, St. Louis, Mo., Vol. I, May 1981, pp. 203-208.

84. Triantafilids, G. E., Discussion - Session I, Proceedings, Fourth Pan-American Conference on Soil Mechanics and Foundation Engineering, San Juan, Puerto Rico, Vol. 3, 1971, pp. 76-79.

85. Valera, J. E. and Donovan, N. C., "Soil Liquefaction Procedures - A Review," Journal of the Geotechnical Engineering Division, ASCE, Vol. 103, No. GT6, June 1977, Proc. Paper 12996, pp. 607-625.

86. Vanmarcke, E. H., "Working Paper on Variance Functions," M.I.T. Department of Civil Engineering, December 1970.

87. Vanmarcke, E. H., "Probabilistic Modeling of Soil Profiles," Journal of the Geotechnical Engineering Division, ASCE, Vol. 103, No. GT11, Proc. Paper 13364, November 1977, pp. 1227-1246.

88. Vanmarcke, E. H., "Reliability of Earth Slopes," J. Geotechnical Engineering Division , ASCE, Vol. 103, No. GT11, November 1977.

89. Vanmarcke, E. H., "On the Scale of Fluctuation of Random Functions," Research Report No. R79-19, M.I.T. Department of Civil Engineering, April 1979.

90. Varaksin, S. V., "Determination of Sand Density Below Groundwater Table," thesis presented to Northwestern University, Evanston, Illinois, in partial fulfillment of the requirements for the degree of Masters of Science, August 1970.

91. Whitman, R. V., "Resistance to Soil Liquefaction and Settlement," Soils and Foundations, Vol. 11, No. 4, 1971, pp. 59-68.

92. Wu, T. H., "Relative Density and Shear Strength of Sands," Journal of the Soil Mechanics and Foundations Division, ASCE, Vol. 83, No. SM1, Proc. Paper 1161, January 1957, pp. 1161-1 - 1161-23.

93. Wu, T. H., "Uncertainty, Safety, and Decision in Soil Engineering," Journal of the Geotechnical Engineering Division, ASCE, Vol. 100, No. GT3, Proc. Paper 10434, March 1974, pp. 324-348.

94. Yegian, M. K. and Whitman, R. V., "Risk Analysis for Earthquake Induced Ground Failure by Liquefaction," M.I.T., Seismic Design Decision Analysis Report No. 26, May 1976.

95. Yoshimi, Y. and Oh-Oka, H., "Liquefaction of Saturated Sand During Vibration Under Quasi-plane-strain Conditions," Proceedings, Third Japan Earthquake Engineering Symposium, 1970.

96. Yoshimi, Y. and Oh-Oka, H., "A Ring Torsion Apparatus For Simple Shear Tests," Proceedings, Eighth International Conference on Soil Mechanics and Foundation Engineering, Vol. 1.2, Moscow, 1973, pp. 501-506.

97. Yoshimi, Y. and Oh-Oka, H., "Influence of Degree of Shear Stress Reversal on the Liquefaction Potential of Saturated Sand," Soils and Foundations, Vol. 15, No. 3, Tokyo, Japan, September 1975, pp. 27-40.

98. Yoshimi, Y. and Tokimatsu, K., "Settlement of Buildings on Saturated Sand During Earthquakes," Soils and Foundations, Vol. 17, No. 1, March 1977, pp. 23-38.

99. Youd, T. L., Discussion on "Seismic Response and Liquefaction of Sands," by Finn, W. D. L., Byrne, P. M., and Martin, G. R., Journal of the Geotechnical Engineering Division, ASCE, Vol. 103, No. GT7, Proc. Paper 13025, July 1977, pp. 827-829.

100. Bazaraa, A.R.S.S., "Use of the Standard Penetration Test for Estimating Settlements of Shallow Foundations on Sand," thesis presented to the University of Illinois at Urbana, Illinois in 1967, in partial fulfillment of the requirements for the degree of Doctor of Philosophy.

101. Box, G.E.P. and Cox, D. R., "An Analysis of Transformations," Journal of the Royal Statistical Society, Series B, Vol. 26, 1964, pp. 211-252.

102. Donovan, N. C., "Earthquake Hazards for Buildings," Building Practices for Disaster Mitigation, Ed. R. Wright, S. Kramer, C. Culver, Building Science Series 46, U. S. Department of Commerce, National Bureau of Standard, February 1973.

103. Donovan, N. C., "A Statistical Evaluation of Strong Motion Data Including the February 9, 1971 San Fernando Earthquake," Proceedings, Fifth World Conference on Earthquake Engineering, Italy, 1973.

104. McGuire, R. K., "Seismic Structural Response Risk Analysis, Incorporating Peak Response Regressions on Earthquake Magnitude and Distance," M.I.T., Department of Civil Engineering, Research Report R74-51, 1974.

105. Terzaghi, K. and Peck, R. B., Soil Mechanics in Engineering Practice, John Wiley & Sons, Inc., New York, New York, 1948.